Experimental Investigation of Bio-sealants Used for Pavement Preservation and Development of a New Strength Test for Asphalt Binders at Low Temperature

A DISSERTATION SUBMITTED TO THE FACULTY OF THE UNIVERSITY OF MINNESOTA

BY

DEBAROTI GHOSH

IN PARTIAL FULFILLMENT OF THE REQUIREMENTS FOR THE DEGREE OF DOCTOR OF PHILOSOPHY

Mihai Marasteanu, Adviser

October 2017

Acknowledgements

After a long journey of three years, today is the day: writing this note of thanks is the finishing touch on my dissertation. It has been a period of intense learning for me, not only in the scientific arena but also on a personal level. Once I heard that it takes a village to raise a child, it is definitely appropriate to say that it takes a whole research community to raise a graduate student. The journey of being a Ph.D. has a significant impact on me. I would like to reflect on the people who have supported and helped me so much throughout this process.

At first, I would like to thank my amazing adviser and teacher Dr. Mihai Marasteanu. I truly mean it when I say that it would have been difficult for me to finish my Ph.D. in three years if he was not my adviser. He taught me how to be organized, discipline and proceed step by step with ideas in research. He is one of the most supportive and understanding faculties I have ever known. I can probably write few pages about the ways Dr. Mihai inspired me and helped me improve. Next, I am grateful to Mugurel Turos who is in charge of the pavement materials laboratory. He made my life a lot easier by being there in the laboratory, teaching me how to handle machinery/equipment and helping me in my laboratory works when I had a busy class schedule. It would have been tough for me to take care of the complicated sample preparation procedure needed for my research if Mugur was not there. I will always remember and admire his adventurous and energetic personality which I discovered while having a lot of extended discussions on traveling.

I would like to thank Dr. Lev Khazanovich, Dr. Lauren Linderman, Dr. Jia-Liang Le and Dr. Glen Meeden for serving as my committee members and helping me with valuable advice. I am thankful to Joseph Labuz, Dominik Schillinger, Otto Strack, Adam Boies and Glen Meeden for the effective courses they taught which helped me enrich the horizon of my knowledge. My labmates Jhenyffer Oliveira and Mateus Aguiar Lima were very generous and helpful to assist me with the testing for my research. Having Marcela Hartman as a groupmate, friend and colleague were refreshing. I would like to thank a number of people working for the civil engineering department who made my graduate life

a lot easier and comfortable: Tiffany Ralston, who had answers to all the questions I faced regarding administrative issues; Gregory Sherar, who was the solution to all the technical problems; Heather Niermans, with a fantasticly smiling face was always enthusiastic to help me regarding payroll issues; Heather Eastlund, who helped me survive the struggle of visa problem I faced while visiting my country with her prompt responses for the paper-works needed to be done online; Merry Rendahl, who taught me several ways about how to write and helped me improve my writing skills.

I want to thank the ever-enthusiastic crowd of MnDOT material office who inspired me and helped me become confident about my career in pavement engineering. Several discussion with my colleagues on transportation engineering helped me broaden my research perspective. I was amazed by the crowd at my defense when I saw all my colleagues I invited from MnDOT came to support me and cheer me up, and that was a moment I will always cherish. Speaking about MnDOT, I would like to convey my special thanks to MnDOT for providing the funding for my research study.

While it is always challenging to cope up with foreign land and language leaving behind family/friends and be productive in studies at the same time, I would like to thank all the members of Bangladeshi Student Association (BDSA) of UMN for providing me a little piece of Bangladesh and touch of having a family here in USA. My special thanks to Mehedi and Taskin for being there all the time as family members and feeding me in my struggling days of graduate life. I am also grateful for having my dearest school friends as graduate students here in almost all the major cities in the USA who were always available providing me the words of encouragement when I needed. It will be unfair if I do not thank Sabina, Lubna, Syeda, Nabila and Munmun for the refreshing road trips in the USA and frequent long talks regarding life and career which were the primary sources of my stress-relaxation. My special thanks to Sabina Islam, a Ph.D. candidate at North Carolina State University, who was the first to inspire me about dreaming big through applying abroad and continuing graduate studies.

I am truly blessed to be a part of a family that values study, career, and hard work over anything else. Besides, I was probably one of the most privileged girls in Bangladesh

having both parents as faculty who always inspired me towards higher studies and successful career. Whenever I felt depressed, my parents were always there to hold me, believe in me and cheer me up in hundred ways. My special thanks to my younger brother, Somudro who always believes in me more than I do and irritates me in a lot of adorable ways which has become the fuel of my life. I am grateful to have my younger sister, Arin who is always just a phone call away anytime of the day to listen to me talk. It is essential to have a good friend as a roommate who will always be there to be a partner in crime. I am thankful to my husband for being that partner, the best friend and the support system of my life who is always there to comfort and encourage me. It is always relaxing to know that I am not alone and if anything goes wrong, my best friend is there to fix it. My special thanks to his family who has a tradition of producing Ph.Ds and eventually knows the value and the pressure of my journey. I will always admire the continued encouragement and enthusiasm my in-laws gave me during my tough days.

Lastly, I am thankful for belonging to such a beautiful campus of the University of Minnesota which never failed to make me smile or amaze me with her scenic beauty in all seasons.

Dedicated to my Parents, Sanjib Ghosh, Ruma Nandi and uncle Bissawjit Ghosh, aunt Mitali De

ABSTRACT

Surface treatment using sealants as a mean of pavement preservation is an important tool for cost-effectively extending service life of pavement. Sealants have become an important tool for cost-effectively extending the service life pavements. Due to the combined negative effects of asphalt aging and thermal cracking, it is always more challenging to choose an appropriate preservation technique for pavements built in cold-regions. Asphalt aging and thermal cracking negatively affect pavements built in cold climates. Therefore, it is important to evaluate the effects of sealants in laboratory conditions before application in the field to ensure effective performance. However, preservation activities cannot effectively address major distresses, such as low-temperature cracking, that can occur when the pavement was built from the very beginning with less durable materials. Therefore, an essential requirement to mitigate low-temperature cracking of pavements for asphalt materials used in the construction of pavement built in cold- regions is ensuring proper fracture properties of the asphalt materials used in construction.

This study has two parts. In the first part, a laboratory evaluation of the effects of adding bio-sealants to both asphalt binder and mixture is performed. The goal is to obtain relevant properties of treated asphalt materials to understand the mechanism by which sealants improve pavement performance. For asphalt binders, a dynamic shear rheometer and a bending beam rheometer were used to obtain rheological properties of treated and untreated asphalt binders. For asphalt mixtures, field cores from both untreated and treated sections were collected and thin beam specimens were prepared from the cores to compare the creep and strength properties of field-treated and laboratory-treated mixture. It is observed that the oil-based sealants have a significant softening effect on the control binder compared to the water-based sealant and traditional emulsion. Oil-based sealants increased rutting and fatigue potential of the binder and helped the low-temperature cracking resistance. For asphalt mixtures, different trends are observed for the field samples compared to the laboratory prepared samples. Similar to binder results, significant differences are observed between the asphalt mixtures treated with oil-based and water-based sealants, respectively. Additional analyses were performed to better understand the

sealant effects. Fourier transform infrared spectroscopy (FTIR) analysis showed that the sealant products could not be detected in mixture samples collected from the surface of the treated section. Semi-empirical Hirsch model was able to predict asphalt mixture creep stiffness from binder stiffness. The results of a distress survey of the test sections correlated well with the laboratory findings.

In the second part, a news binder strength testing method is proposed with the goal to provide an effective tool for selecting asphalt binders that are crack resistant. A modified Bending Beam Rheometer (BBR) is used to perform three-point bending strength tests, at constant loading rate, on asphalt binder beams at low temperature. Based on the results, a protocol for selecting the most crack resistant material from binders with similar rheological properties is proposed.

Table of Contents

LIST OF TABLES

LIST OF FIGURES

Chapter 1: INTRODUCTION

1.1 Background

Pavement preservation is playing an increasingly significant role in maintaining our aging pavement infrastructure under severe budget constraints. One key component is the use of surface treatments based on application of sealants. The selection of sealants for use in cold climates has remained a difficult task. Cold temperature significantly limits the number of sealant materials that perform well over many years (Masson et al., 1999). Recently, several new products, called bio-sealants, have been used to treat aging pavement surfaces. These sealants are expected to seal the cracks resulting in impervious pavement surfaces pavement surfaces and to reverse the oxidation/aging process. The effect of sealants on the low-temperature properties of binder and mixture has always been a matter of significant concern. Therefore, it is essential to investigate the effects of these sealants on the properties of asphalt binder and mixture.

A well-planned strategy is a key requirement for a durable pavement infrastructure. That strategy should include applying cost-effective treatments to a structurally sound pavement, preserving the pavement system, and preventing future deterioration. Preservation activities are beneficial to mitigate normal deterioration that occurs with aging pavements, but they cannot effectively address major distresses, such as low-temperature cracking, that occurs when a pavement was built from the very beginning with less durable materials.

The prevailing failure mode in asphalt pavements constructed in the northern part of the US is cracking due to low-temperature shrinkage stresses. Restrained by the layers below, the top layer of the pavement relieves built up tensile stresses by forming transverse cracks on the surface. The low-temperature cracking manifests as a set of almost-parallel, surface-initiated transverse cracks of various lengths and widths. Other types of degradation are related to the existence of these transverse cracks: water penetrates through the pavement cracks and weakens pavement base and subbase through freeze-thaw cycles. During winter, the presence of water may lead to differential frost heaves of the pavement. Under traffic loads, water and fine

materials are pumped out, causing a progressive deterioration of the asphalt layer. Finally, these cracks expedite moisture-related issues and pothole formation at the crack location and lead to poor ride quality. Therefore, to build durable pavements that can be effectively maintained using current pavement preservation techniques, it is critical to select asphalt materials that resist low-temperature cracking

1.2 Objectives

This thesis investigates new materials and methods of characterization that can lead to improvements in pavement preservation. The mechanism of pavement preservation that occurs when bio-sealants are applied to the surface of asphalt pavements is discussed through laboratory analysis. It also proposes a new method for selecting asphalt materials that have better cracking resistance at low temperatures.

The mechanisms of bio- sealants were investigated by quantifying the effect of bio-sealants on the material properties of asphalt that can lead to improvements in pavement performance, developing a laboratory sample preparation method that closely mimicked the field-application of sealants, and determining if bio-sealants are more effective than traditional asphalt sealants.

In addition, a simplified strength testing method is proposed. The new method uses a modified BBR to perform three-point bending strength tests on asphalt binder beams at low temperature, with the final goal of developing a specification for binder selection similar to the current performance grading (PG) specification.

1.3 Research Approach

The thesis describes the following research tasks:

- Performed relevant literature review

- Developed laboratory sample preparation method that can simulate the application procedure of sealants in the field
- Performed experimental investigation on field samples obtained from cores and on laboratory prepared samples
    - For asphalt binders: obtained rheological and fracture properties using Dynamic Shear Rheometer (DSR) and Bending Beam Rheometer (BBR) testing methods
    - For asphalt mixtures: performed BBR creep and strength test at low temperature.
- Performed statistical analyses to
    - Evaluated the effect of applying different types of sealants to the control asphalt binder and asphalt mixture
    - Evaluated the effectiveness of using laboratory sample preparation methods to simulate actual field conditions.
- Investigated the feasibility of using semi-empirical methods to predict mixture properties from binder properties, and vice-versa.
- Evaluated the BBR strength test and propose a new testing method for asphalt binders.

1.4 Organization of Thesis

The objective and motivation for this study are presented in Chapter 1. Chapter 2 presents a literature review on pavement preservation. Chapter 3 describes the materials used in the investigation and the testing protocols used to obtain rheological and strength properties of the investigated materials. The results of the asphalt binder testing are presented in Chapter 4, and the results of asphalt mixture testing are shown in Chapter 5. The results from the previous two chapters were analyzed using the Hirsch semi-empirical model and are presented in Chapter 6. The investigation to establish a new testing protocol for binder strength test is presented in

Chapter 7. Chapter 8 contains the conclusions of this research and recommendations for future work.

Chapter 2: LITERATURE REVIEW

2.1 Introduction

Chapter 2 presents an overview of pavement preservation and current pavement preservation practices. Because bio-sealants are expected to serve a purpose similar to fog seals and oil-based rejuvenator, the effects of fog seals and oil-based rejuvenators are presented in detail. A review of laboratory evaluation for fog seals, rejuvenators, and bio-fog seals follows.

2.2 Pavement Preservation

Pavement preservation involves the timely application of carefully selected surface treatments to maintain or extend a pavement's service life. The purposes of pavement preservation are to reduce aging and restore serviceability. The key is to apply the right treatments to the right roads at the right time when the pavement is still in good condition, with no structural damage. An effective pavement preservation program includes the use of a range of preventive maintenance techniques and strategies, such as fog seal, chip seal, slurry seals, crack sealing, thin hot-mix overlay (both dense- and open-graded), thin cold-mix treatment, Novachip, very thin and ultra-thin overlays, and micro-surfacing.

Zubeck et al. found that crack sealing and patching represent the most extensively used applications in pavement preservation treatments, followed by chip seals, fog seals, and slurry seals (Zubeck et al., 2007). Gransberg summarized a survey of U.S. public highway and road agencies that use chip seals as a part of their roadway maintenance program (Gransberg, 2005). A total of 72 individual responses from 42 U.S. states and 12 U.S. cities and counties were received as mentioned in the study. The survey concluded that the chip seal could be successfully used on high-volume roads if it is installed before pavement distress becomes severe or the structural integrity of the underlying pavement is breached. However, fog seals are the most cost-effective preventive maintenance tool and should be considered for routine maintenance programs (Simpson, 2006). Fog seals are low-cost and are used to restore "flexibility" to an existing HMA pavement surface. Hicks et al. also mentioned that fog seals might be used to seal

a pavement surface or to address raveling in an existing chip seal. However, they are not effective when applied to pavements with wide cracks, low friction numbers, ruts or shoving, or structural deficiencies (Hicks et al., 1997). Zukbeck and Mullin mentioned about the challenges of pavement preservation in cold region which include issues with construction as well as issues while the treated road is in service (Zukbeck and Mullin, 2012). In-service challenges include usage of studded tires for winter traction, snow and ice removal operations and exposure to cold and moisture. If the aggregate is not properly embedded into the substrate, snow plow damage may occur during the winter months. As a solution for mitigation of winter pavement damage, Croteau et al. suggested the use of multilayer systems with fine aggregate or use of a premium binder (Croteau et al., 2005). Pavement failure modes and mitigation in cold regions are explained elsewhere by Doré and Zubeck (Dore and Zubeck, 2009).

2.2.1 Agencies Practices

Pavement preservation techniques and their application vary among different states. Some of the more significant state practices are presented below.

An intensive study of surface treatments by Utah Department of Transportation on Utah pavements indicated that Chip Seal Courses (CSC) has a significantly longer life and the fog seal showed little, or no impact on the performance of the pavement distresses studied (Romero and Anderson, 2005). Based on the relative cost of both treatments and the performance observed through this study, it is recommended that Utah Department of Transportation expand the use of chip seal course.

Washington Department of Transportation (WSDOT) conducted a study on several aspects of chip seals to incorporate changes in its preservation program for expanding the use of the lower-cost option (Mahoney et al., 2014). The changes were based on literature review, a survey of state DOTs and a series of chip seal oriented meetings held over a span of five years. As a part of the investigation on seal practice in different states, when WSDOT conducted a survey, it was reported that most DOTs do not have a set cycle of applying an HMA overlay and chip seal cycle in alternating sequence. Only six states placed at least one Bituminous Surface Treatments between HMA overlay, however, some states do conduct this practice without a set

cycle. Most DOTs are interested in an alternating application of HMA and chip seals as they attempt to make their pavement preservation dollars stretch further (Mahoney et al., 2014).

When comparing the cost of preventive maintenance versus delaying more extensive treatments TxDOT estimates that this delay costs 4X more which broadly agrees with prior WSDOT findings (Webb, 2010). The authors noted that > 66% of the state DOTs apply chip seals over existing HMA surface courses to address oxidation or light to moderate surface distress issues associated with HMA (Peshkin et al., 2010).

Wood and Olson (2007) presented a history of the chip seal program at Minnesota Department of Transportation (MnDOT) that resulted in significant improvements and a successful implementation. MnDOT currently uses chip seals for both high and low traffic roads. Recently, MnDOT initiated a study to investigate the types and methods of selecting pavement preservation techniques that are ongoing in Minnesota and to develop set of guidelines or best practices for local agency engineers and maintenance supervisors in the development of pavement preservation programs within their agencies (Wilde et al., 2014).

2.3 Pavement Preservation using Fog-Seal, Rejuvenator, and Bio-Sealants

The literature reviews from previous sections conclude that surface treatment using chip seal is the most common practice and many studies have been performed on chip seal. However, chip seals include limitations such as aggregate loss, relatively long curing times for non-polymer modified emulsions, loose aggregate chips which can cause windshield damage, noise due to the rough surface, and need of warm weather to allow for construction. Fog seals can be used to prevent or at least reduce the occurrence of an aggregate loss in chip seals and extend the service life of the pavement. Other benefits of fog seal are low cost, ease of construction, and a desirable black appearance, to name a few. Asphalt-based fog sealants have been successfully used for surface treatments for many years. However, harmful sealants, such as coal tar-based products, have been banned by the Minnesota Legislature since January 1, 2014. These sealants contain high concentrations of chemicals called polycyclic aromatic hydrocarbons (PAHs), and environmental mixtures of PAHs are carcinogenic. A study by Minnesota Pollution Control

Agency revealed that about 67% of total PAHs in the sediments of 15 metro-area storm-water ponds were from coal tar-based sealants (.

The studies show that some of the products investigated were defined as sealants and others were defined as rejuvenators or a combination of the two. The main difference between a fog seal and a rejuvenator seal is in the chemical make-up. An asphalt rejuvenator is a petroleum product based on maltene (a lighter component of asphalt), whereas a fog seal is an asphalt-based emulsion. Rejuvenators have oils which help reduce the viscosity and soften the existing binder by restoring maltenes lost to the oxidative aging process resulting in improved flexibility and reduction in cohesive failure. A fog seal should theoretically slow down the deterioration rate by limiting the pavements exposure to the elements which can lead to oxidative aging that stiffens the asphalt binder making the pavement more susceptible to cracking (Wood and Olson, 2009). Three most common fog seals in practice are SS-1h (Anionic Slow Setting Emulsion), CSS-1h (Cationic Slow Setting Emulsion) and CQS (Cationic Quick Setting Emulsion). The effects of traditional CSS-1h on rheological properties of asphalt binder and mixture were investigated and compared with the effects of newly emerging products in this study.

Several significant field studies have been conducted on fog seal or rejuvenator application which helped develop guidelines and specification (A. Johnson, 2000; Janisch and Gaillard, 2006; Stroup-Gardiner, 2009; Urbanek et al., 2013; Im and Kim, 2015). Since this study focuses on the laboratory evaluation of sealants, a brief literature review of recent laboratory investigation on pavement preservation using fog seal and oil-based rejuvenators is presented next.

2.3.1 Laboratory Evaluation of Fog Seals and Rejuvenators

Many studies mentioned about softening effect when analyzing rejuvenator treated asphalt binder, mixture or RAP/RAS in the laboratory using different testing methods.

Mogawer et al. (2013) focused on the use of asphalt rejuvenators in high RAP and RAS mixtures to offset the stiffness effects of the aged binder from RAP and RAS without negatively impacting the performance of the mixtures (Mogawer et al., 2013). These rejuvenators may help

the hardened binder from the RAP/RAS co-mingle with the virgin binder. The rheological properties obtained from generating master curves along with the results from LAS and MSCR tests confirmed that the rejuvenators had a softening effect on the virgin binders and reduced the stiffness of the binders. For example, the results from the MSCR test showed a decrease in rutting resistance with the addition of rejuvenators (Mogawer et al., 2013). Similar observation of softening the effect reduced rutting resistance and increased moisture susceptibility upon adding rejuvenator was reported by other studies (Lin et al., 2012; Shen et al., 2007, Nahar et al., 2014). Lin et al. investigated the influence of using rejuvenator seal materials (RSM) on both asphalt mixtures and aged asphalt binder (Lin et al., 2012). The effect of three types of materials (RSM) composed of a petroleum solvent and a rejuvenator available in China was studied where the rejuvenators were added to PG 70-22 at 5% by weight of the binder. The laboratory test results showed that the RSM-treated aged binder exhibited lower the viscosity, lower complex modulus and higher phase angle which indicated softening of binder and thus increasing rutting potential. Similar findings were obtained for RSM-treated HMA when RSM significantly increased the rutting depth of HMA. Moreover, the RSM treated HMA showed lower ITS, higher creep strain and lower skid resistance as compared with untreated HMA. Similar findings of a decrease in rutting resistance of rejuvenator-treated asphalt binder and mixture were observed in a study by Shen et al., where the researchers aimed to investigate the effects of rejuvenator on aged-asphalt binder and mixture (Shen et al., 2007). They conducted a series of DSR and BBR tests on rejuvenator-treated aged binder along with the control binder to study both high and low-temperature performance. Besides, to evaluate the mixture performance, wheel tracking test was performed to determine rutting resistance at high temperature and thermal stress restrained specimen (TSRS) was used to evaluate the fracture properties at low temperature (Shen et al., 2007). Nahar et al. focused on the rheological and microstructural assessment of rejuvenated asphalt (Nahar et al., 2014). Virgin binder was aged in the laboratory using an accelerated procedure based on the rotational cylinder aging tester, RCAT, to consistently mimic RAP binder (Nahar et al., 2014*)*. Two distinct rejuvenators were selected for this study, which was mixed with the laboratory aged binders for 15 minutes at 150°C. Three mixtures were prepared using 10%, 20% and 25% rejuvenators with the aged binder. Rheological measurements were conducted at 30, 40, 50 and 60°C using a Dynamic Shear Rheometer (AR 2000ex rheometer

from TA Instruments), and the results were shifted to a reference temperature of 30°C using the time-temperature superposition principle (Nahar et al., 2014). As expected and reported in the literature (Shen et al., 2007; Zaumanis et al., 2013; Asli et al., 2012) upon addition of rejuvenators, the master curve of the blend is found to shift to lower values because of softening. A study by Chiu and Lee also reported about resulting softening effect when applied three different types of rejuvenators on a highly aged parking lot pavement, which had shown some severe raveling (Chiu and Lee, 2006). Cores were taken from the pavement before and after the treatments and binders were extracted from different layers of the cores to examine the effects of these treatments based on viscosity. The application of these rejuvenators caused a reduction in pavement surface friction (about 20% reduction in British Pendulum Number (BPN)) and pavement surface texture (about 10 % reduction in Macro Texture Depth (MTD)) (Chiu and Lee, 2006). Similar observations of a reduction in Macro Texture Depth and temporary reduction in skid resistance were also reported by the extensive study on fog seals and rejuvenators conducted in California (Stroup-Gardiner et al., 2009; Cheng et al., 2014 and 2015). Zaumanis et al. evaluated the effectiveness of rejuvenators in terms of penetration for the production of very high (40% to 100%) reclaimed asphalt pavement (RAP) content mixtures (Zaumanis et al., 2013). The study used penetration index (PI) and the penetration–viscosity number (PVN) as the indicators of oxidative hardening and cracking. A report by NCAT in 2012 concluded that adding a recycling agent (i.e., a rejuvenator) can be helpful to restore the performance properties of recycled binder to offset the higher binder stiffness and improve the mixture resistance to cracking when high RAP/RAS contents are used (Zaumanis et al., 2013).

Hugener et al. investigated the idea of reactivating the old binder in reclaimed asphalt pavement (RAP) using vegetable oil-based rejuvenator (Hugener et al., 2013). The authors found that rejuvenators are not suited for uncoated minerals because they can only activate the old binder, but not act as a binder by themselves (Hugener et al., 2013). Boyer mentioned that applying the rejuvenator at periodic intervals can restore the asphaltene-maltene balance to maintain a ductile, pliable pavement which is particularly applicable to pavements in the hot, dry southwestern section of the country (Boyer, 2000). Brownridge mentioned that for a rejuvenator to penetrate it cannot be retarded by blending with asphalt binder because that stops the

absorption which might result in loss of the rejuvenation effectiveness (Brownridge, 2010). The diffusion and mixing of binders in a blend depend upon several factors, including compatibility of binders, the temperature of mixing, performance grade of the virgin and recycled binder, and the percentage of recycled binder in the blended binder (Tran et al., 2012). A study by Al-Qadi et al. (2006) described that the sealant with an appropriate consistency at the recommended installation temperature would provide a better effectiveness and would ensure appropriate bond strength (Al-Qadi et al., 2006). Ali and Sobhan analyzed several factors which are important to determine the amount of rejuvenator to be added to the mix which includes hardness of the existing binder and the reaction between the binder and rejuvenator (Ali and Sobhan, 2012). A recent study by Wang et al., analyzed the rejuvenating effect on aged asphalt by means of a Mortar Transfer Ratio (MTR) test, which concerns the ratio of asphalt mortar that moves from recycled aggregates (RAP aggregates) to fresh added aggregates when aged asphalt is treated with a regenerating agent and comes into contact with fresh aggregates. The proposed MTR test analyzes the regeneration in terms of the softening degree on aged asphalt when the rejuvenator is applied (Wang et al., 2017).

2.4 Bio-Fog Seal

Among all these various surface treatments, this study focuses on some different types of fog seal, known as a bio-fog seal, which has been introduced recently as alternative surface sealers for streets, highways, shoulders, and recreation trails. The use of these emerging products may provide a sustainable alternative to traditional petroleum-based products and reduce adverse environmental impacts. Common bio fog seal product includes RePlay®, Anova™, Biorestor. The most commonly claimed benefit is their ability to prevent and reverse harmful oxidation factors to asphalt pavements (life extension). It is also commonly claimed that they penetrate efficiently and cure in 15 to 30 minutes, which allows for minimal road closure time. In addition, some bio fog seals are clear and do not affect pavement markings, their application rates are often lower than traditional fog seal (as low as 0.02 per square yard), and are considered to be environmentally friendly.

Next section presents some studies on newly introduced bio-sealants which are RePlay and JOINTBOND.

2.4.1 Recent Studies on Bio Fog Seal

Pennsylvania department of transportation conducted a research project on evaluating a new soy-based sealer named RePlay, developed by BioSpan Technologies (Medina and Tyson, 2009). RePlay, an Agricultural Oil Seal and Preservation Agent, is an asphalt sealant which is 88% biobased and 40% of which is sourced from soybean oil (Figure 11) (BioSpan Technology, 2010). This product was reported to be very useful in drastically reducing the presence of air (for oxidation) and water into the pavement. The oil increases the flexibility of the aged, brittle pavements penetrating deep into the surface of the pavement with an average of 0.75 to 1.25 inches, and thus adding lost oil to the asphalt (Medina and Tyson, 2009). This results in adding years to the service life of asphalt surfaces, filling cracks, and reducing the oxidation process of the roadway when applied every 3-5 years. According to the manufacturer, the process of introducing new SBS and SBBS polymers to the mix has made RePlay exceptional from other conventional surface sealants. The BioSpan Technology claims that the product contains approximately 15% polymers, which increases the resistance to raveling, rutting, and cracking and thus strengthen the pavements (Biospan Technologies, 2010). The objective of the research project by PennDOT was to evaluate RePlay's effectiveness at reducing permeability without reducing durability or skid resistance to an unacceptable level (Medina and Tyson, 2009). As a result, a series of skid tests, field observations and a permeability test were planned in to evaluate and determine the performance of the RePlay. The RePlay was applied by the company representatives using their equipment following the manufacturer's specifications. The product smelled like citrus degreaser and developed a glossy and slippery surface to walk on. The effect of the application of the product was noticeable within minutes, softening the asphalt surface and the joint seals and with the changes in color (FIGURE 2.1 and 2.2). Only some coarse aggregates were observed to be wet after 15 minutes. The researchers drove over the treated asphalt surface and braked several times aggressively after 35 minutes. The road was open just after an hour and five minutes later of the application of the BioSpan-RePlay. A similar type of observations was

also made in a similar project of evaluating treated pavements using RePlay which was funded by Minnesota Local Road Research Board (LRRB) and conducted in 2011 (Olson, 2011).

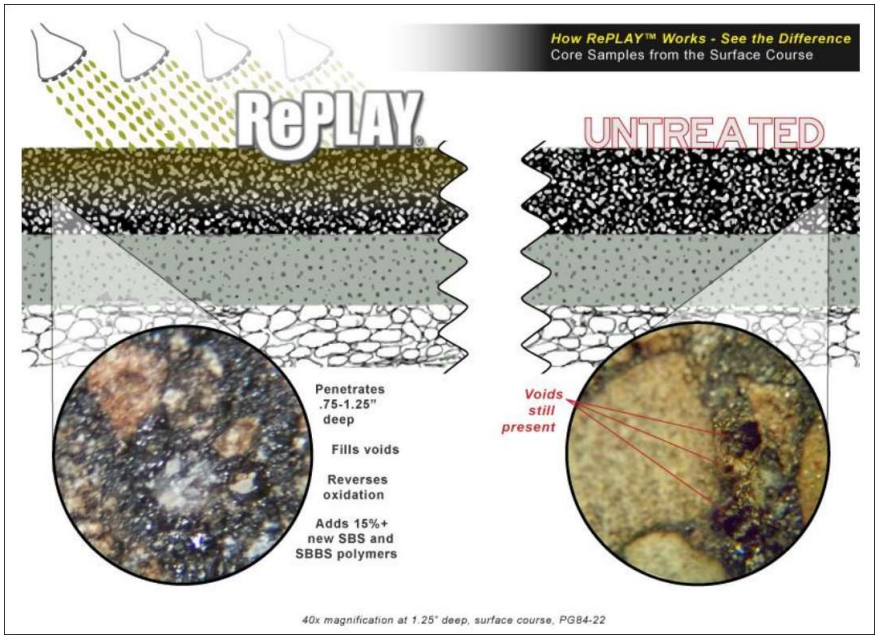

FIGURE 2.1 Polymer penetration with RePlay® of a PG 84-22 asphalt concrete sample at 1.25" depth compared to untreated sample (source BioSpan Technologies Inc. at http://biospantech.com/)

FIGURE 2. 2 Change of Colors from a Light Gray to a Dark Grayafter Application of RePlay (Medina and Tyson, 2009, pp.26).

Three cores were taken in the treated lane with BioSpan-RePlay, and three cores were taken from the adjacent untreated lane for the project conducted by PennDOT (Medina and Tyson, 2009). Permeability tests were performed on both types of cores to determine the change. Skid testing values were obtained prior to the application of the product, two weeks after the application and at the end of the project. The permeability tests were conducted as per ASTM PS 129 method (ASTM, 2009). Permeability was found not to be an issue because both the treated and untreated cores were found to be impermeable. The coefficient of the water permeability was determined to be the same for both experimental and control sections. A significant loss in friction and reflectivity of pavement markings were observed in the treated pavement even after two weeks of the application of the product. There was no visible evidence of the application of BioSpan-RePlay after 18 months of the application. Same deterioration was observed in winter for both the treated and untreated sections. The BioSpan Technologies claimed that the use of RePlay for 3-5 years substantially saves the excessive cost of repaving (BioSpan Techonology, 2010). However, PennDOT concluded that safety concerns associated with the use of RePlay as pavement sealers, along with inconclusive evidence of having a benefit to extending pavement life, outweighed the benefits of its use.

Two sections of very different pavement conditions were selected for the Minnesota LRRB project (Olson, 2011). One of the sections was a fifteen years old, cracked and raveled bicycle/pedestrian trail and the other was a driveway without any distresses constructed within the last five years. The application of the RePlay followed the same procedure, as mentioned before, according to the manufacturer's specification. A significant difference was observed in the behavior of water when applied to both newer and older pavement, respectively, before and after application of RePlay (Olson, 2011). The water was more prone to penetrate into the older bicycle/pedestrian trail than into the newer driveway before application of RePlay. Once the RePlay was applied, water ran off the paved surfaces at a high rate of speed without wicking into the surface, for both new and old pavements. This observation contradicts the observation from the PennDOT project that equal permeability was measured in the pavements before and after the application of RePlay (BioSpan Techonology, 2010). The authors of the LRRB report mentioned that visual inspections of pavements before and after application of RePlay also confirmed about the top layer of asphalt getting sealed after the application (Olson, 2011. This

was a helpful observation for the pavements experiencing high foot/ pedestrian traffic all year long, especially in hottest weather. The conventional sealants were observed to have the problems of becoming soft and sticky during hot weather periods and thus affecting pedestrian traffic negatively. The equipment needed to apply the RePlay included a sprayer and a flatbed truck. The truck is very common for most agencies and the sprayer would cost between $15,000 and $20,000. The application of the product can be performed by only two people and requires very little traffic control. As restriping pavement is not mandatory after the application of RePlay, it makes the process less expensive than applying chip seal coating where there are pavement markings. The application cost of RePlay using contract labor results has an equivalent cost of applying a chip seal coat, and it appears to be more cost-effective in some cases.

Recently, BioBasedNews.com published an article on the benefits of using RePlay at Tyndall Air Force Base in Florida (BioSpan Technology, 2010). The manufacturer stated that airports are extremely environmentally sensitive because of jet fuels, vehicle exhausts, and the demand for electrical power and heating and cooling puts tremendous stress on the environment. RePlay is considered as an environment-friendly surface sealant.

The Flexible Pavement Division of the Central Road Research Institute (CRRI) of New Delhi, India released a report from April 2010 on their research evaluating BioSpan premier asphalt product, RePlay, Agricultural Oil Seal and Preservation Agent (BioSpan Techonology, 2010). As described in the report, field tests were conducted by CRRI team on a six-lane toll road in July 2009, and after allowing eight weeks for RePlay to penetrate adequately, 24 core samples, 12 unmodified and 12 modified with RePlay were collected. Through the analysis of the collected samples using ASTM International standards, RePlay was proved to be a sealant that improves the properties of bitumen present in the road surface and bituminous mix (BioSpan Techonology, 2010).

Another newly introduced sealants, Joint Stabilization (Joint Bond®) Treatment is marketed as a rejuvenator designed to prevent the deterioration of the longitudinal joint without damaging pavement markings. This product is also intended to make the pavement impervious to water and salt brine. A project by Maine DOT was carried out to determine if JOINTBOND®

extends the useful life of the construction joint by reducing permeability at the joint (Gayne, 2013). JOINTBOND, manufactured by D&D Emulsion, Inc., and distributed by Pavement Technology, Inc., is a post-applied polymerized maltene-based emulsion product composed of a petroleum resin oil base and SBR copolymer uniformly emulsified with water (Williams, 2011). This product penetrates the pavement's surface and affects the chemistry of the in-place asphalt binder to help prevent joint deterioration and separation. JOINTBOND was designed to help minimize asphalt maintenance by penetrating newly placed asphalt pavement and stabilizing the critical area surrounding the longitudinal construction joint (Gayne, 2013). A total of 11 miles were treated in this project. The treated area appeared as a darkened stain on the centreline joint at this point, the day after treatment. According to the manufacturer, the pavement should show little sign of the treatment and no damage to the pavement markings. The product/ installation is expected to be evaluated by the Transportation Research Division over a two-year period for effectiveness through being monitored for signs of joint degradation and permeability at the centerline joint. The investigation initially reported that the JOINTBOND product changed the white lines to a more yellow color (FIGURE 2. 3).

FIGURE 2. 3 Application of JOINTBOND product. (Gayne, 2013, pp. 19).

JOINTBOND® has now been applied to 950+ miles of joint on Tennessee Department of Transportation interstates and state routes. TDOT approved the use of JOINTBOND application as a fix instead of milling/repaving new paving joints where contractors do not meet joint density requirements (FIGURE 2. 4) (Calvert, 2008).

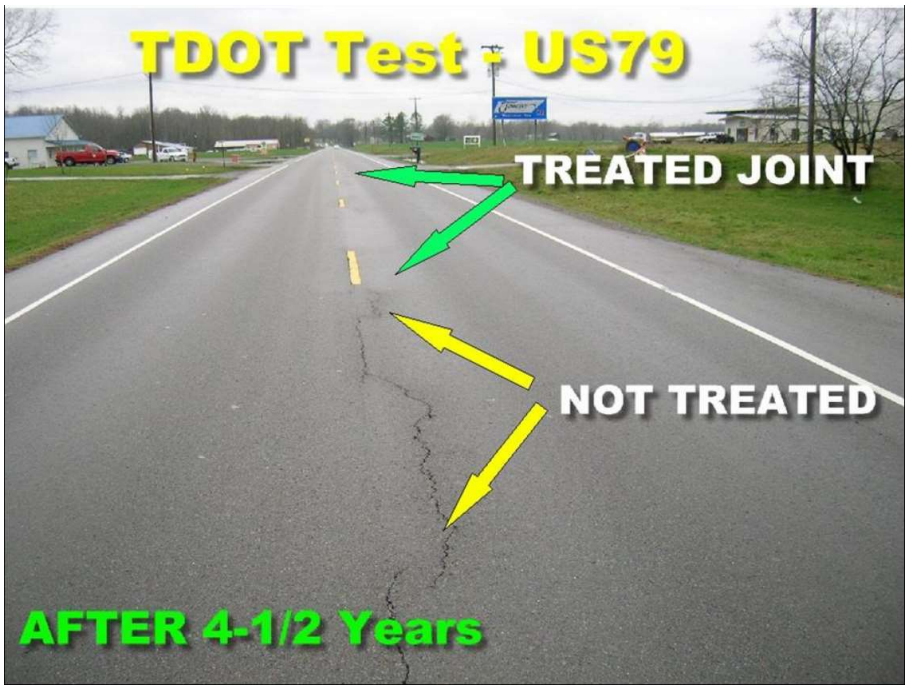

FIGURE 2. 4 Effect of JOINTBOND Application on Tennessee Roads. (Calvert, 2008).

The university of Arkansas conducted a similar study on HMA longitudinal joint evaluation and construction in 2011 (Williams, 2011). The authors of the study used field core density and field permeability, as well as infiltration, as reasonable indicators of joint quality. The study investigated some joint construction techniques, to generate a recommendation for appropriate methods that can be used to improve longitudinal joint quality, which can be easily implemented within an existing quality control/quality assurance (QC/QA) program. Among eight construction joint techniques, only the JOINTBOND product appeared to both increase density and decrease permeability, though the method of application did not intuitively cause the anticipation of an increase in density (Williams, 2011). However, when the Joint Stabilization (Joint Bond®) treatment was applied to two test sections of TH 95 in Minnesota in 2008 in Minnesota, field visits in 2009, after rain events, did not reveal any noticeable performance difference between the treated and untreated sections (Watson, 2009).

2.5 Summary of Literature Review

The following findings can be made from literature review:

- Application of sealants depends on the environment, cost, and needs to be applied at the right moment.

- All states have developed guidelines for preventive maintenance techniques based on requirements that do not follow a hard rule.

- Oil-based rejuvenators have a significant softening effect on asphalt binder and mixture, which results in a reduction of rutting resistance.

- Cold-temperature regions face more challenges in choosing suitable sealants for surface-treatments because pavements in perennial frost areas experience local failures due to degradation of the underlying permafrost. Other challenges include a short and relatively cold construction period, a need for snow and ice removal, and exposure of pavement to cold and moisture.

- Comparatively, more field studies have been performed on chip seals than other types of seals. A very limited number of studies on newly introduced bio-sealants and their benefits have been completed so far.

- Many studies that included a laboratory evaluation of binders treated with sealants blended heated binder and sealants to prepare samples. Direct mixing of binder and sealant does not represent the spraying application of surface-treatments used in actual field conditions. There is no laboratory procedure to simulate the application process of sealants to pavement surfaces, which is a critical step in designing effective products in laboratory conditions rather than conducting expensive field testing.

Chapter 3: MATERIALS AND TESTING METHODS

The materials used in this investigation and the testing methodology used to evaluate the properties of these materials are presented in the next sections 3.1 through 3.3.

3.1 Materials

The investigation of newly introduced bio-sealants is a part of MnDOT project (Ghosh et al., 2016). In this study, two types of oil-based bio-sealants, OB1, OB2, one type of water-based bio-sealant, WB1 and one type of traditional emulsion, E1, were investigated. The materials used in this study come from a field project conducted by MnDOT on CSAH 75 in Wright County, Minnesota. The road and shoulder were paved full width in 2013 using a MnDOT type SPWEB340C mix design. Treatments were installed between August and October of the 2014 construction season as follows:

- RePlay (OB1), an Agricultural Oil Seal & Preservation Agent, is an asphalt sealant which is 88% bio-based rejuvenator; of which 40% is derived from soybean oil (*Kindler, 2009*). The remainder 12% of the OB1 composition is recycled materials; particularly polystyrene, that is especially used to impart essential polymers to the asphalt binder (*Levy, 2012*). It is carbon negative, non-toxic, and safe for any nearby plant life if over-sprayed. This polymer-bearing, proprietary fog treatment product for bituminous pavement was sprayed over 2680-ft of the bituminous shoulder at a rate of 0.020 gallons per square yard.
- Biorestor (OB2) is a proprietary fog treatment product for bituminous pavement. Biorestor was applied as a fog treatment over 1338-ft of the bituminous shoulder at a rate of 0.015 gallons per square yard (OB2_a) and a rate of 0.020 (OB2_b) gallons per square yard to another 1326 ft.
- JOINTBOND (WB1), manufactured by D&D Emulsion, Inc., and distributed by Pavement Technology, Inc., is a post-applied polymerized maltene-based emulsion product composed of a petroleum resin oil base and SBR copolymer uniformly emulsified with water. It is a proprietary product that is designed for stabilizing the area surrounding

longitudinal construction joints. JOINTBOND was applied as a fog seal over 3000 ft of the bituminous shoulder at a rate of 0.073 gallons per square yard.

- CSS-1h (E1) is a slow set cationic emulsion with a relatively low viscosity that is made using relatively hard base asphalt. In July 2014, a 1:1 dilution of CSS-1h was applied to 1000-ft of Wright CSAH 75 as a bituminous fog seal at a rate of 0.1 gallons per square yard in the westbound shoulder.

Four field cores from each type of treated section along with the control section were collected. Three cores were taken from the control and the treated sections a few days after treatments were applied, and one core was taken 8 months later. The earlier three cores received a random core numbering of 1, 2, and 3 for each treatment type. Core number 4, from all treated section, was collected eight months later. A summary is shown in Table 3.1.

TABLE 3. 1 Cores used in the study

Type	Number of cores	Rate of Application (gallon/sy)
Control Section	3+1	
Control Section + Emulsion (E1)	3+1	0.10
Control Section + OB2 (0.015)	3+1	0.015
Control Section + OB2 (0.02)	3+1	0.020
Control Section + OB1	3+1	0.015
Control Section + WB1 CSAH 75	3+1	0.073

3.2 Experimental Testing

The following paragraphs provide a brief description of the test methods used to obtain rheological and strength properties of the asphalt binders and mixtures investigated in this study.

3.2.1 Asphalt Binder Testing

For asphalt binder testing, the current test methods used to obtain the performance grade of asphalt binders were used. A Dynamic Shear Rheometer (DSR) was used to obtain binder properties at intermediate and high temperatures.

Low-temperature stiffness and relaxation properties of binder were determined using a bending beam rheometer (BBR).

3.2.1.1 Dynamic Shear Rheometer Testing

Characterization of the viscous and elastic behavior of binder at intermediate to high temperatures is performed in accordance with the AASHTO T 315 (*Determination of rutting and fatigue factors using a Dynamic Shear Rheometer (DSR)*) test method. The AASHTO T 315 test method helps determine the high-temperature rutting factors as well as the intermediate temperature fatigue factor (*AASHTO T-315, 2006*). The samples are tested using 25-mm diameter parallel plates and 8-mm diameter parallel plates based on requirement. One of the parallel plates is allowed to oscillate with respect to the other at preselected frequencies and angular rotation (i.e., torque). The required amplitude depends upon the value of the complex shear modulus of the binder being tested. The DSR samples are tested in a thermally controlled test chamber, capable of maintaining the desired testing temperature within a tolerance of ±0.1°C. The DSR test is performed at a loading frequency of 10 rad/s. The complex modulus (G*) and phase angle (δ) are calculated automatically as part of the operation of the rheometer using a proprietary computer software supplied by the instrument manufacturer. The complex shear modulus and the phase angle are defined as the resistance to shear deformation of the binder in the linear viscoelastic region.

3.2.1.2 Bending Beam Rheometer Test

The BBR is used to perform low-temperature creep tests on thin beams of asphalt binders conditioned at the desired temperature for one hour *(AASHTO T-313, 2006)*. The asphalt beam (101.6x12.5x6.25mm) is tested in a three-point bending configuration. A constant load is applied instantaneously and maintained for all the duration of the test (240s) while the deflection at the mid span of the beam is continuously recorded (Figure 3.1).

FIGURE 3.1 BBR Testing Setup for Binders.

Correspondence principle and elastic solution for a simply supported beam are used to obtain the creep compliance. The creep stiffness, *S(t)*, equal to the inverse of the creep compliance, *D(t)*, is calculated as:

$$S(t) = \frac{\sigma}{\varepsilon(t)} = \frac{P \cdot l^3}{4 \cdot b \cdot h^3 \cdot \delta(t)} \tag{1}$$

where

S(t)	flexural creep stiffness, function of time,
σ	maximum bending stress in the beam, MPa,
$\varepsilon(t)$	bending strain (mm/mm), function of time,
P	constant load = 980±50mN ,
l	length of specimen (101.6mm),
b	width of specimen (12.7mm),
h	height of specimen (6.35mm),
$\delta(t)$	deflection at the midspan of the beam at time t, and

t time.

The m-value which is the slope of log stiffness versus log time curve is computed according to:

$$m(t) = \left| \frac{d \log S(t)}{d \log(t)} \right| \quad [2]$$

Both stiffness and the m-value are used to determine the critical temperature.

3.2.2 Asphalt Mixture Testing

Low-temperature creep and strength properties of asphalt mixtures are obtained using the Indirect Tension Tester (IDT) performed on cylindrical specimens loaded in compression along the diameter *(AASHTO)*. Due to the localized effect of the sealant at the surface of the pavement, in this study, a BBR-Pro device was used to obtain the creep and strength properties of asphalt mixtures, which allows testing of miniature mixture beams of different layers, see Figure 1. This approach is more suitable to check the level of penetration and effect of the sealant by testing beams from the various depth of the obtained cores. The approach is based on two testing methods developed by Marasteanu et al. *(Marasteanu et al., 2009 and 2012)* using a modified Bending Beam Rheometer (BBR) called BBR Pro. This method can be used to investigate the effect of surface aging, microcracking, and compaction on the mechanical properties of asphalt pavements by testing thin layers of asphalt mixtures recovered from different depths, which is not possible with the current IDT procedure. The testing procedures are described in detail elsewhere *(Marasteanu et al, 2009; Velasquesz et al., 2010)*. An example of a BBR asphalt mixture beam is shown in Figure 3.2, while Figure 3.3 shows the steps required to prepare mixture beams from a cylindrical specimen or core.

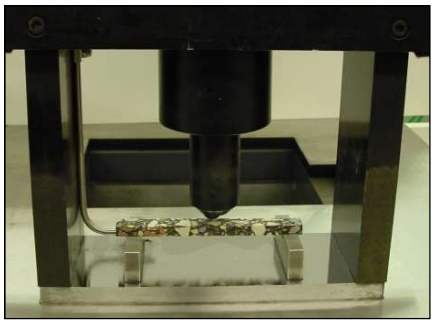

FIGURE 3.2 Bending Beam Rheometer with thin asphalt mixture (Marasteanu et al., 2009).

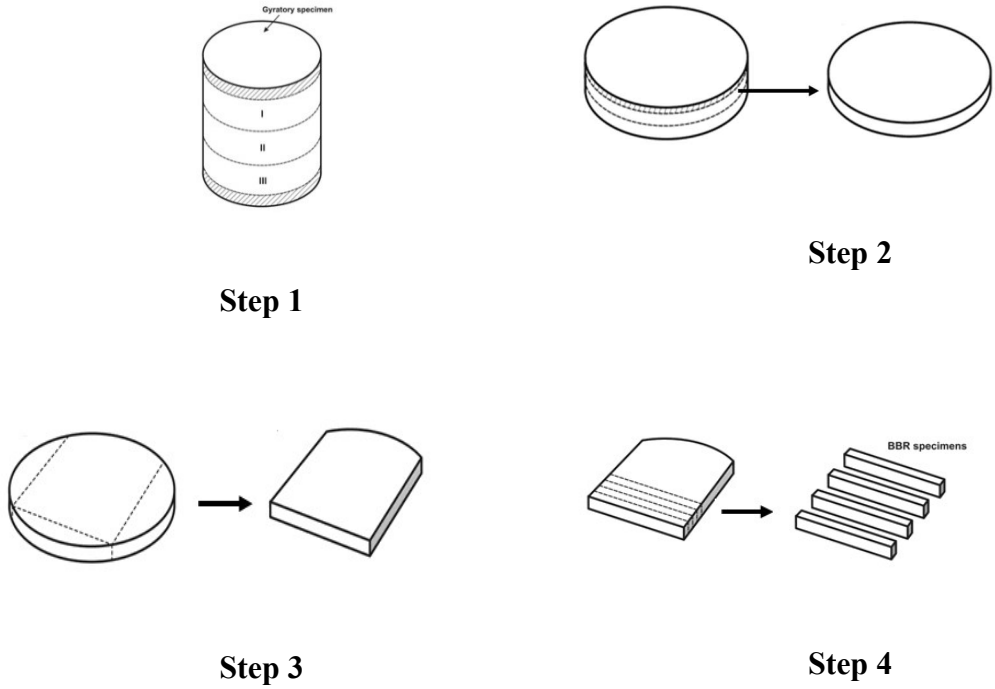

FIGURE 3.3 Asphalt Mixture Beam Preparation (Marasteanu et al., 2009).

BBR creep tests with duration of 500 sec followed by a recovery period of 500 sec were performed on all samples. For samples undergoing both creep and strength test, at the end of the recovery period, ramp loading at a constant loading rate was applied until the beams broke. The rate was chosen such that a load of 43N was obtained in 150 sec. Since asphalt mixtures are less

temperature susceptible than asphalt binder, all testing was done in chilled air in the BBR bath at -24ºC and -12ºC. A total of 576 beams were tested using 3 replicates from each layer for each core of each treated and control sections. Both asphalt binders and asphalt mixtures from the field projects were used in the investigation. A PG 58-28 binder used in the construction project was used in the experimental work, which included rheological methods such as Dynamic Shear Rheometer (DSR) and Bending Beam Rheometer (BBR) to investigate the high, intermediate and low-temperature properties of both treated and untreated binders. For asphalt mixture, field cores were obtained from both the control and sealant-treated pavement sections, and asphalt mixture beam specimens were prepared to be tested using BBR.

3.3 Summary

BBR creep tests, with a duration of 500 sec followed by a recovery period of 500 sec, were performed on all samples. For samples that underwent both creep and strength tests, ramp loading at a constant rate was applied at the end of the recovery period until the beams broke. The rate was chosen such that a load of 43N was obtained in 150 sec. Since asphalt mixtures are less temperature susceptible than asphalt binders, all testing was done in chilled air in the BBR bath at -24ºC and -12ºC. A total of 576 beams were tested using 3 replicates from each layer for each core of treated and control sections.

Chapter 4: ASPHALT BINDER TESTING

4.1 Introduction

In Chapter 4, the asphalt binders sample preparation methods are discussed, and the results of the rheological testing are presented. One asphalt binder, a PG58-28, was used as a control and four types of sealants were applied using different methods and rates.

4.2 Asphalt Binder Sample Preparation

For laboratory testing, it is important to identify the amount of sealant applied to the binder. This is necessary to be able to simulate actual field conditions in which the sealant is applied on the surface of the pavement. Two key parameters are needed to determine this amount. The first one is the application rate used in the field, and the second one is the penetration depth of the seal into the asphalt layer.

4.2.1 Determination of Sealant Application Rate

Two methods are used to determine the application rate of bio-seal treatments. In one method, nonwoven geotextile pads are used to measure the application rates. In this method, 2ft by 2ft square pads were weighed before and after the seal application. The application rate was converted to gallons per square yard using the measured specific gravity from field samples. In the other method, gallons applied to the treated area are determined by measuring the size of the treated section with a foot meter, and obtaining the volume of the treatment from the distributor truck metering system. In this research effort, this latter method was used since the information provided by MnDOT followed this method.

To obtain the penetration depth, a literature search was conducted. It was found that according to the manufacturers of the products BioSeal's product Biorestor adds agricultural oils and polymers to the asphalt cement in the top 1/2" of the pavement and RePlay Penetrates deep into asphalt (2-3 cm) *(BioSpan Technology, 2010)*.

Based on the application rates provided by MnDOT and penetration information from literature, the amount of seal to be added to the asphalt binder was calculated as follows. In all calculations, it was assumed that the asphalt mixture contained 5% binder (by weight) and 95% aggregates. The specific gravity of aggregates was assumed to be 2400kg/m3. Based on the penetration amount of literature, the weight of aggregate affected by sealant per surface area was calculated followed by the calculation of affected binder-weight (Column 7 and 8 of Table 4.1). The results are presented in Table 4.1, and the calculation steps are listed in table 4.2.

TABLE 4.1 Calculation of Seal Amount as a Percent of Binder Weight

1	2			3	4	5	6	7	8	9
Section (Target Rate)	Gallons	Area (ft^2)	Gallons/ yd^2	Penetration depth (from literature) inch	Spraying Rate liter/m^2	Sealant Density kg/liter	Sealant Weight kg/m^2	Aggregate Weight kg/m^2	Binder Weight kg/m^2	Percent Sealant (by weight)
OB1 A(0.020)	35.4	16080	0.02	1.18	0.09	0.80	0.07	71.93	3.60	2.0
OB1 B(0.020)										
OB2_a A(0.015)	37.78 x 42.9%	9366	0.015	0.5	0.07	0.80	0.06	30.48	1.52	3.7
OB2_b B(0.015)										
OB2_b C(0.020)	37.78 x 57.1%	9282	0.021	0.5	0.09	0.80	0.08	30.48	1.52	5.0
OB2_b D(0.020)										
E1 (0.10)	77.8	7000	0.1	unknown	0.45	0.9	0.41	Depends on penetration		
WB1 A(0.08)	180	22193	0.073	unknown	0.33	0.95	0.31	Depends on penetration		
WB2 B(0.08)										

TABLE 4.2 Calculation Steps of Table 4.1

Calculation Steps of Table 4.1	
Column 3=	obtained from the literature
Column 4=	Column 7 * 4.52731481 (to convert from Gallon/sq. y to Liter/sq. m)
Column 5=	Density of sealants was measured in lab

Column 6=	Column 4*Column 5
Column 7=	Density of Aggregate (assumed 2400kg/m^3) * Column 3 * 0.025 (to convert inch to m)
Column 8=	Column 7 * 5% binder(binder % from mix design)
Column 9=	Column 6/ Column 8

4.2.2 Application Procedure

There is no specific method to add sealants to a binder. A number of methods were developed in this investigation ranging from the direct mixing of hot binder and sealant to application of sealants to the surface of testing specimens. After the trial procedures of sample preparation described below, the sealants were applied to both RTFOT and PAV aged binder using two methods: simple mixing, and a laboratory-developed pipette method.

4.2.1.1 Mixing with heated binder

In this method, the RTFO-aged and PAV-aged, respectively, binders were heated at 150˚C and mixed with the four sealant products that were kept at room temperature. After 5 minutes of mixing, the samples were left at room temperature until the next day, when they were tested. Some authors used this mixing procedure in their laboratory investigations of rejuvenated binders *(Nahar et al., 2014; Lin et al., 2010; Yang et al., 2014)*. A fixed amount sealant representing 4% by binder weight was used based on the data in Table 4.1, in which the percent varied from 2% to 5% for OB1 and OB2 to match the field application rate. The amount for WB1 and E1 could not be calculated due to lack of information on their penetration from literature (Table 4.1). As a consequence, an intermediate amount of 4% was selected for all sealants to maintain consistency. The boiling liquid was observed forming when the WB1 was added to the heated binder, see Figure 4.1. The addition of Ob1 resulted in a very sticky and odorous mixture.

FIGURE 4.1 Mixing WB1 and Heated Binder.

In this mixing procedure, the exact amount of the applied seal is known. However, this procedure does not simulate actual field conditions. As a consequence, besides using this procedure, it was necessary to develop another method of sample preparation which can closely mimic the field application. The pipette method was developed and considered another way of sample preparation for this study after going through some trial procedures like spraying and brushing. The detail description is given below.

4.2.1.2 Spraying

In the actual field, the sealants were applied using a spraying truck. To simulate the spraying, in this method, the sealant was applied to the DSR and BBR testing specimens using a small spraying bottle. The weight of one spray was calculated to be approximately 0.015gm. This was done by weighing the bottle before and after one spray. The specimens were kept for 72 hours at room temperature (Figure 4.2) and tested. Spraying allows the seal to disperse on the surface of the sample, which damages the surface. As a result, the method was found unsuitable to use for further investigation.

FIGURE 4.2 DSR large plate specimen after 72 hours from spraying the sealant.

4.2.1.3 Brushing

When the spraying method didn't work, the brush was thought to be used as an alternative medium to apply sealant. In this method, the sealant was applied using a brush. The amount of sealant to be applied was determined using sealant weight (kg/m2) from Table 4.1 and multiplying by the DSR sample surface area. In the case of brushing, it is impossible to control the amount applied since the absorbing capacity of the brush was unknown. The condition of the DSR specimen 72 hours after brushing is shown in Figure 4.3. In this procedure, it is difficult to control the amount of seal applied to the surface since the brush absorbs some seal as well and the sample surface gets distorted.

FIGURE 4.3 DSR_large plate specimen after 72 hours from brushing.

After failing to use spraying and brushing methods, pipette method was introduced overcoming the issues of the inability of controlling the exact amount of sealant application and sample surface distortion.

4.2.1.4 Pipette Method

In the pipette procedure, the sealant is applied with a measuring pipette to control the number of drops and then spread on the surface of the DSR and BBR specimens using a plastic non-absorbent strip (Figure 4.4). The density for all sealants was calculated to be around 0.80 kg/liter. The measuring dropper counts 0.5 ml for 25 drops. Therefore, each drop measures 0.016 gm. Based on the field application rate (provided in Table 4.1) and laboratory sample surface area, the number of drops to be applied were calculated. Table 4.3 contains detailed information on the number of drops to be applied on binder sample based on surface area for both 2% and 4% sealant by binder weight. The detail calculation step is provided in Table 4.4. Two drops were applied to the DSR large plate and one drop to the DSR small plate specimen, respectively based on the calculation described in Table 4.3 for both application rate of 2% and 4% sealant of binder weight. The number of drops used to treat the beams was 8 for 2% sealant by binder weight which simulates the spraying rate of 0.02 gallon/sy in the field. Since the BBR beam sample has significant surface area compared to DSR sample, the number of drops calculated for 4% sealant by binder weight is 15 which simulates the spraying rate of 0.045 gallon/sy. Sixteen drops were used instead of 15 drops as the double of 8 drops. PAV-aged binder beams were tested using only 8 drops. Since the asphalt mixtures in the field sections were less than 2 years old at the time the cores were collected, additional BBR testing was performed on the RTFO-aged binder, treated using 8, 16 and 32 drops. This was done to try and better match the aging condition of the binders and mixtures. The DSR samples were tested after 3 days and 48 days from the application of the sealant, whereas, the BBR samples were tested after 3 days of sealant application. The DSR samples were stored in the freezer at 4ºC for being tested after 48 days. For testing after 3 days, the DSR samples and BBR samples were kept at the room temperature. This pipette method was observed to be the most suitable method since it can

closely mimic the field application procedure and thus this method was used for further investigation.

TABLE 4.3 Calculation of Number of Drops for Binder Sample

1	2		3	4	5	6	7	8	9	10	11	12
Sample type	DSR Sample Diameter		Sample surface area	Binder Weight Table 4.1	Binder Weight	Weight per drop	Weight Sealant per sample	Drops per sample (calc.)	Drops per sample (applied)	Weight Sealant per sample	Drops per sample (calc.)	Drops per sample (applied)
	mm						2% Sealant (Binder Weight)			4% Sealant (Binder Weight)		
	Actual	Tested	mm^2	kg/m_2	kg	gm	gm			gm		
DSR large pl.	25	18	254.47	3.60	0.0009	0.016	0.018	1.15	2	0.037	2.29	2
DSR small pl.	8	10	78.54		0.0003		0.006	0.35	1	0.011	0.71	1
BBR Beam			1587.50		0.0057		0.114	7.14	8	0.229	14.29	16

TABLE 4. 4 Calculation Steps of Table 4.3

Column 4=	Binder weight per surface area affected by sealant application in the field, calculated in Table 4.1.
Column 5=	Column 3*Column 4/1000000
Column 6 =	Measured in the laboratory
Column 7=	Column 5 *1000* 2% (OB1) (from Table 4.1 column 9)
Column 8=	Column 7/ Column 6
Column 9=	rounding up Column 8 to the nearest number
Column 10=	Column 5 * 1000*4% (OB2) (from Table 4.1 column 9)
Column 11=	Column 10/ Column 6
Column 12=	rounding up Column 11 to the nearest number

FIGURE 4.4 Sample Preparation Using Pipette Method.

A flow chart of the testing plan of the proposed study is presented in Figure 4.5.

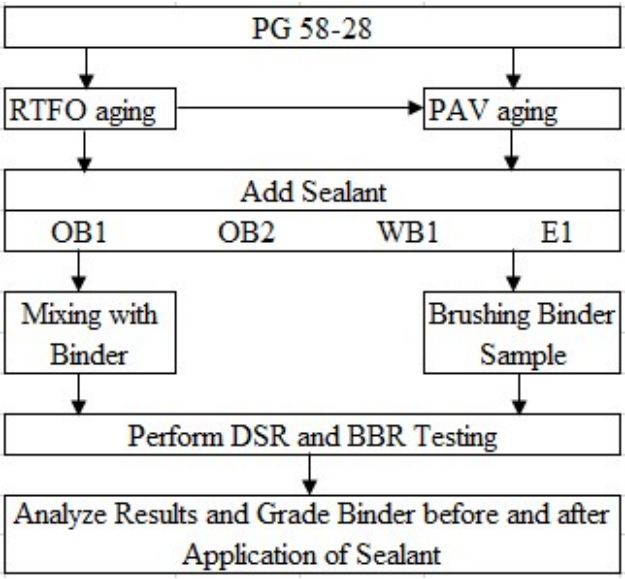

FIGURE 4.5 Testing Plan of Asphalt Binder.

4.3 Rheological Master Curves

Frequency sweeps were performed in 6°C increments from 4°C to 70°C using Dynamic Shear Rheometer. Small plate geometry was used for tests performed from 4°C to 34°C, and large plate geometry was used for testing from 34°C to 70°C.

Examples of |G*| master curves generated at a reference temperature of 22°C are shown in Figures 4.6 to 4.10. Upon aging, the master curve shifts toward higher complex modulus values (Figure 4.6). The addition of oil-based-sealants shifts the master curve of the blend back to lower values, as intended and reported by other studies (*Nahar et al., 2014; Shen et al., 2007; Zaumanis et al., 2013*). Several trends can be observed by visual inspection. In RTFOT case, OB2 produces the most significant changes (softening) of the original binder. OB1 comes in as second. However, for PAV binders, OB1 produces the most significant softening. These changes are more significant when the simple mixing procedure is used, as expected (Figure 4.6 and 4.8). For pipette, both OB1 and OB2 produce the most softening effect. Simple mixing procedure exhibited more softening effect than

pipette method because of blending hot binder with sealant, whereas in pipette method the softening effects depended on the penetration rate of the sealant (Figure 4.7 and 4.9).

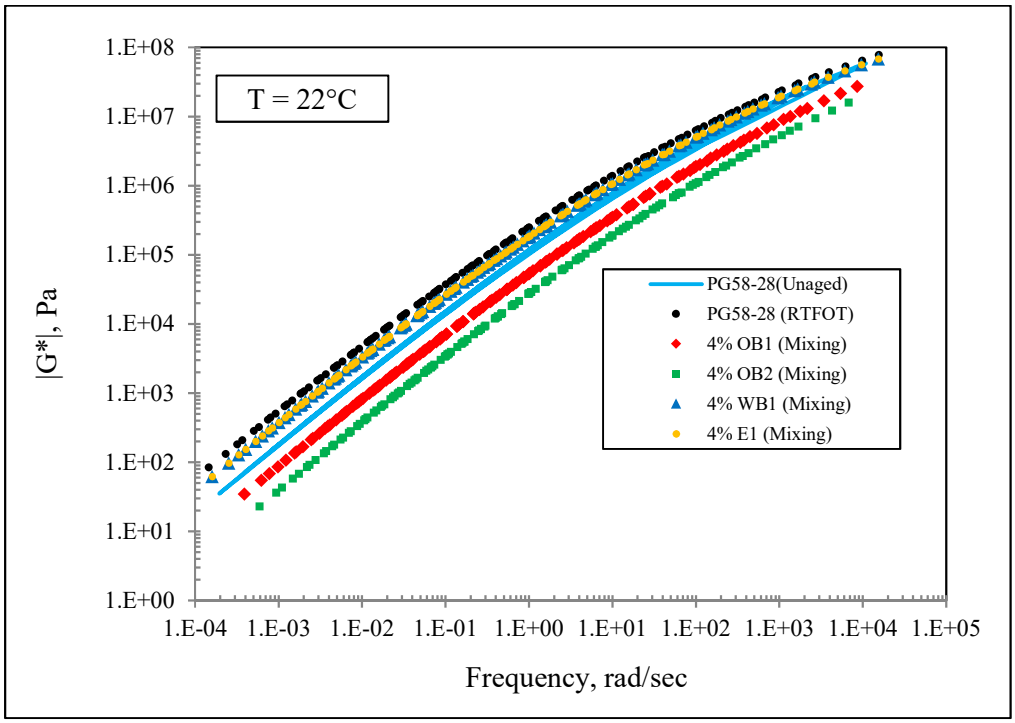

FIGURE 4.6 |G*| Master Curves for RTFOT and Simple Mixing Procedure.

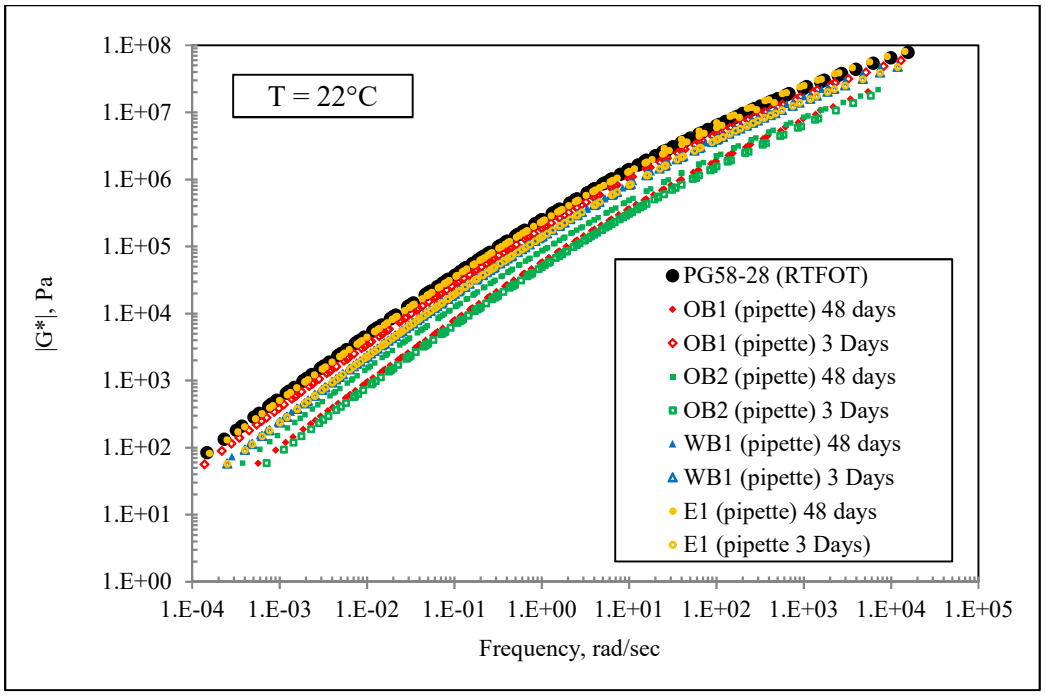

FIGURE 4.7 |G*| Master Curves for RTFOT and Pipette Method.

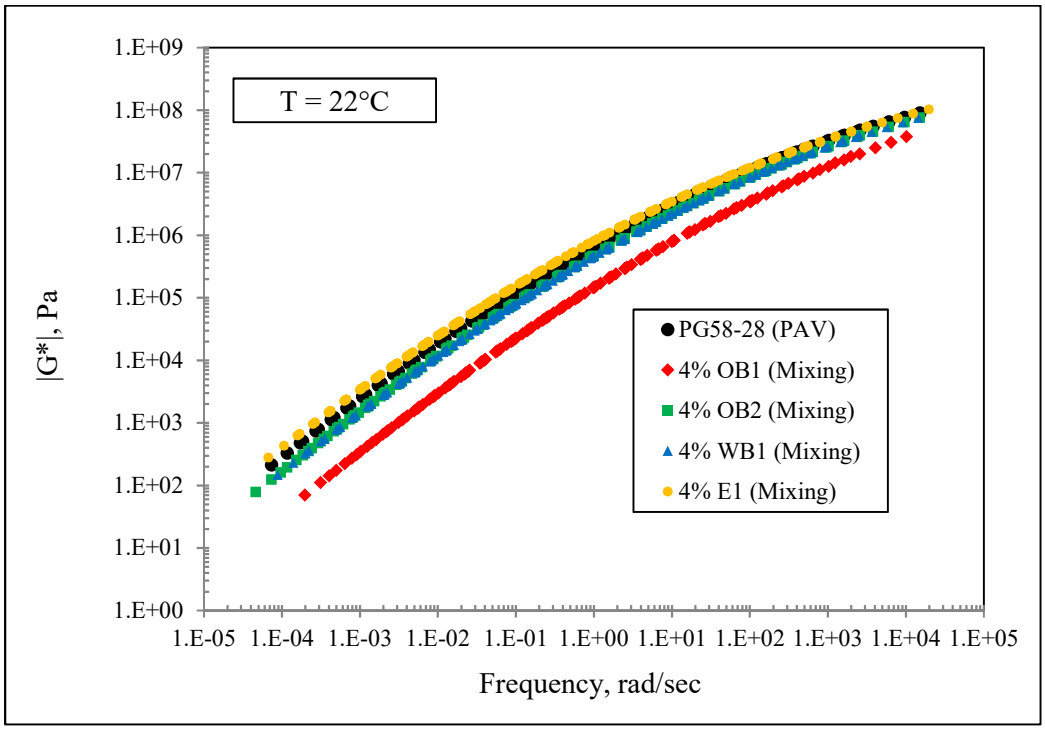

FIGURE 4.8 |G*| Master Curves for PAV and Simple Mixing Procedure.

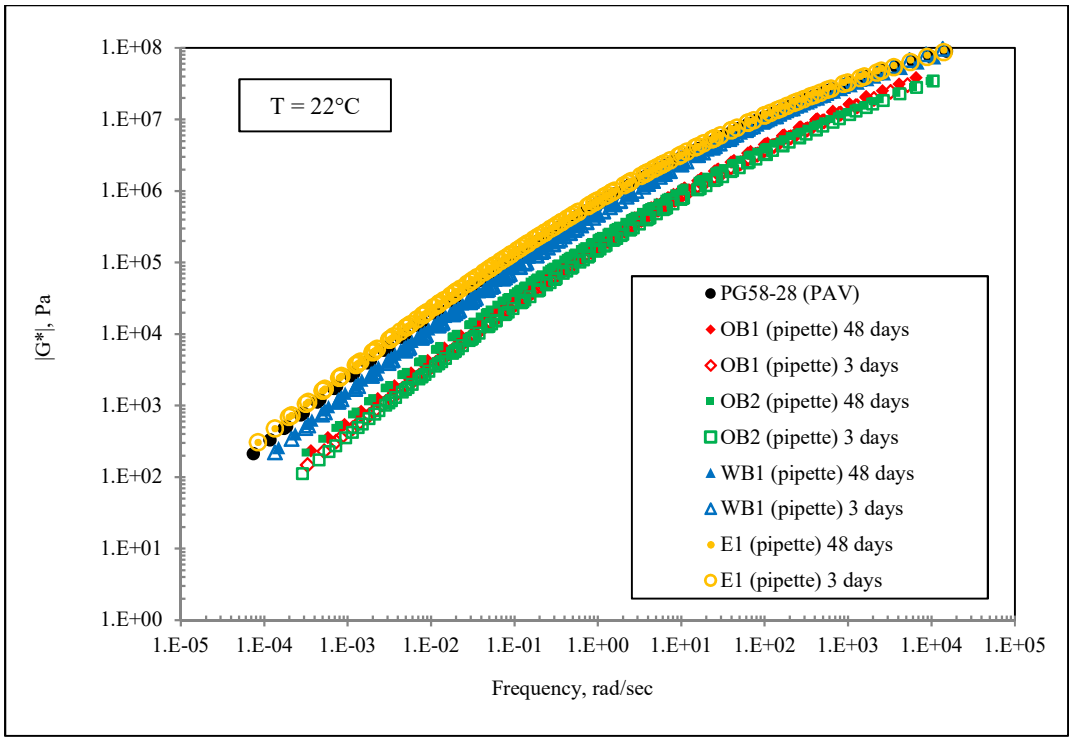

FIGURE 4.9 |G*| Master Curves for PAV and Pipette Method.

The results of applying the seal by brushing and by spraying on the surface of a prepared DSR large plate sample of the PAV-aged binder are presented in Figure 4.10. These two methods were abandoned due to poor control of application weight.

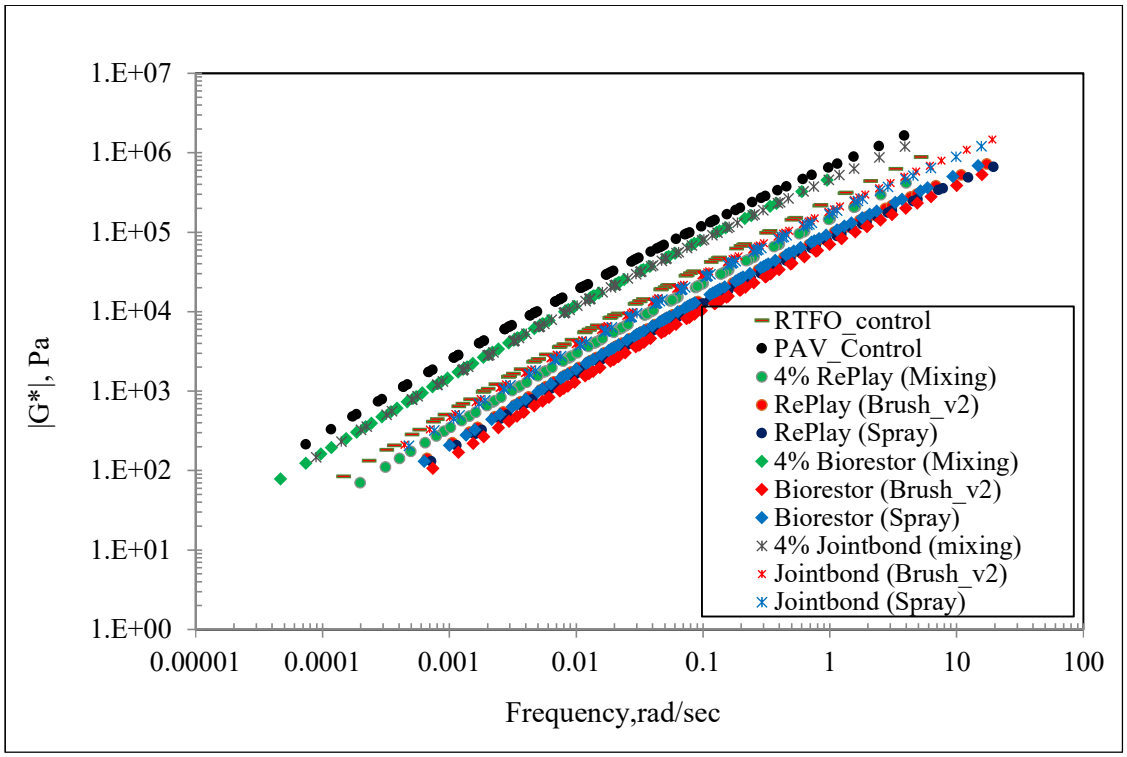

FIGURE 4.10 DSR Master Curve (Large Plate) of PAV-aged PG 58-28 for Three Different Procedures.

4.4 Performance Grade Specification Criteria

To better understand the effect of sealants to the properties of the PG58-28 asphalt binder, calculations were performed to determine the specific changes in the low, intermediate, and high temperature criteria used to obtain the performance grade of the binder. The performance grade (PG) of the virgin and blended binders was determined in accordance with AASHTO M320. The following plots represent the change in rutting factor, fatigue factor, stiffness, and m-value due to different application procedure as well as different storage time for different sealants (Figure 6.1-). The plots show that for the mixing procedure, oil-based OB1 and OB2 have a very significant effect comparing with the control binder and binder treated with WB1 or E1. The application of water-based WB1 and E1 don't bring any major changes in the rutting parameter compared with the control binder.

4.4.1 Rutting Factor

The changes in rutting factor with temperature due to different sample preparation and storage time are presented through Figures 4.11 to 4.14. Figure 4.15 shows the comparison of the RTFOT |G*|/sin δ values at 58°C. It can be observed that the largest change occurs for the OB1 and OB2 sealants when simple mixing is used. The reduction in the rutting factor is almost three-fold. It can also be observed that mixing procedure results in more significant changes compared to the pipette procedure. The 3-day and 48-day results also appear to indicate that the softening effect of the sealant application decreases with time. The results are also shown in Table 4.5. Similar observation of softening effect and reduction in rutting resistance were also reported by other researchers when they compared rheological properties of control binder with oil-based rejuvenator treated binders (*Mogawer et al.,2013; Lin et al., 2013, Shen et al., 2007*).

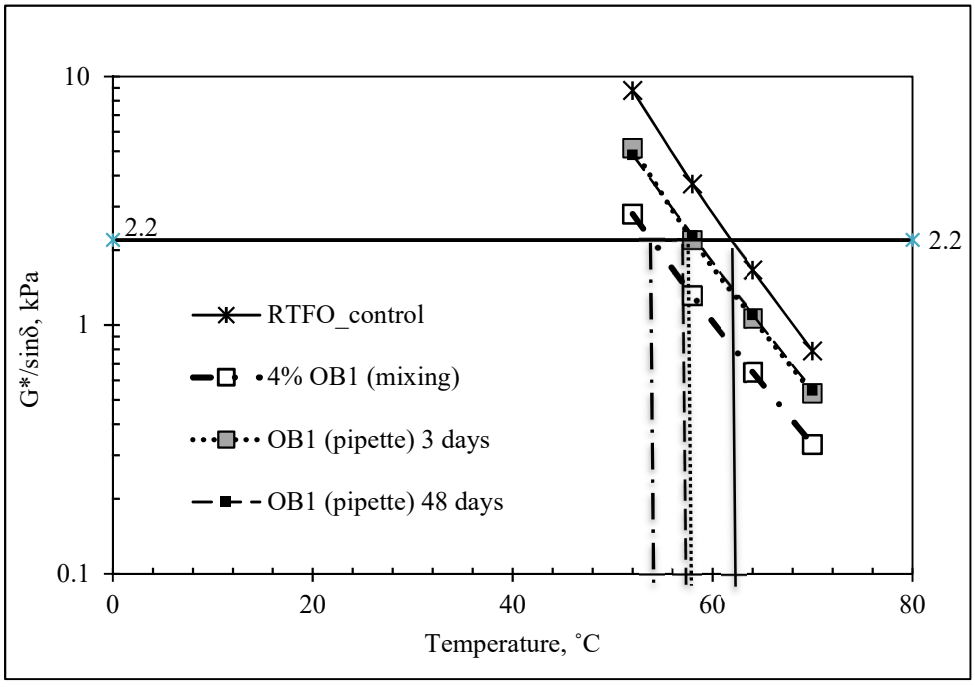

FIGURE 4.11 Change in Rutting Factor of Binder Treated with OB1 due to Different Application Process and Storage Time.

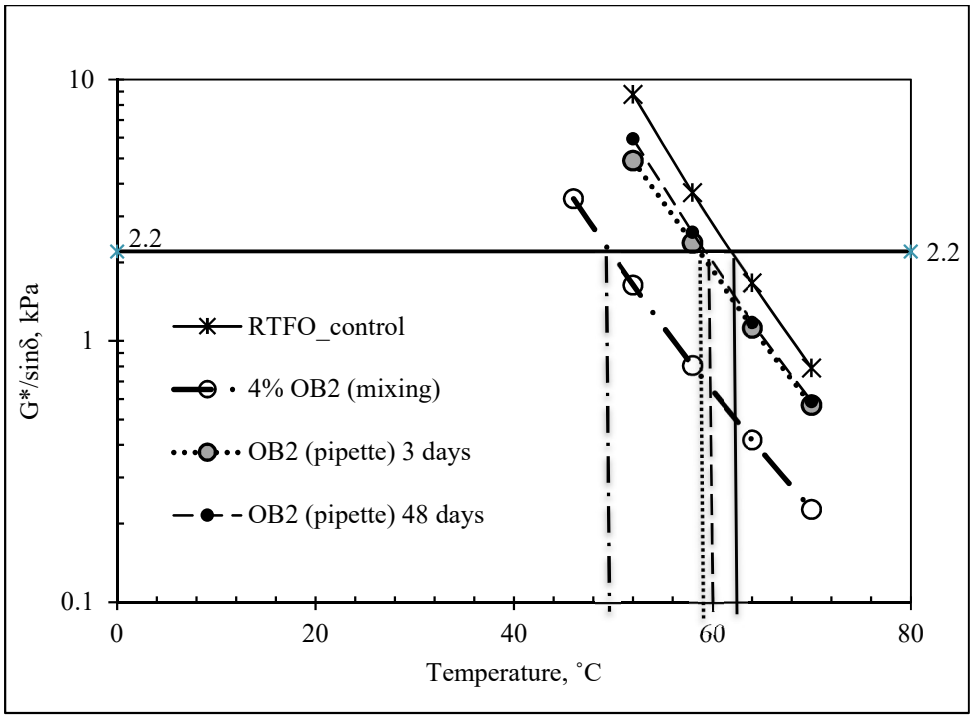

FIGURE 4.12 Change in Rutting Factor of Binder Treated with OB2 due to Different Application Process and Storage Time.

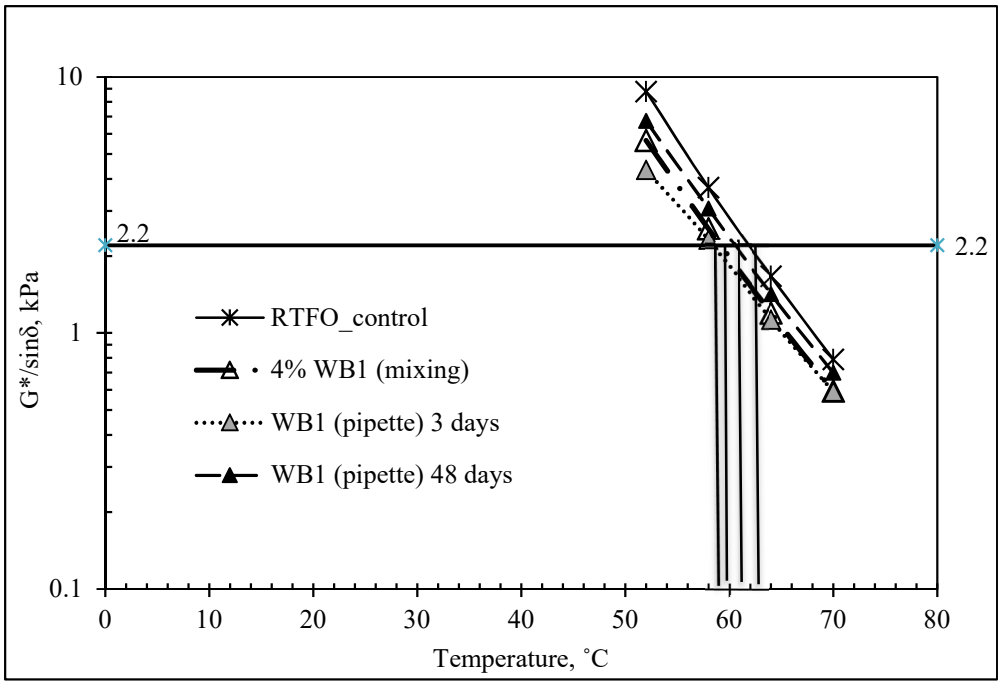

FIGURE 4.13 Change in Rutting Factor of Binder Treated with WB1 due to Different Application Process and Storage Time.

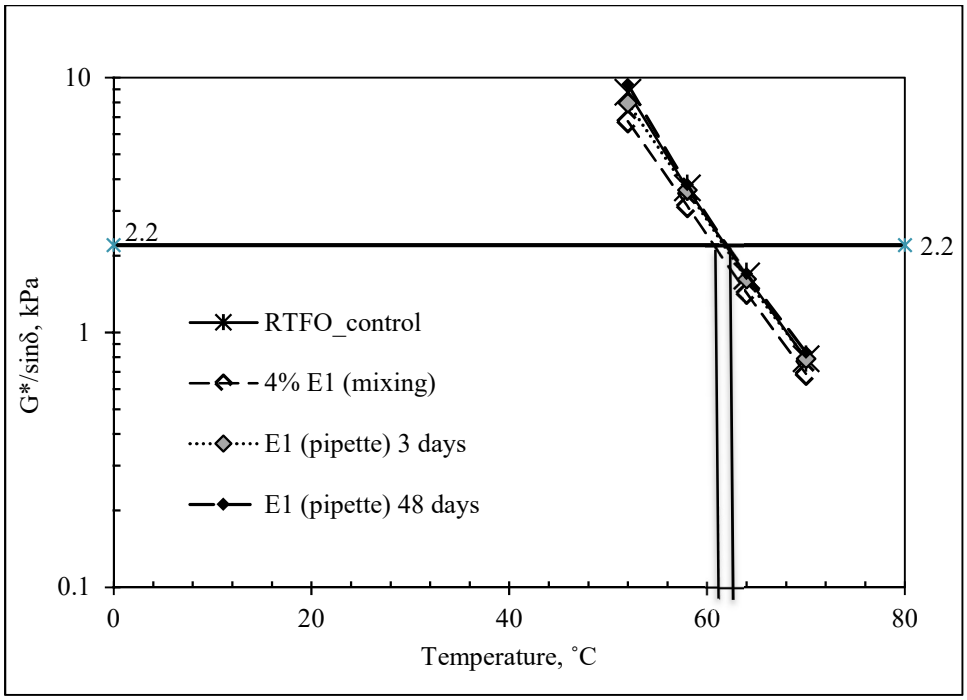

FIGURE 4.14 Change in Rutting Factor of Binder Treated with E1 due to Different Application Process and Storage Time.

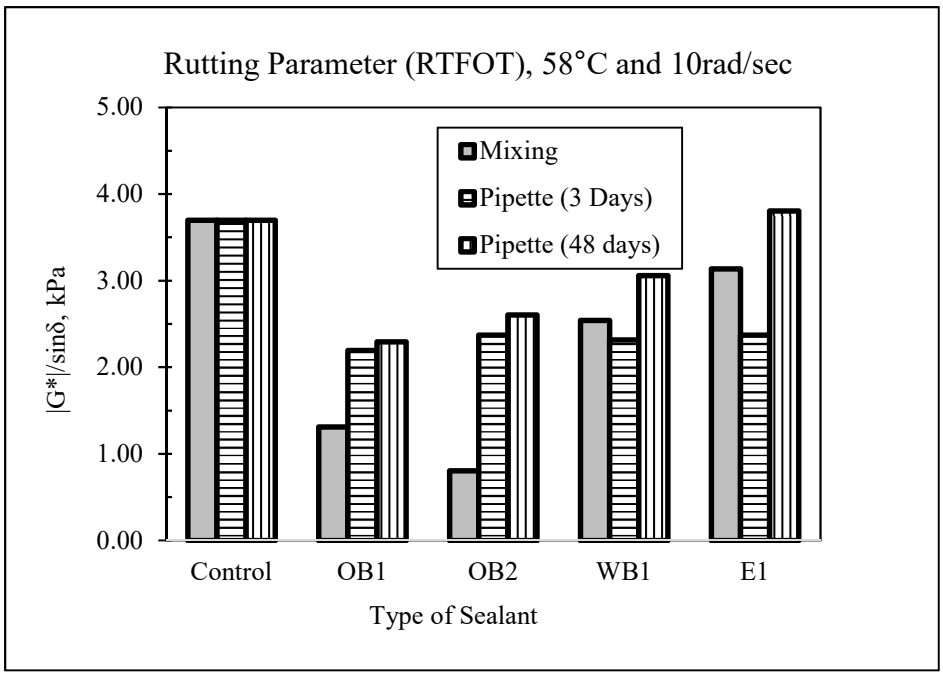

FIGURE 4.15 RTFOT |G*|/sinδ Results at 58°C.

TABLE 4.5 RTFOT Rutting Factor, |G*| and Phase Angle at 58ºC and 10rad/s

Specimen	Application Procedure	Rutting Factor (|G*|/sin δ), kPa	|G*| kPa	Phase Angle degrees
Control		3.70	3673	83.49
OB1	Mixing	1.31	1308	85.85
	Pipette(3 days)	2.19	2182	83.96
	Pipette(48 days)	2.29	2281	84.44
OB2	Mixing	0.80	802.2	86.60
	Pipette(3 days)	2.37	2360	84.44
	Pipette(48 days)	2.60	2590	84.19
WB1	Mixing	2.54	2539	84.40
	Pipette(3 days)	2.31	2304	84.77
	Pipette(48 days)	3.06	3042	83.95
E1	Mixing	3.14	3119	83.96
	Pipette(3 days)	2.37	3596	84.44
	Pipette(48 days)	3.80	3776	83.12

4.4.2 Fatigue Factor

For PG 58-28 binder, the fatigue factor is determined at 19ºC. Table 4.6 and Figure 4.16 show the fatigue properties at two different temperatures obtained from DSR testing, which is need for interpolating the fatigue factor at 19ºC.

TABLE 4.6 Fatigue Factor, |G*| and Phase Angle at 10rad/s

		16˚ C			22˚ C		
Specimen	Application Procedure	Fatigue Factor (|G*| x sin δ) kPa	|G*|, kPa	Phase Angle	Fatigue Factor (|G*| x sin δ) kPa	|G*|, kPa	Phase Angle
Control	No sealant	5614	7384	49.49	2418	2944	55.2
OB1	Mixing	1717	2038	57.41	683.1	774.2	61.92
	Pipette(3 days)	1694	2005	57.65	751.8	853.1	61.79
	Pipette(48 days)	2225	2648	57.17	890.1	1015	61.29
OB2	Mixing	1683	2006	57.04	670.8	763.8	61.43
	Pipette(3 days)	1564	1884	56.13	647.2	746	60.18
	Pipette(48 days)	1922	2425	52.42	846.3	1013	56.64
WB1	Mixing	4353	5554	51.6	1830	2175	57.29
	Pipette(3 days)	4927	6060	54.39	1994	2320	59.25
	Pipette(48 days)	4551	5787	51.86	1971	2347	57.1
E1	Mixing	6520	8863	47.36	2739	3428	53.04

	Pipette(3 days)	5728	7662	48.39	2603	3211	54.13
	Pipette(48 days)	6362	8468	48.71	2634	3238	54.45
Fatigue Criteria: |G*| x sin δ = maximum 5000 kPa at 19˚C for PG 58-28							

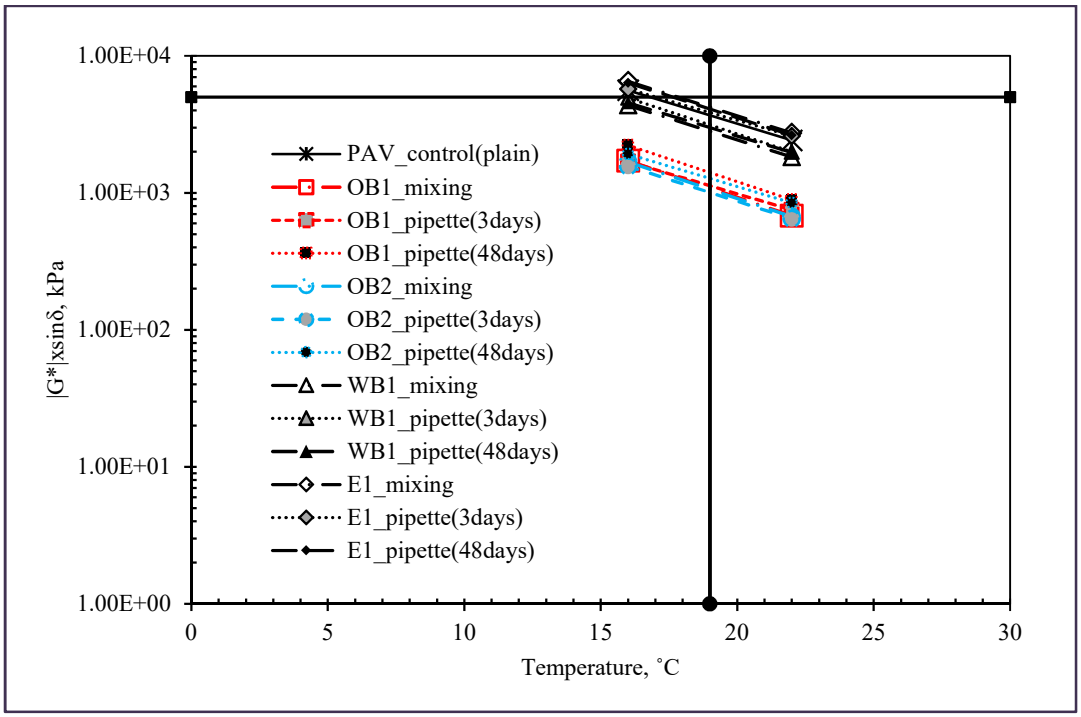

FIGURE 4.16 PAV |G*|sinδ Results at 19°C.

Figure 4.17 shows the changes in the fatigue PAV |G*|sin δ values at 19°C. The largest softening effect is again observed when OB1 and OB2 are simply mixed with the PAV binder. Less pronounced differences are observed between the different application procedures and the 3-day, and 48-day results indicate only a minimal reduction in the softening effect with time.

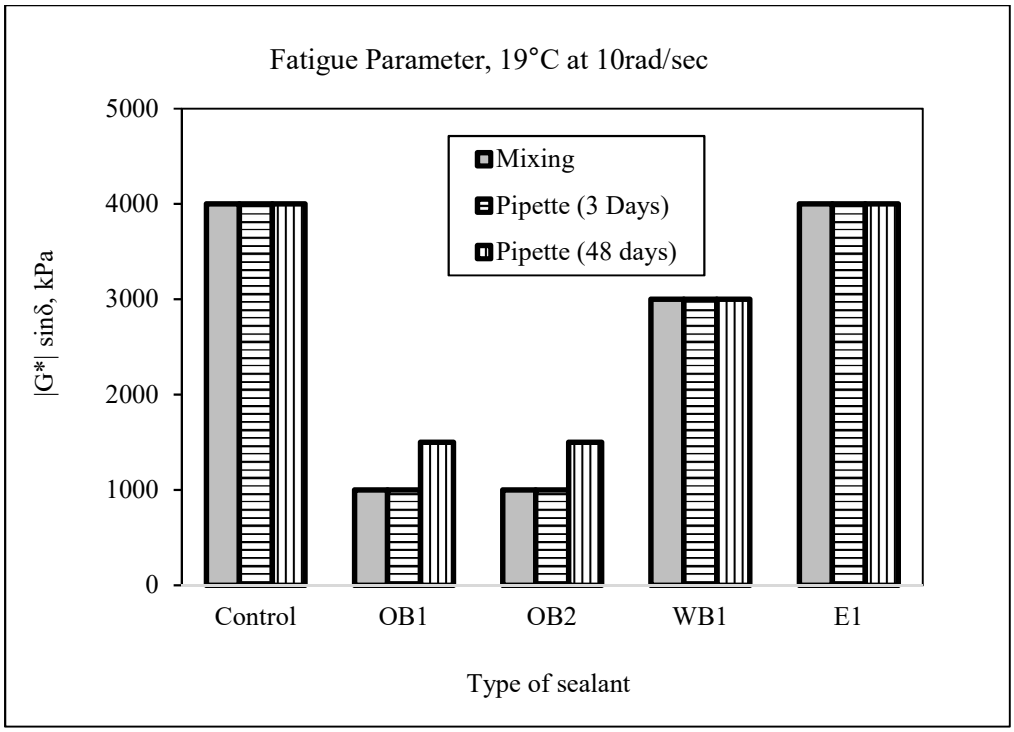

FIGURE 4.17 PAV |G*|sinδ Results at 19°C.

4.4.3 Creep Stiffness and m-value

For low-temperature characterization, all beams were tested first at -24°C. Based on the m-value and S results obtained at -24ºC, some materials were tested at -30ºC and some at -18ºC. As a consequence, the beams treated with OB1 and OB2 were eligible to be tested at -30ºC whereas, beams treated with WB1 and E1 were tested at -18ºC.

While there was no storing time for the beams prepared after sealant application using mixing procedure, for the pipette method, the BBR tests were performed after 3 days from sealant application. Lack of materials did not allow testing samples after 48 days. Also, it was quite challenging to store BBR samples for 48 days. The creep stiffness and m-value at 60sec using two different methods are presented in Table 4.7 and 4.8 for two different temperatures.

TABLE 4.7 Creep Stiffness and m-value at 60 sec using Pipette Method

Stiffness and m-value at 60sec (Pipette_3 days)							
PAV-aged PG 58-28 with Sealants	Temperature	Stiffness, S (MPa)			m-value		
	℃	Sample 1	Sample 2	avg	Sample 1	Sample 2	avg
Control	-18	187	185	186	0.378	0.356	0.367
	-24	436	457	446	0.301	0.296	0.298
OB1	-18	171	155	163	0.339	0.316	0.327
	-24	304	335	319	0.277	0.285	0.281
OB2	-18	163	195	179	0.363	0.358	0.361
	-24	349	360	354	0.286	0.289	0.287
WB1	-18	233	232	232	0.347	0.348	0.348
	-24	448	458	453	0.281	0.286	0.284
E1	-18	240	244	242	0.354	0.368	0.361
	-24	438	479	459	0.243	0.283	0.263

TABLE 4. 8 Creep Stiffness and m-value at 60 sec Using Mixing Method

Stiffness and m-value at 60 sec (Mixing)							
PG 58-28 (PAV-aged)	Temperature	Stiffness, S (MPa)			m-value		
	℃	Sample 1	Sample 2	Average	Sample 1	Sample 2	Average
Control	-24	436	457	447	0.301	0.296	0.299
	-18	187	185	186	0.378	0.356	0.367
OB1	-24	129	123	126	0.431	0.421	0.426
	-30	377	398	387	0.341	0.326	0.333
OB2	-24	158	134	146	0.406	0.398	0.402
	-30	400	318	359	0.314	0.276	0.295
WB1	-24	409	410	410	0.308	0.320	0.314
	-18	161	159	160	0.394	0.396	0.395
E1	-18	248	243	245	0.293	0.360	0.327
	-24	524	524	524	0.293	0.293	0.293

Figures 4.18-4.22 show the changes in the PAV BBR parameters S(60s) and m(60s), where S represents the creep stiffness, and m represents the slope of the creep stiffness versus time curve on a double logarithmic scale. The Figure 4.14 below shows the significant softening effect of oil-based OB1 and OB2 when using mixing procedure. Mixing procedure ensures a perfect blending of hot binder and the sealant which results in a large drop in stiffness.

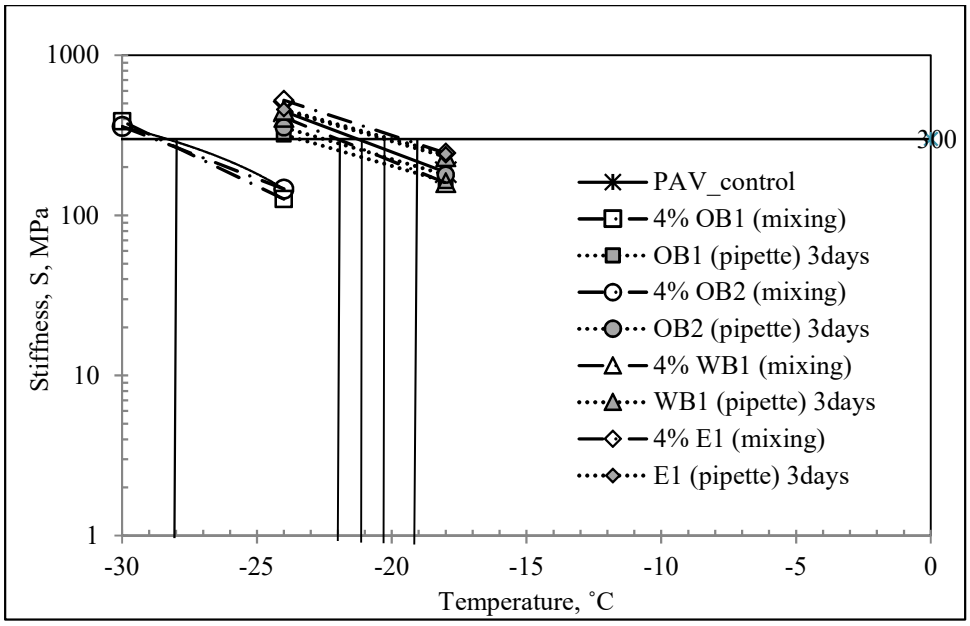

FIGURE 4.18 Change in Creep Stiffness due to Pipette Method.

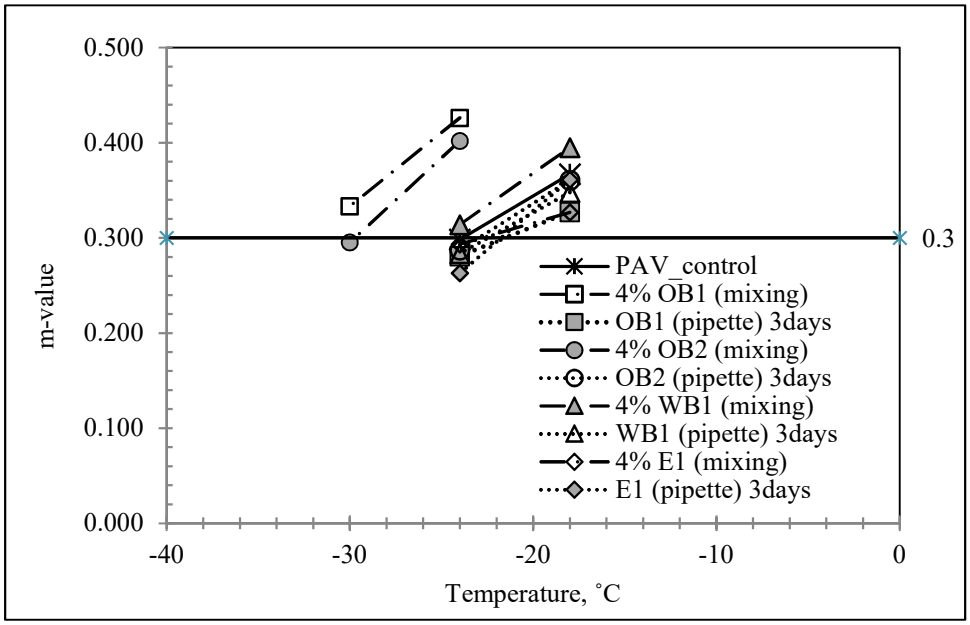

FIGURE 4.19 Change in m-value due to Pipette Method.

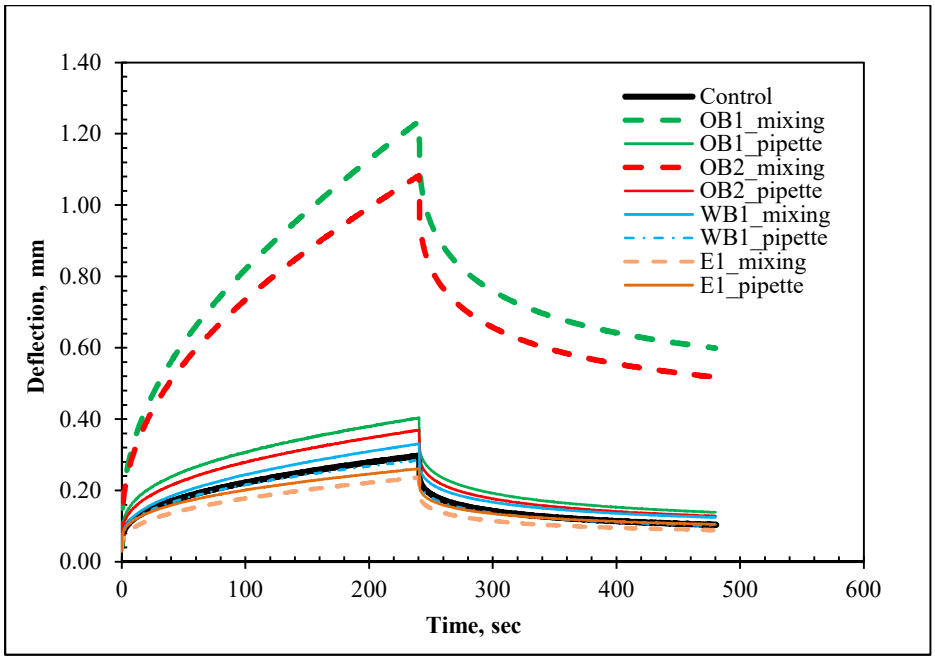

FIGURE 4.20 Deflection vs. Time for PAV-aged PG 58-28 at -24ºC.

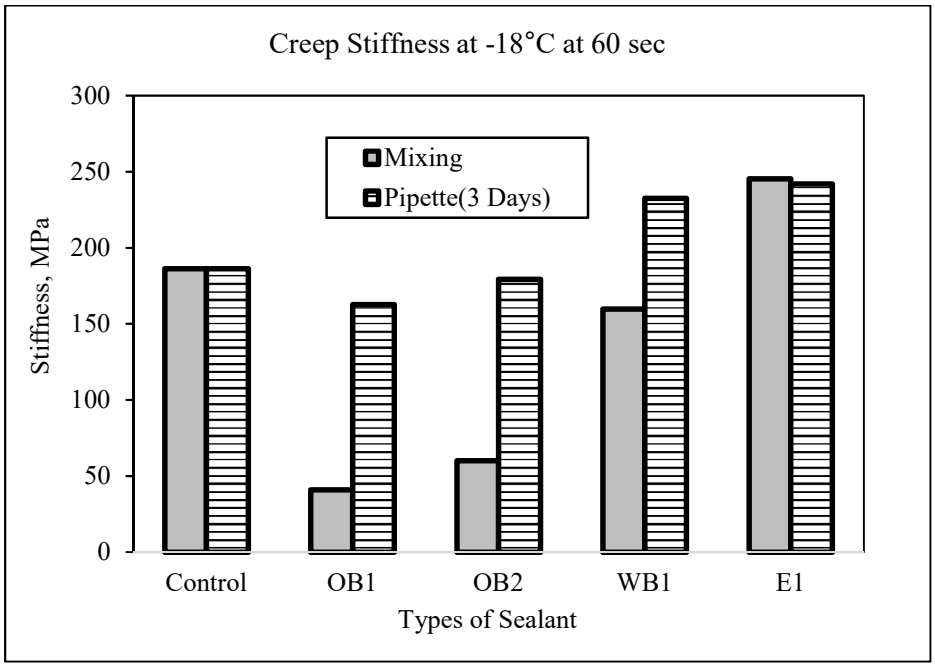

FIGURE 4.21 PAV S(the 60s) Results at -18°C.

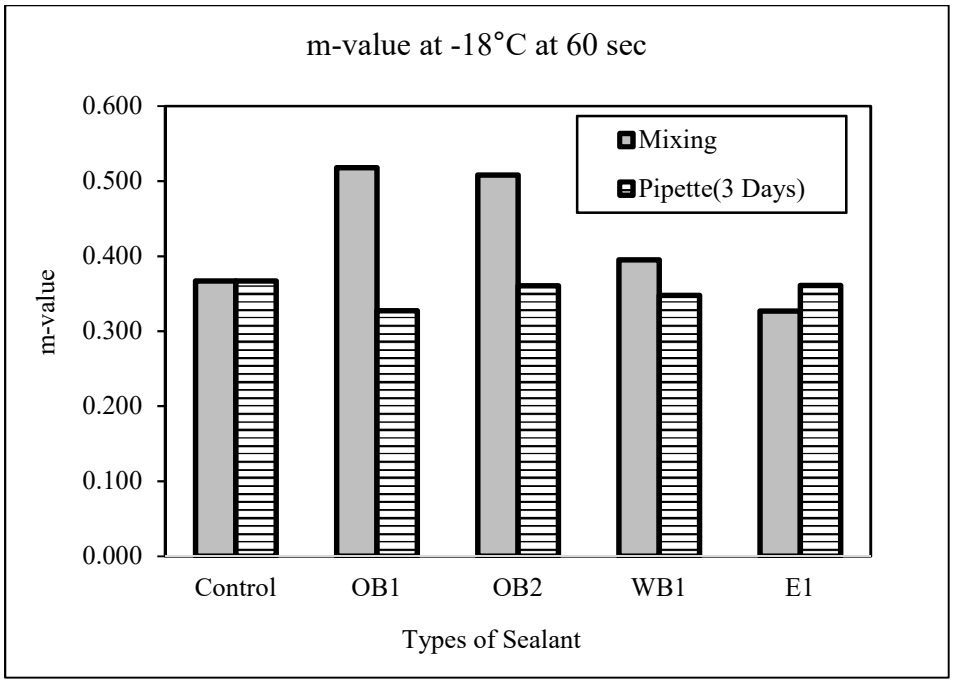

FIGURE 4.22 PAV m(60s) Results at -18°C.

The most significant reduction in creep stiffness is again observed for OB1 and OB2 and the simple mixing procedure. This change is accompanied, as expected by a significant increase in m-value. It is however noted that for the pipette method the changes are much less pronounced for both S and m-value. It is also interesting to observe the increase in stiffness achieved by the application of the emulsion, without a major decrease in m-value.

To better evaluate the changes produced by the application of sealants, the exact temperature values for the high and low failure criteria were tabulated rather than the specification temperatures (Table 4.9). The BBR tests were not conducted for 48 days due to difficulty in storing the beams.

TABLE 4.9 Change in Performance Grade

	Mixing 4%	**Pipette(3 days)**	**Pipette(48 days)**
Control PG 58-28	PG 62-31		
OB1	PG 54-38	PG 58-33	PG 58-…
OB2	PG 50-38	PG 58-32.5	PG 59-…
WB1	PG 59-31	PG 58-30	PG 61-…
E1	PG 61-29	PG 62-30	PG 62…

A number of important observations can be made. The simple mixing procedure results in significant changes in the PG of the original binder, a clear indication that this procedure cannot simulate the blending mechanisms that occur in field conditions.

4.5 Additional Binder Testing

Since low-temperature cracking is a phenomenon observed in the long-term aged pavement, the BBR test is performed on PAV-aged binders. However, in this project, the asphalt mixtures in the field sections were less than 2 years old at the time the cores were collected. As a consequence, additional BBR testing was performed on RTFO-aged binder at -24ºC, treated using the pipette method and three application rates (Figures 4.23 and 4.24). This was done to try and better match the aging condition of the binders and of the field mixtures. Four replicates were tested for each case and the average value discarding the outliers was reported. In all cases, increasing the application rate increased the stiffness of the treated binder, which is contrary to expectations for the oil based sealants. Surprisingly, the increase in stiffness is accompanied by increase the m-value, which is also contrary to expectations with an exception for E1 with 32 drops. However, the oil-based sealants (OB1 and OB2) still soften the binder comparing with the control binder regardless of the application rate.

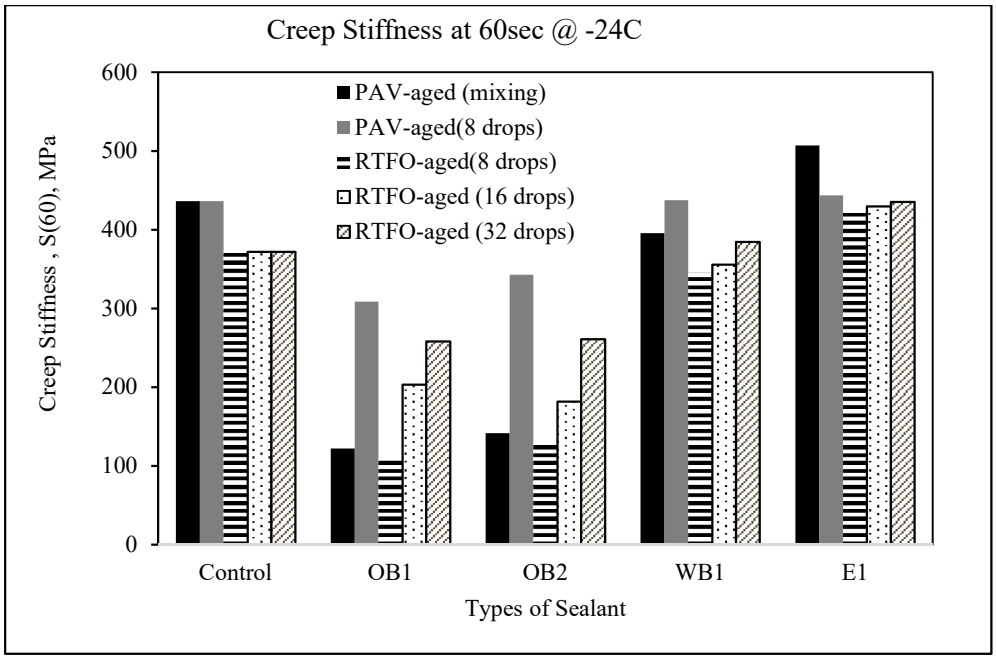

FIGURE 4.23 Change in Creep Stiffness due to PAV-aging, RTFOT-aging and Different Application Rate of the Sealant.

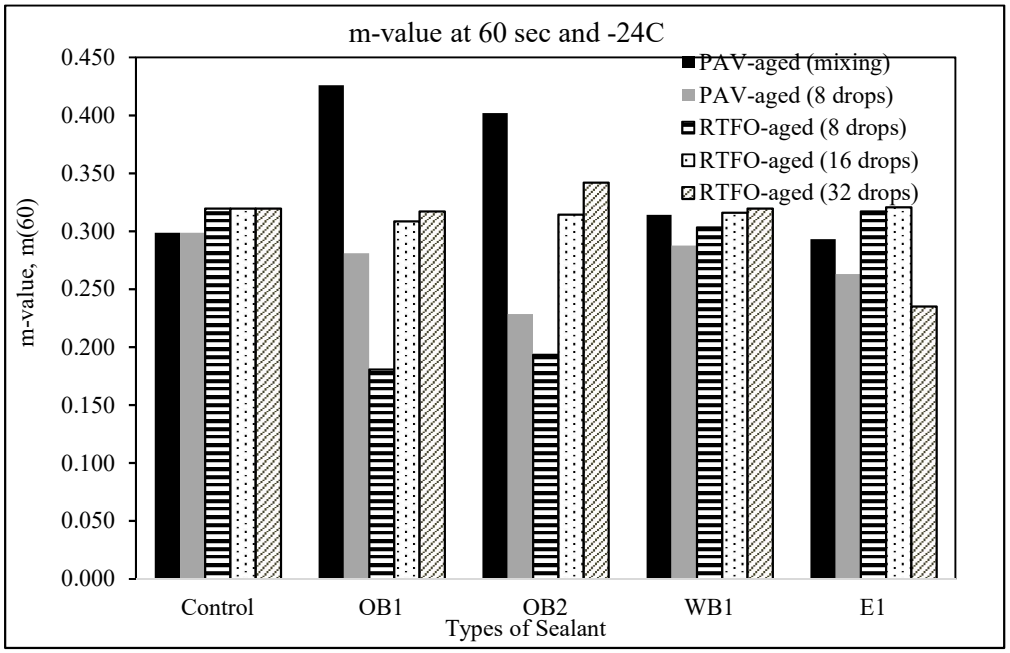

FIGURE 4.24 Change in m-value due to PAV-aging, RTFOT-aging and Different Application Rate of the Sealant.

4.6 Summary of Asphalt Binder Testing

The rheological properties of aged-asphalt binder before and after treatment were obtained by performing DSR and BBR tests in the laboratory. Two methods were used for applying sealant: simple-mixing and a laboratory-developed pipette method. The simple mixing method resulted in a significant softening effect, whereas the pipette method was found to be more realistic and closer to field observations. Application of oil-based sealants tends to increase rutting potential. Conversely, reduction in creep stiffness was observed in presence of oil-based sealants when compared to the control section which makes the binder less brittle and helps reduce low-temperature cracking. A more detailed analysis of the testing results is presented in Chapter 6.

Chapter 5: ASPHALT MIXTURE TESTING

5.1 Introduction

The sample preparation procedure, testing plan, and results obtained on asphalt mixture samples are discussed to evaluate the effectiveness of sealant application on asphalt mixture.

5.2 Asphalt Mixture Sample Preparation

5.2.1 Beam Cutting Process

Asphalt mixture beams were prepared according to the method presented in Chapter 3. This method includes several cutting steps from a gyratory compacted cylinder or field core to the actual BBR beams. In the 1st step, each core receives four horizontal cuts resulting in four layers of around 6 mm each, called a top, bottom, middle, and last. Each layer is then cut into six beams with the dimensions of approximately 1 =125.0mm, b=12.5mm, D=6.25mm.

Four field cores from each type of treated section along with the control section were collected. Initially, the cores were labelled according to the treatment they received with a random core numbering of 1, 2, and 3 for each type. The fourth core from all type of treated section was collected eight months later. The top 3 mm was removed from Core No. 1, 2 and 4 to obtain a smooth surface. However, for Core No. 3 the original top surface was not removed to compare the properties of the shaved and unshaved cores.

Four cores from each type were cut into 4 layers, horizontally. Each horizontal layer was then cut vertically to obtain 6 beams. As a result, a total of 576 small mixture beams were obtained from all the cores. The beams were measured after the cutting process. The width and thickness of the beams were measured in three different points using a standard laboratory caliper. The thickness measured ranged from 4.14 to 7.29 mm with a 6.69% of

the coefficient of variation and was plotted in Figure 5.1. A normal distribution of the measured values is observed.

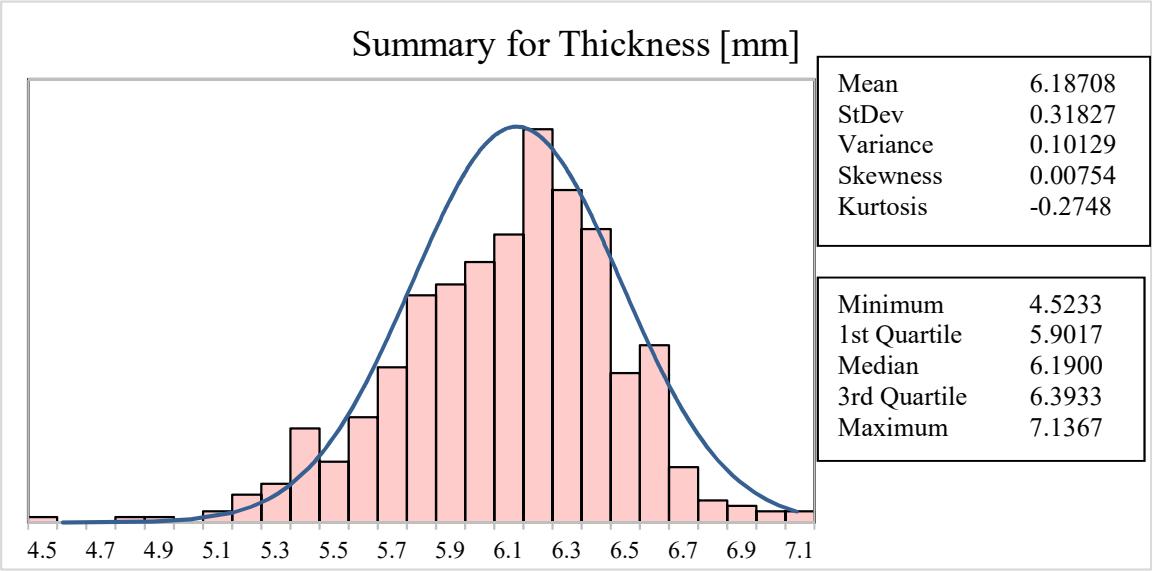

FIGURE 5.1 Statistics for BBR Mixture Beams Thickness.

The width of the beams had a low coefficient of variation of 1.32%. Width measured values ranged from 11.70 to 13.51 mm showing the consistency of the values and how normally distributed they were (Figure 5.2).

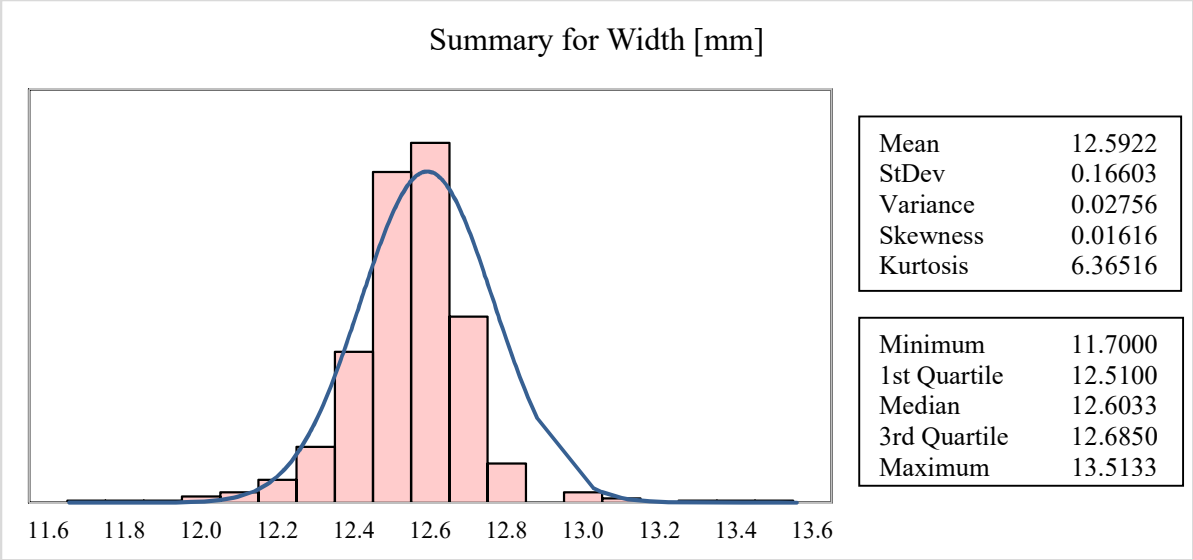

FIGURE 5.2 Statistics for BBR Mixture Beams Width.

5.2.2 Sealant Application

The pipette method, developed for binder sample preparation to simulate the application of sealant in the field was also used for mixture sample preparation. The lower part of the cores is not affected by the application of the sealants that occurs at the surface since it is highly improbable that the sealants applied in the field penetrate more than 29 mm, as indicated by some of the manufacturers. As a consequence, the beams cut from the bottom layer (4^{th} layer) of the cores were used in this experiment. In this procedure, the sealant is applied with a measuring pipette to control the number of drops as described in the previous section 4.2 and then spread on the surface of the BBR specimens using a plastic non-absorbent strip (Figure 5.3a). The number of drops to be applied is calculated in Table 5.1 based on spraying rate of sealant in the field. The spraying rate used in Table 5.1 is based on column 6 of Table 4.1. Due to lack of materials, the beams were treated using 8 drops only. The detail calculation step is provided in Table 5.2. The condition of beams before and after treatment in the laboratory is presented in Figure 5.4b. The number of drops used to treat the beams in the laboratory was 8 which simulates the spraying rate of 0.02 gallon/sy in the field. The spraying rate of WB1 and E1 was about 0.09 gallon/sy, which resulted in around 30 drops (Table 5.1). However, due to lack of mixture specimens

and to perform analysis based on consistent sample preparation procedure for all the sealants, the mixture beams were treated with 8 drops of sealants.

(a)

(b)

FIGURE 5.3 Preparation of Laboratory Treated Mixture Beams.

TABLE 5. 1 Calculation of no. of Drops for Mixture Beams

Calculation of No. of Drops of Sealant for Mixture Beams						
1	2	3	4	5	6	7

Sample type	BBR Sample Surface Area	Spraying Rate of Sealant.	The weight of Sealant. per Sample	Weight of one drop of Sealant	No. of Drops of Sealant per sample	Drops applied per sample
		by weight				
	mm^2	kg/m^2	gm	gm		
BBR Beam_OB1	1587.50	0.07	0.111	0.016	6.95	7
BBR Beam_OB2_a	1587.50	0.06	0.095	0.016	5.95	6
BBR Beam_OB2_b	1587.50	0.08	0.127	0.016	7.94	8
BBR Beam_WB1	1587.50	0.31	0.492	0.016	30.76	31
BBR Beam_E1	1587.50	0.41	0.651	0.016	40.68	41

TABLE 5. 2 Calculation Steps of Table 5.1

Column 3=	Column 6 From Table 4.1
Column 4=	Column 2 * Column 3*1000
Column 5 =	Measured in Laboratory
Column 6=	Column 4 / Column 5

A flow chart of the testing plan of the study is presented in Figure 5.4.

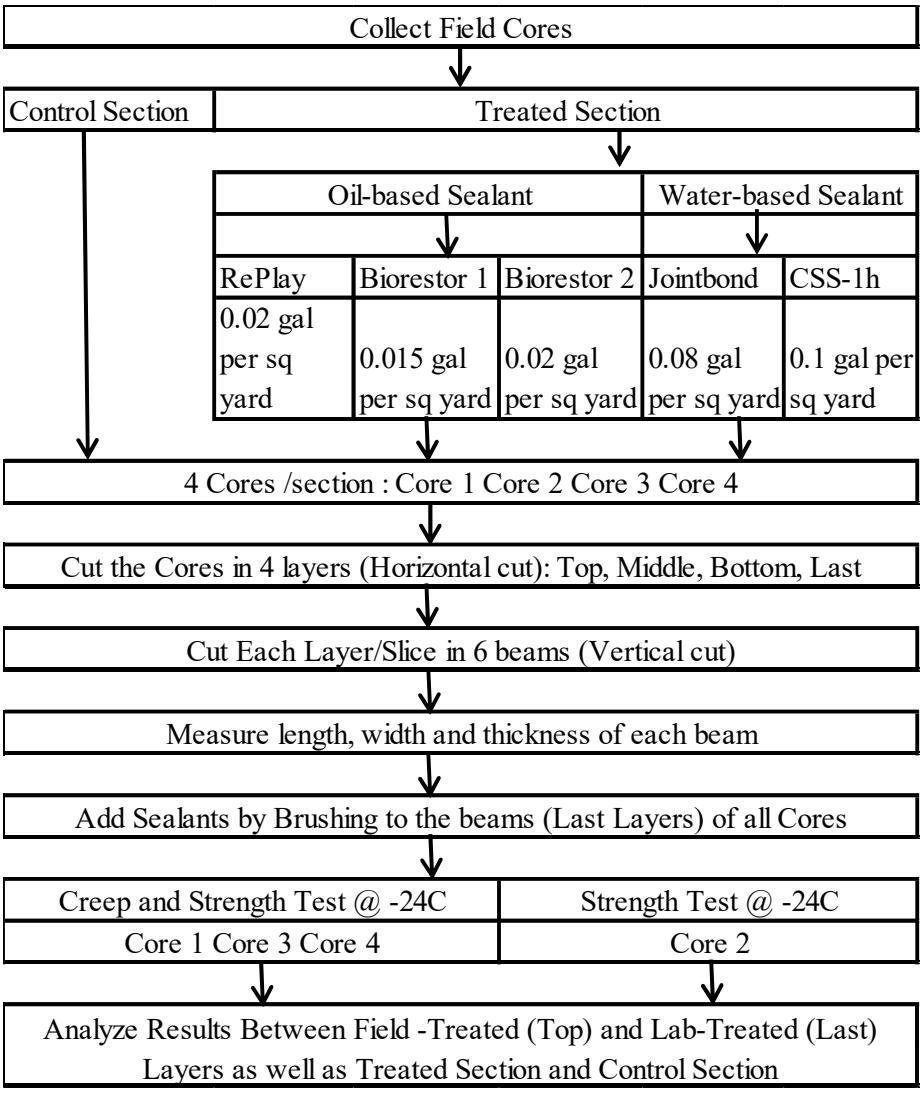

FIGURE 5.4 Testing Plan of the Study.

5.3 Testing Method

The laboratory treated mixture beams were tested after 1 month of sealant application in the laboratory, whereas the beams from the surface of the field cores were tested after about 9 months of sealant application in the field. Both creep and strength tests were performed on the beams cut from Core No. 1, 3 and 4. Only strength test was conducted on the beams from Core No. 2. All tests were performed using BBR Pro.

In this strength test, a constant loading rate was applied, such that a load of 43N was obtained in 150 sec until the beams broke. BBR creep tests with duration of 500 sec followed by a recovery period of 500 sec were performed on all samples from Core No. 1, 3 and 4 along with the strength test at the end of the recovery period. A total of 576 beams were tested in air, 288 beams at -24ºC and 288 beams at -12ºC; 3 replicates from each layer for each core of each treated and control sections.

5.4 Experimental Result

5.4.1 Creep Stiffness

Three replicates were tested for each case, and the average value was reported discarding the outliers. Figures 5.5 to 5.8 show the creep stiffness average values for the field treated and laboratory treated at -24ºC and -12ºC, respectively.

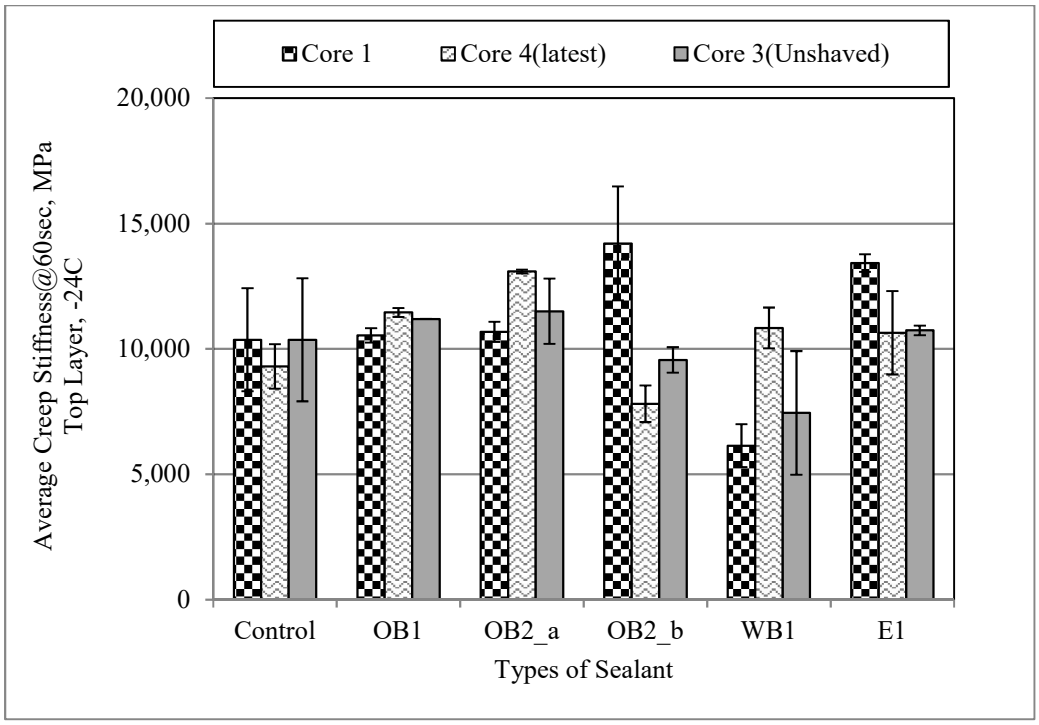

FIGURE 5.5 S(60s) Results at -24ºC of Mixture Beams from Field Treated/Top Layer.

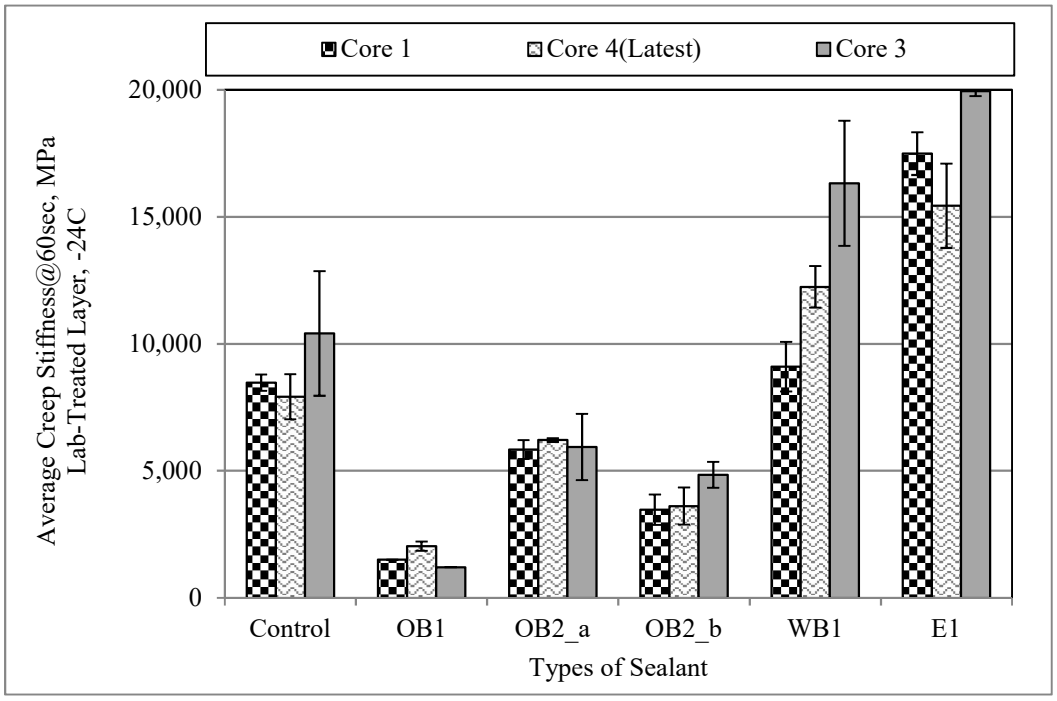

FIGURE 5.6 S(60s) Results at -24ºC of Mixture Beams from Lab-Treated Layer.

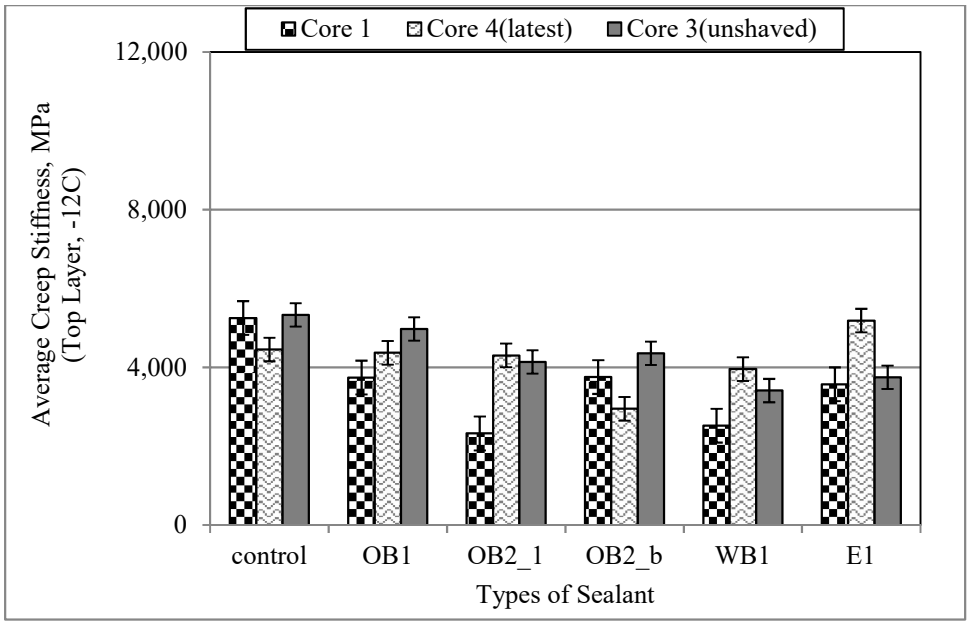

FIGURE 5.7 S(60s) Results at -12ºC of Mixture Beams from Field Treated/Top Layer.

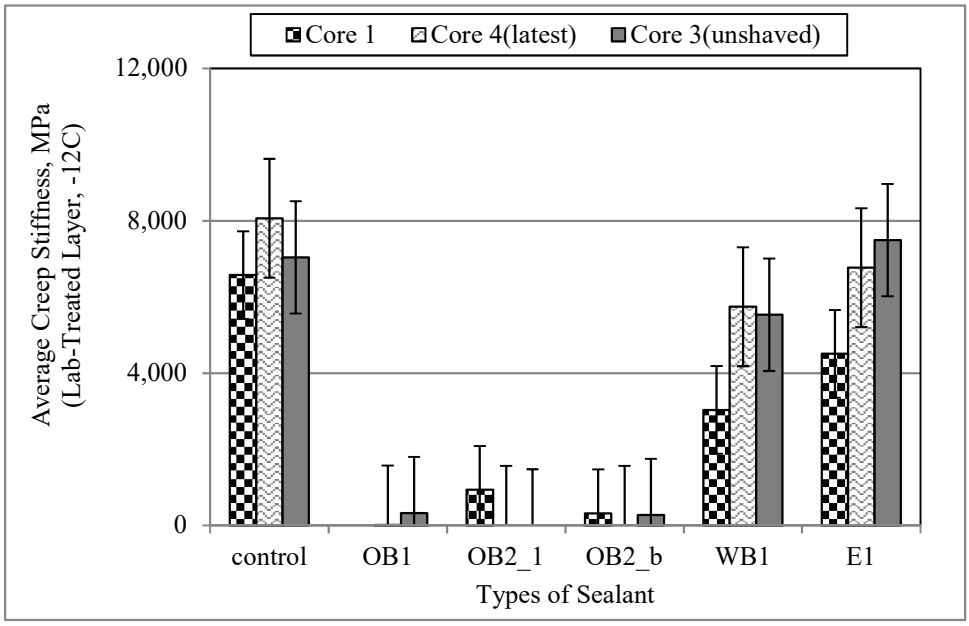

FIGURE 5.8 S(60s) Results at -12ºC of Mixture Beams from Lab-Treated Layer.

A number of observations can be made. The beams from the top layer of the control section (Figures 5.5 and 5.7) have similar stiffness values for all cores, while the beams from the bottom layer (Figures 5.6 and 5.8) were less stiff and the values were scattered. Oil-based sealants, OB1 and OB2 (OB2_a and OB2_b) increased the stiffness of the control for the field treated samples. However, a significant decrease is observed for the laboratory treated samples, similar to the results reported in many other studies.

5.4.2 m-value

Figures 5.9 to 5.12 show the m-value averages for the field treated and laboratory treated samples at -24ºC and -12ºC, respectively. Very small changes can be observed in the field treated samples. On the contrary, significant increases in m-value averages can be noticed on the laboratory treated samples when using oil-based sealants.

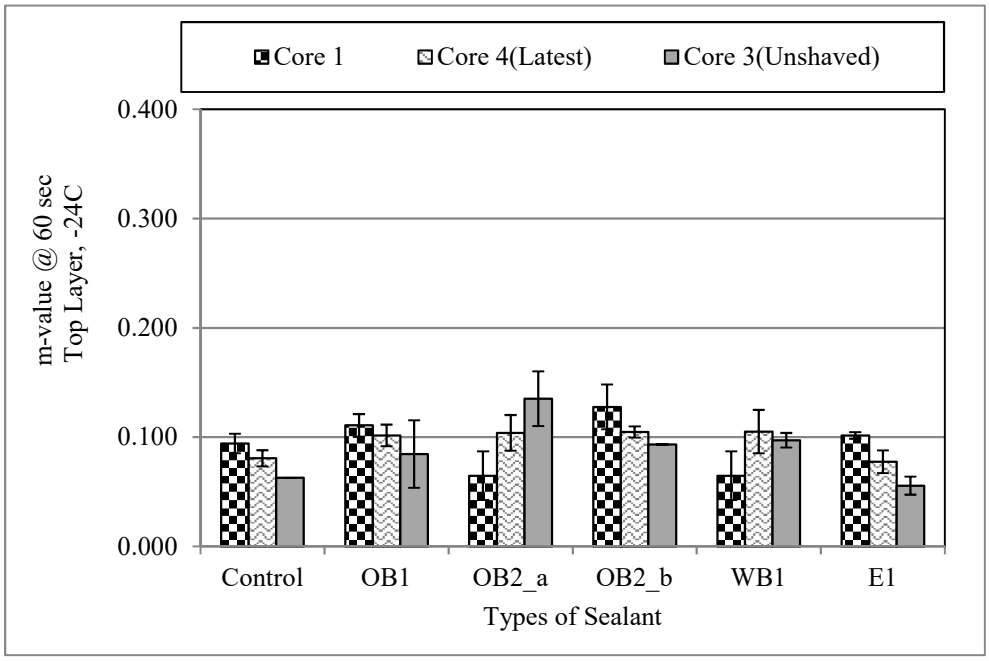

FIGURE 5.9 m-value(60s) Results at -24ºC of Mixture Beams from Field Treated/Top Layer.

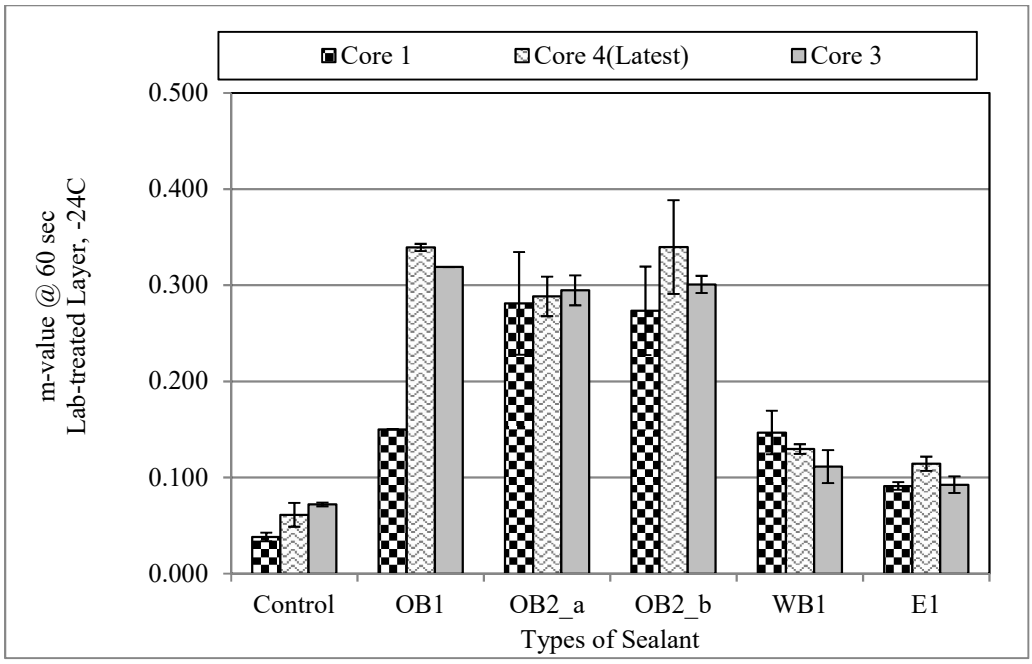

FIGURE 5.10 m-value(60s) Results at -24ºC of Mixture Beams from Lab-Treated Layer.

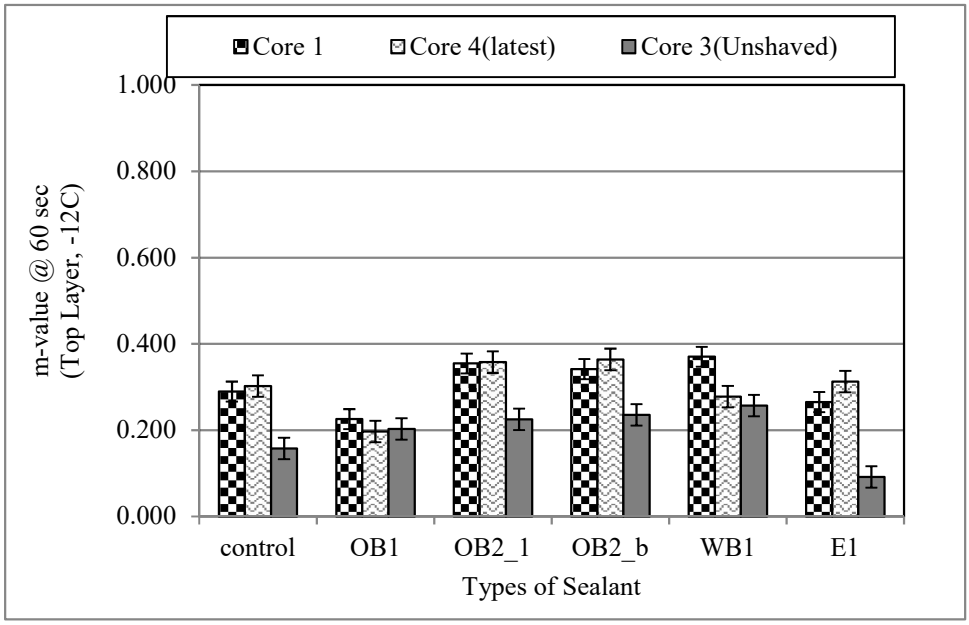

FIGURE 5.11 m-value(60s) Results at -12ºC of Mixture Beams from Field Treated/Top Layer.

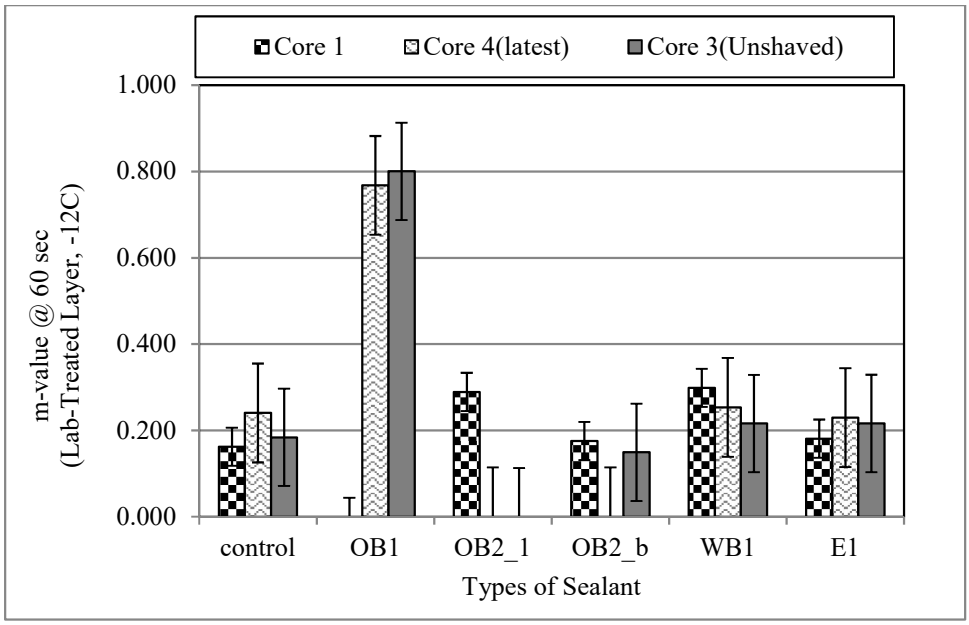

FIGURE 5.12 m-value(60s) Results at -12ºC of Mixture Beams from Lab-Treated Layer.

5.4.3 Strength

Strength tests were also performed on the mixture beams using BBR Pro, a modified BBR machine developed by Marasteanu et al. (2012) *(18).* Unlike the original BBR that applies constant loads, this BBR Pro can apply loads at different rates. The stress and failure strain results are shown in Figures 5.13 to 5.20 for two different temperatures. A small change in both strength and strain at failure are observed for the field-treated mixture beams (Figures 5.14, 5.16, 5.18 and 5.20). For the laboratory treated samples, no major changes in strength were observed, except a decrease in strength when OB1/OB2 was applied in the laboratory (Figures 15 and 17). Average strength and failure strain at -12ºC for the mixture beams treated with oil-based OB1 or OB2 in the laboratory was not possible to obtain due to beam-breaking because of the high softening issue (Figures 5.17 and 5.21). However, for the failure strain, 3 to 6 times higher values were observed for OB1 and OB2 (Figures 5.19 and 5.21).

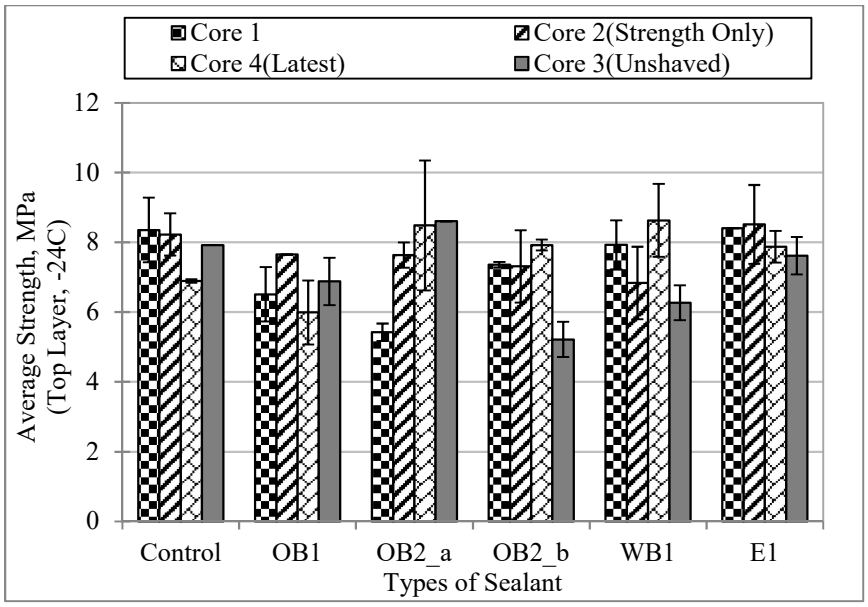

FIGURE 5.13 Strength at -24ºC of Mixture Beams from Field Treated/Top Layer.

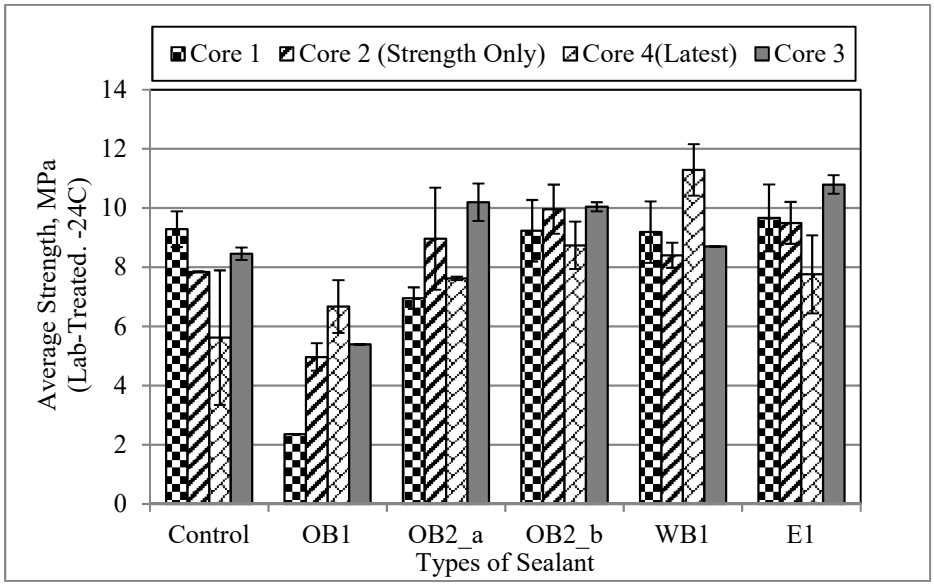

FIGURE 5.14 Strength at -24ºC of Mixture Beams from Lab-Treated Layer.

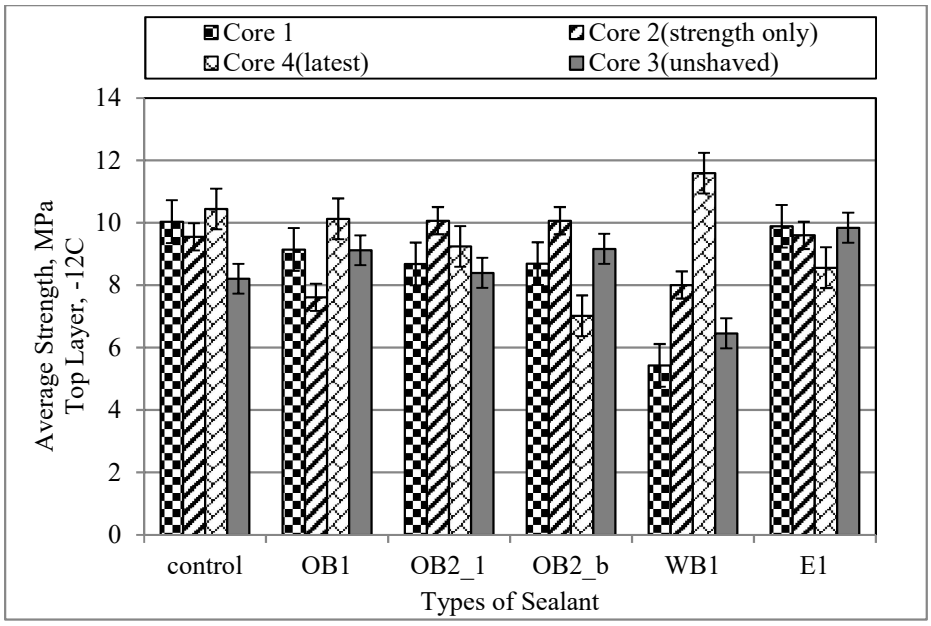

FIGURE 5.15 Strength at -12ºC of Mixture Beams from Field Treated/Top Layer.

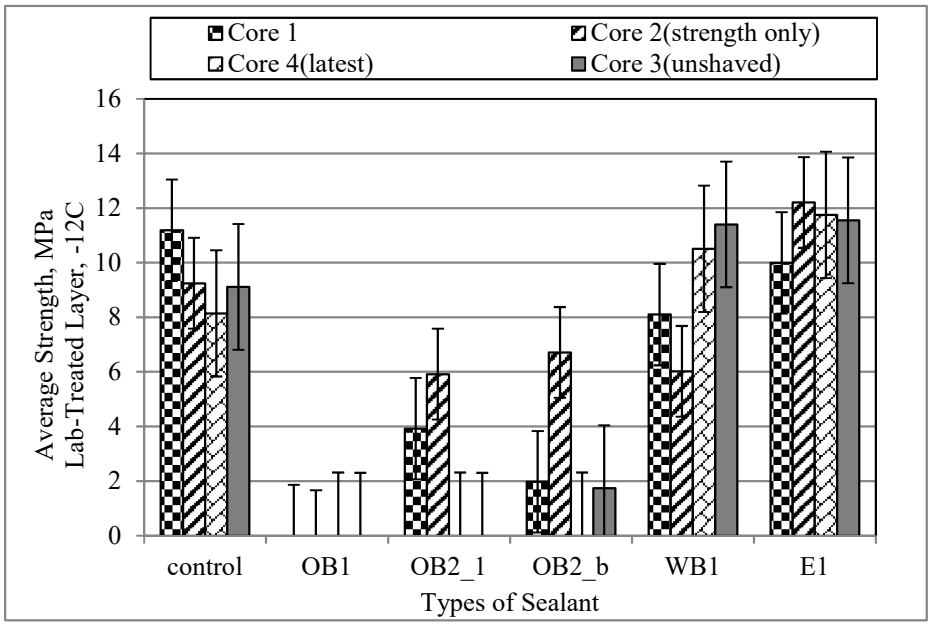

FIGURE 5.16 Strength at -12ºC of Mixture Beams from Lab-Treated Layer.

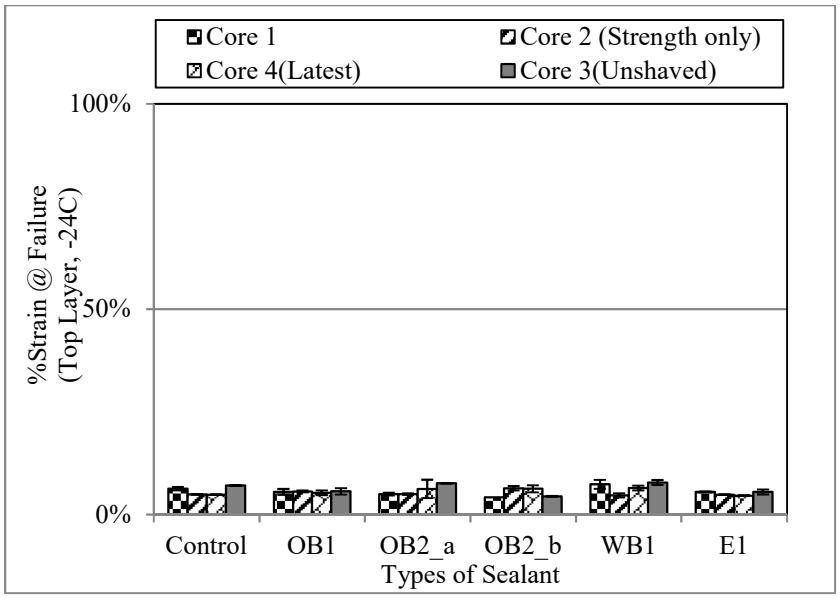

FIGURE 5.17 %Strain at Failure at -24ºC of Mixture Beams from Field Treated/Top Layer.

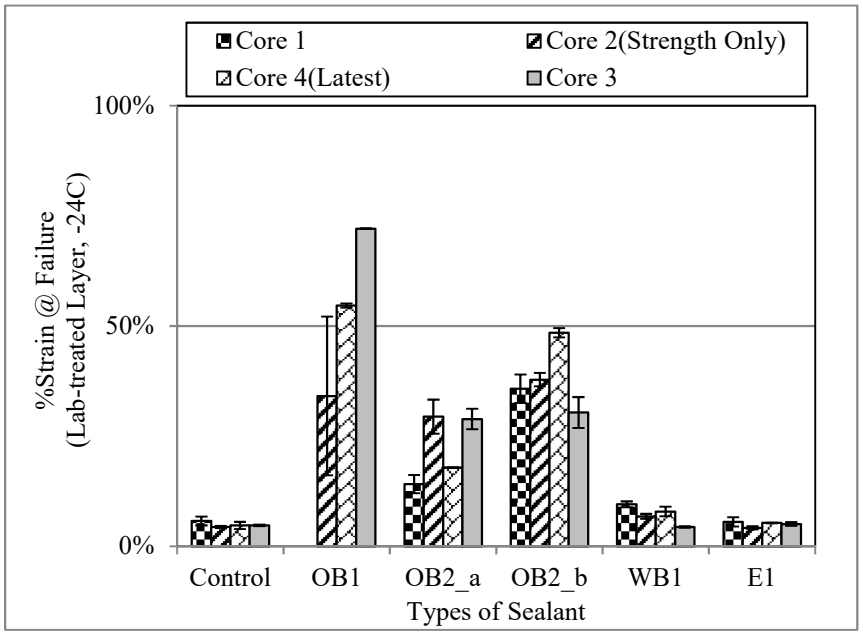

FIGURE 5.18 %Strain at Failure at -24ºC of Mixture Beams from Lab-Treated Layer.

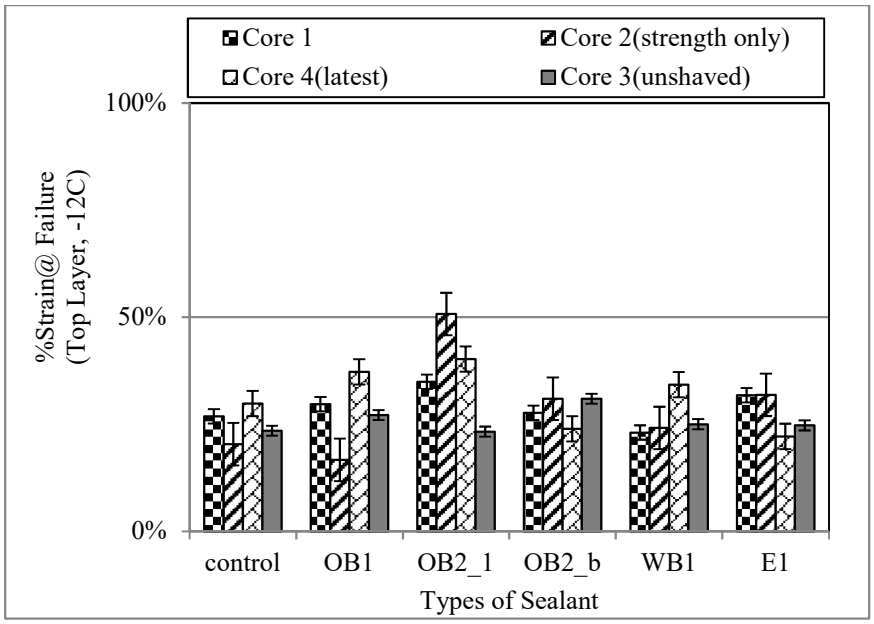

FIGURE 5.19 µStrain at Failure at -12ºC of Mixture Beams from Field Treated/Top Layer.

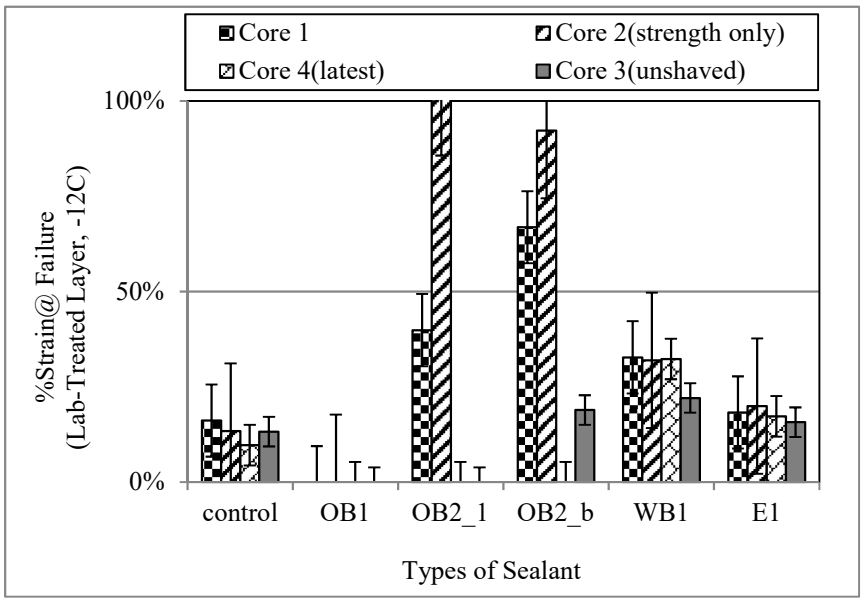

FIGURE 5.20 %Strain at Failure at -12ºC of Mixture Beams from Lab-Treated Layer.

5.5 Shaved vs. Unshaved Top Surface

As described earlier, Core 1, 2 and 3 were received from the field few days after sealant application. Top 3mm was removed from Core 1 and 2 to obtain smooth surface.

Since the exact penetration of the sealant in the field is unknown; there might be a chance that removing top 3 mm surface will result in removing the treated surface. In this regard, Core 3 remained unshaved to run a comparison analysis between shaved and unshaved samples. The following plots represent low-temperature mixture properties at -12ºC and -24ºC. A fixed pattern was observed in all cases for the test temperature of -12ºC. The creep stiffness was reported to be consistently higher for the unshaved surface (Core 3) than the shaved surface (Core 1) (Figure 5.22). This is expected since the unshaved top surface is more aged due to binder oxidation than the shaved top surface where the top 3mm was removed. As a consequence, m-value decreased for Core 3 comparing with Core 1 (Figure 5.24). Average strength and strain at failure at -12ºC were observed to be smaller for Core 3 than Core 1 (Figures 5.26 and 5.28). The obtained test results at -24ºC followed a fixed pattern only for the beams treated with water-based WB1 and E1, with an exception for m-value (Figure 5.23, 5.25, 5.27 and 5.29). Creep stiffness, and average strength was observed to be lower for Core 3 than Core 1 when tested at -24ºC (Figure 5.23 and 5.27). Figure 5.29 shows that micro-strain increases a very small amount for Core 3 comparing with Core 1 at -24ºC.

5.5.1 Creep Stiffness

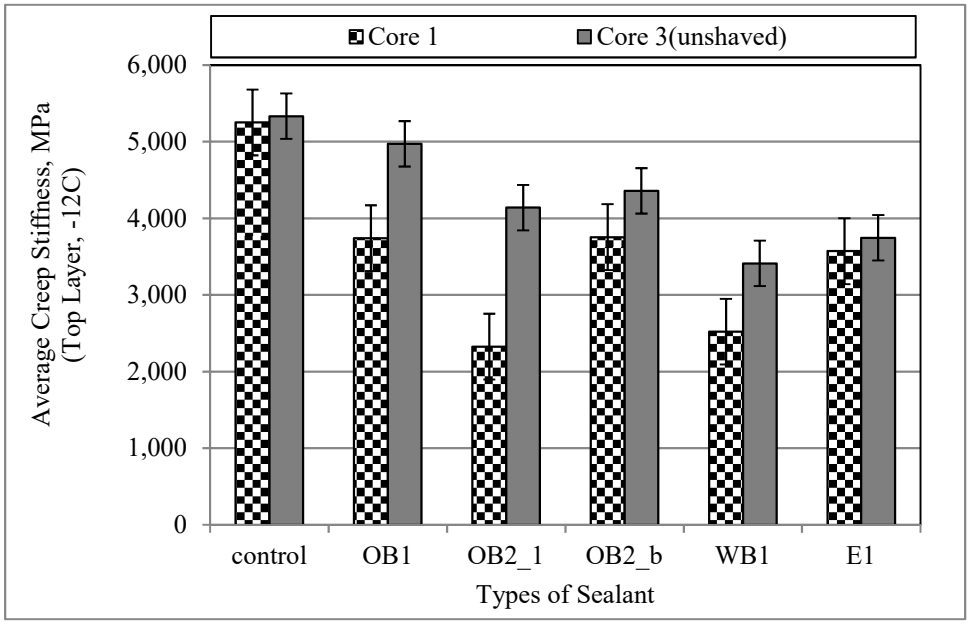

FIGURE 5.21 Creep Stiffness of Mixture Beams for Shaved and Unshaved Top Surface at -12ºC.

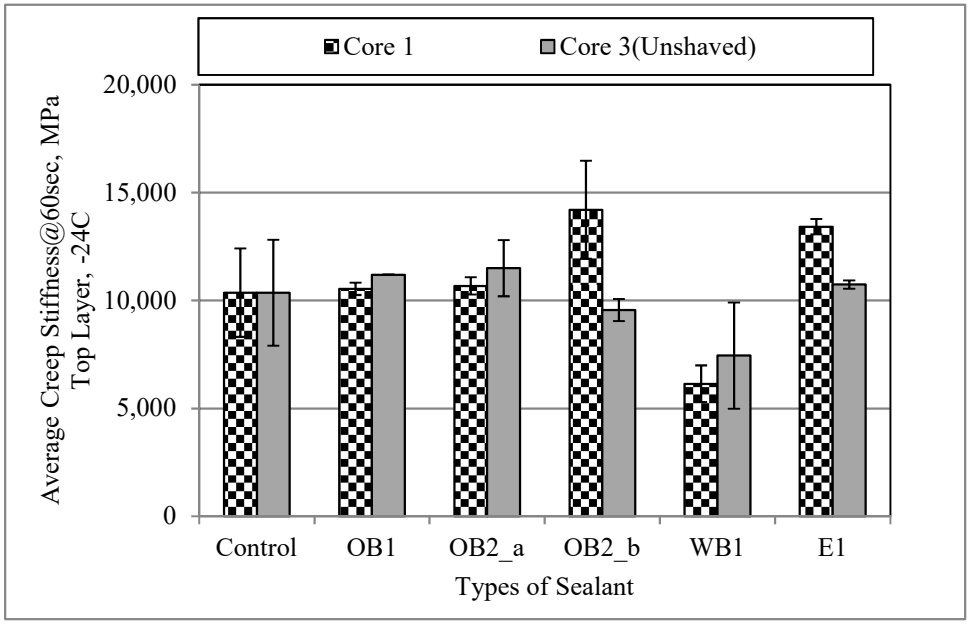

FIGURE 5.22 Creep Stiffness of Mixture Beams for Shaved and Unshaved Top Surface at -24ºC.

5.5.2 m-value

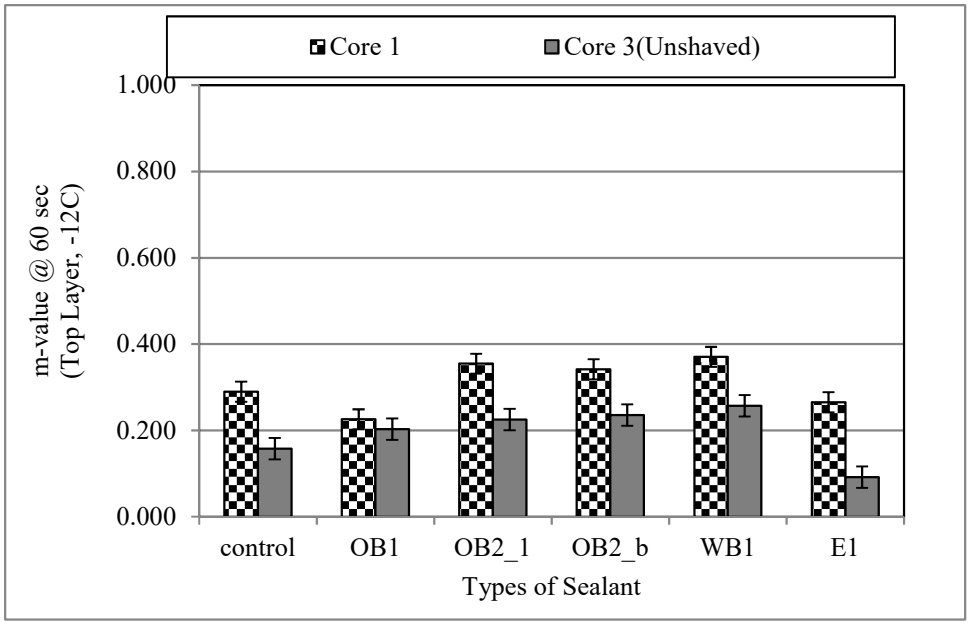

FIGURE 5.23 m-value of Mixture Beams for Shaved and Unshaved Top Surface at -12ºC.

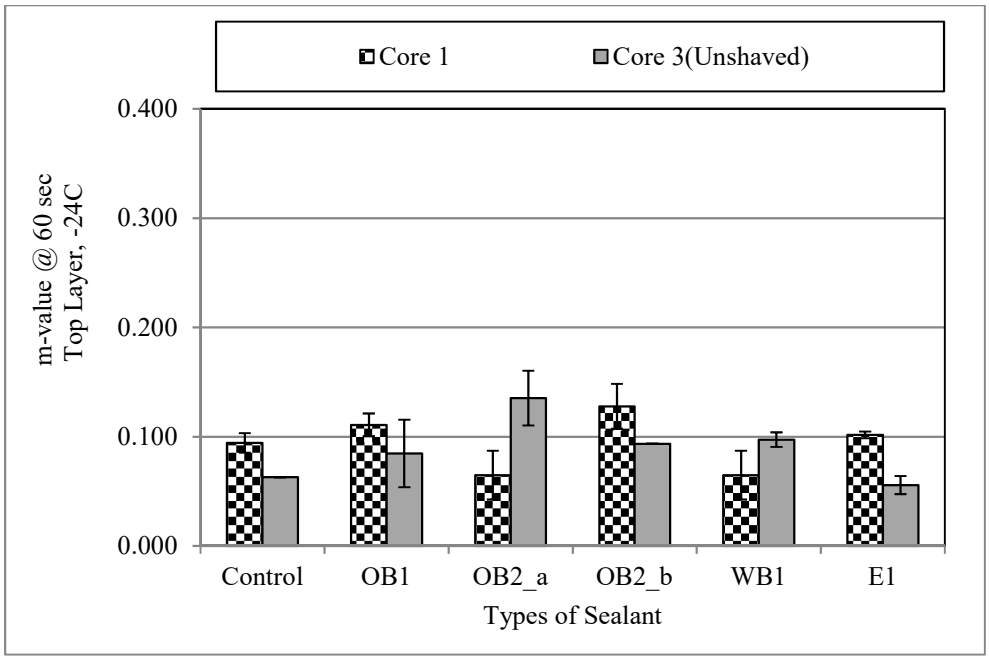

FIGURE 5.24 m-value of Mixture Beams for Shaved and Unshaved Top Surface at -24ºC.

5.5.3 Average Strength

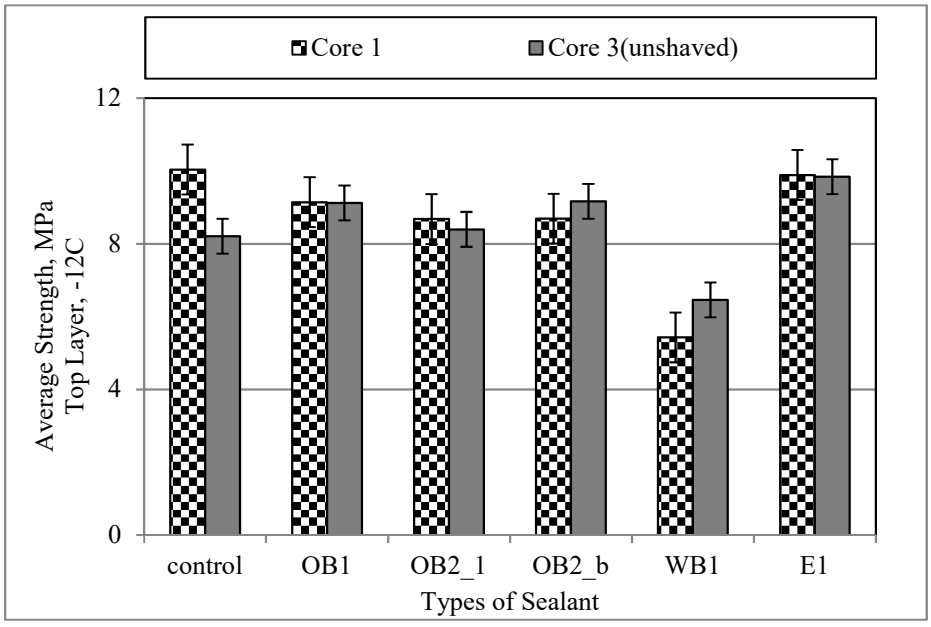

FIGURE 5.25 Average Strength of Mixture Beams for Shaved and Unshaved Top Surface at -12ºC.

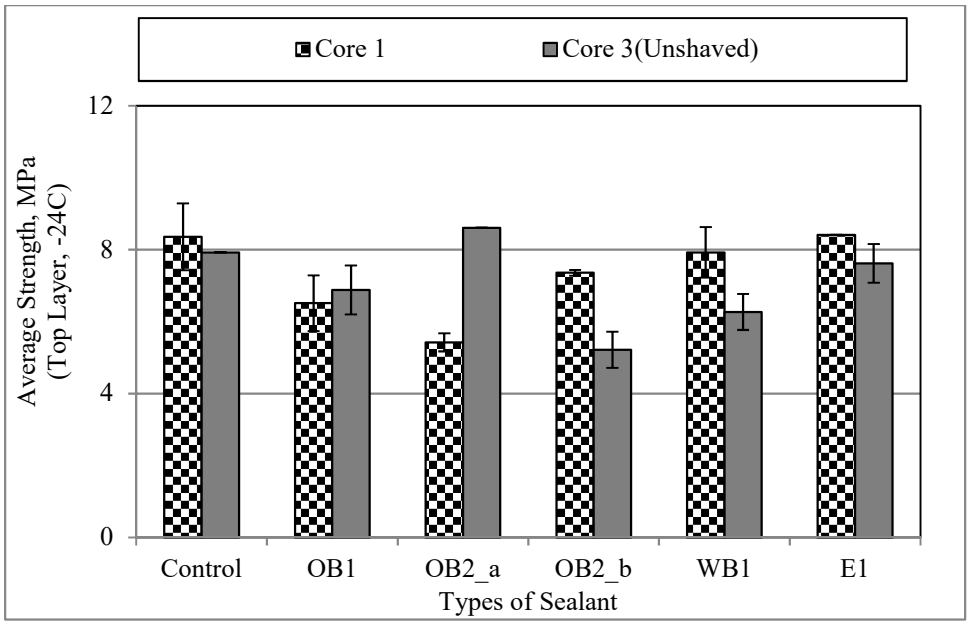

FIGURE 5.26 Average Strength of Mixture Beams for Shaved and Unshaved Top Surface at -24ºC.

5.5.4 Strain at Failure

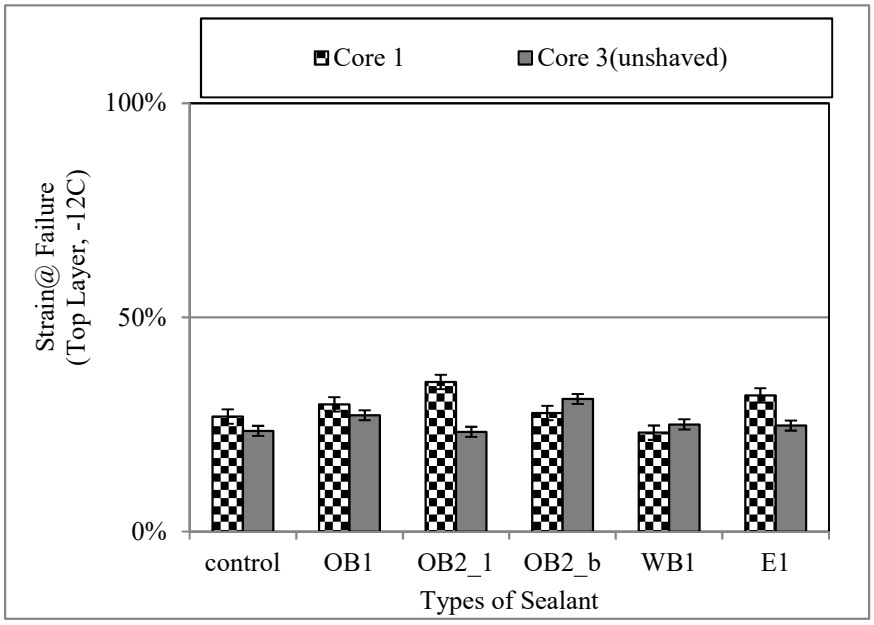

FIGURE 5.27 %Strain at Failure of Mixture Beams for Shaved and Unshaved Top Surface at -12ºC.

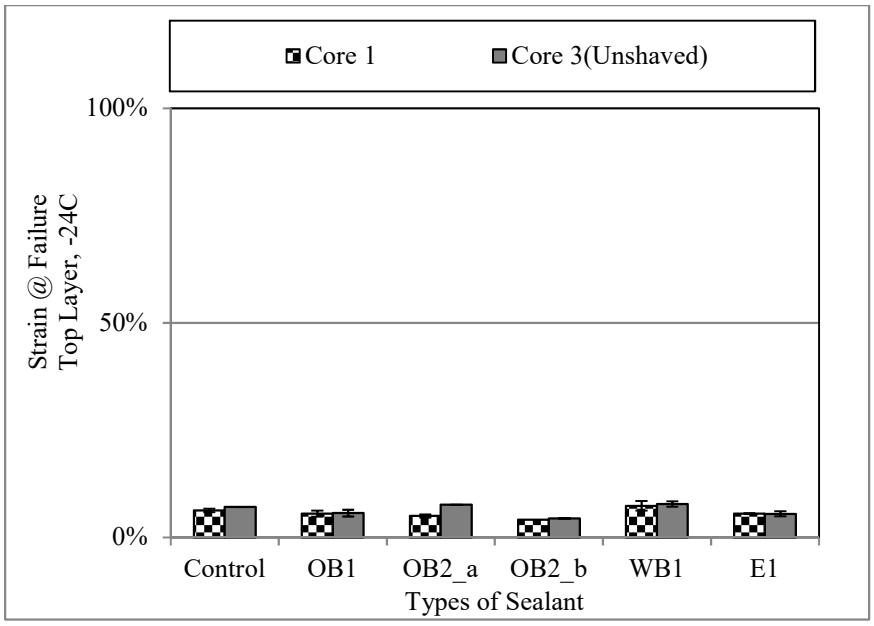

FIGURE 5.28 %Strain at Failure of Mixture Beams for Shaved and Unshaved Top Surface at -24ºC.

5.6 Effect of Ageing on Pavement Layers

As described earlier, the cores were cut in four layers; top/field-treated layer, middle layer, a bottom layer and last/lab-treated layer. Beams from each layer were tested at -24C and -12C to observe the effect of sealant penetration through layers. In this analysis part, only Core 1 and Core 4 were selected for each treated and control section to study the effect of aging based on layers. This is because Core 1 was obtained after 3 weeks of sealant application and Core 4 was obtained after 8 months. In addition, both cores went through same sample preparation and testing procedure unlike Core 3 and Core 2 where Core 3 had its top 3mm removed, and only strength test was conducted on Core 2. Since the beams from the lab/last layer of the treated section were treated in the laboratory before testing; the last layer was not considered for the analysis. The results at -24C are presented below.

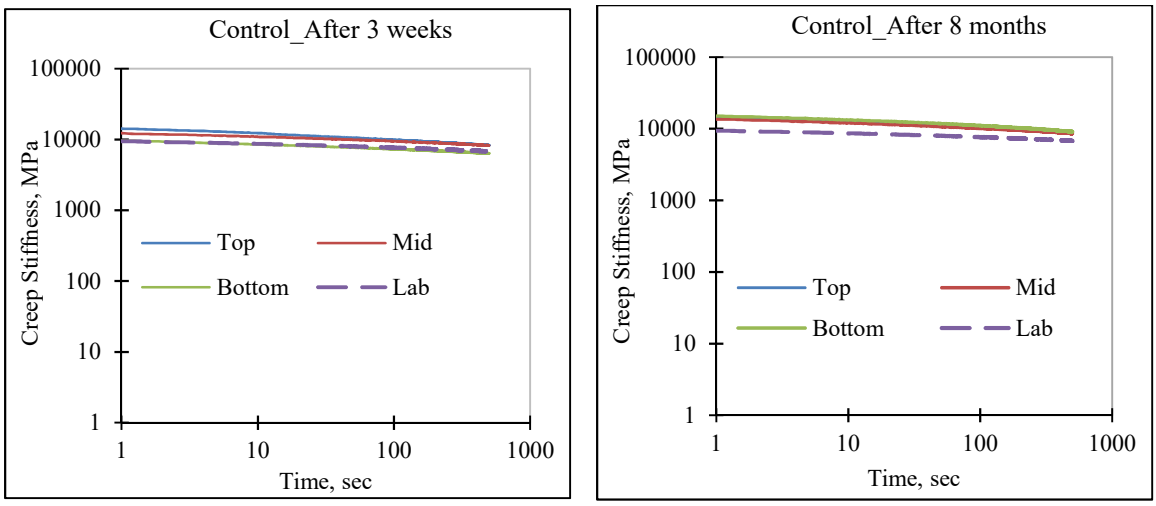

FIGURE 5.29 Creep Stiffness vs. Time at -24C for Control Section (a) After 3 weeks; (b) After 8 months.

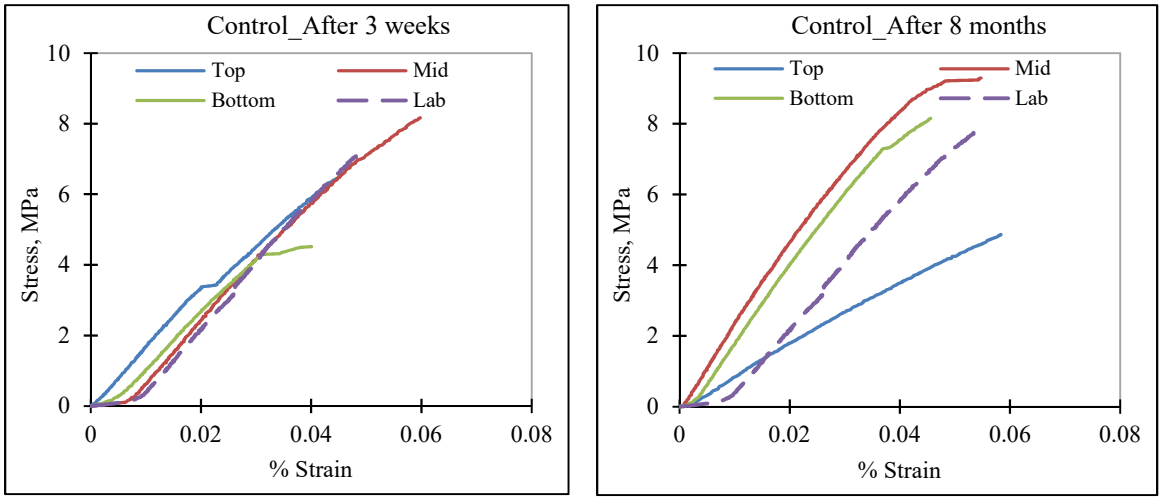

FIGURE 5. 30 Stress-Strain Curve at -24C for Control Section (a) After 3 weeks; (b) After 8 months.

A minor increase in creep stiffness and strength is observed after 8 months (Figure 5.29b). The bottom and last/lab layer resulted in lower creep stiffness compared to top/mid layer in both cases as expected.

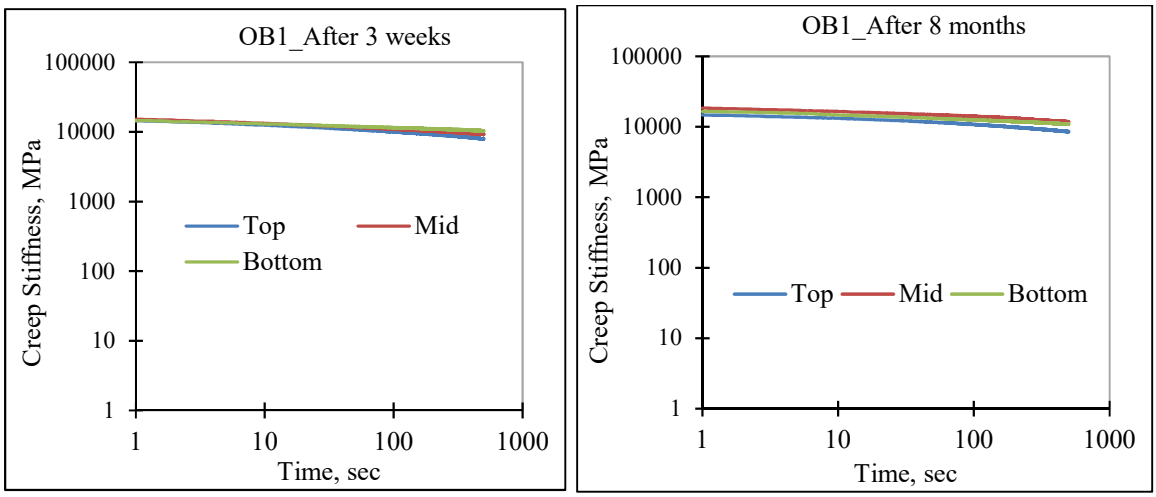

FIGURE 5.31 Creep Stiffness vs. Time at -24C for OB1 Treated Section (a) After 3 weeks; (b) After 8 months.

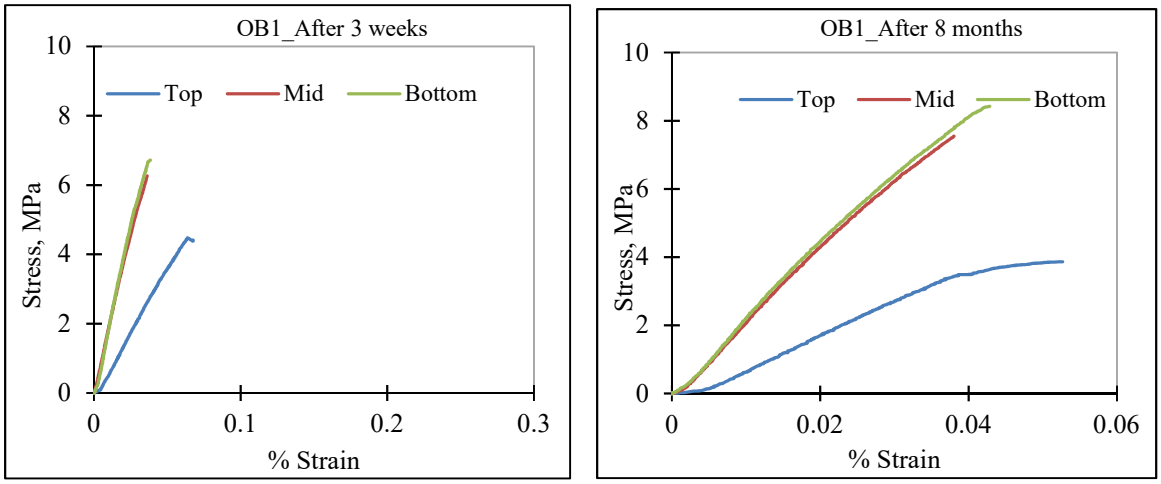

FIGURE 5.32 Stress-Strain Curve at -24C for OB1 Treated Section (a) After 3 weeks; (b) After 8 months.

While no difference in creep stiffness was observed among layers after 3 weeks of sealant application, creep stiffness of the top layer after 8 months was observed to be lower than mid/bottom layers (Figure 5.31). The strength was observed to increase after 8 months when comparing the results of the beams from first 3 layers (Figure 5.32).

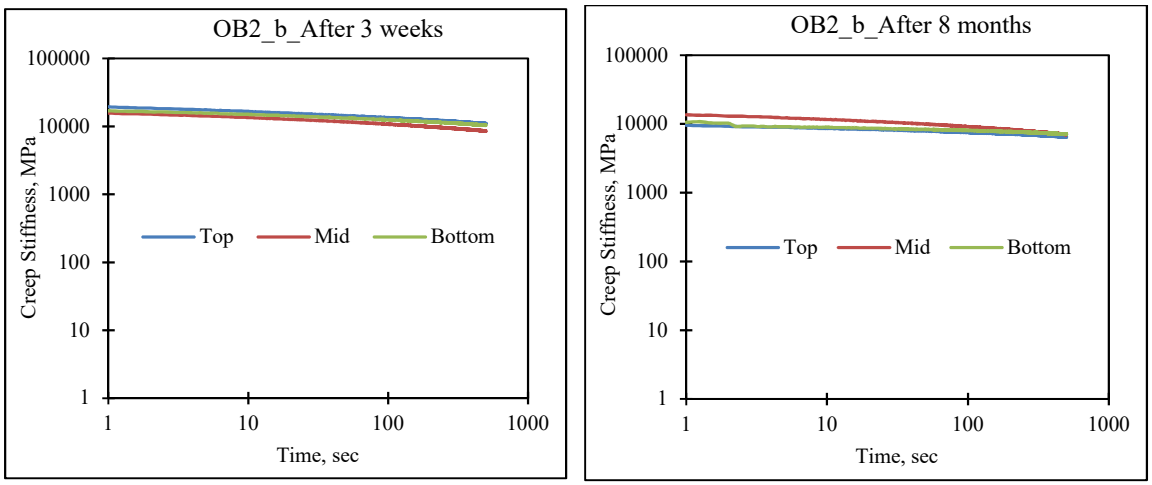

FIGURE 5.33 Creep Stiffness vs. Time at -24C for OB2_b Treated Section (a) After 3 weeks; (b) After 8 months.

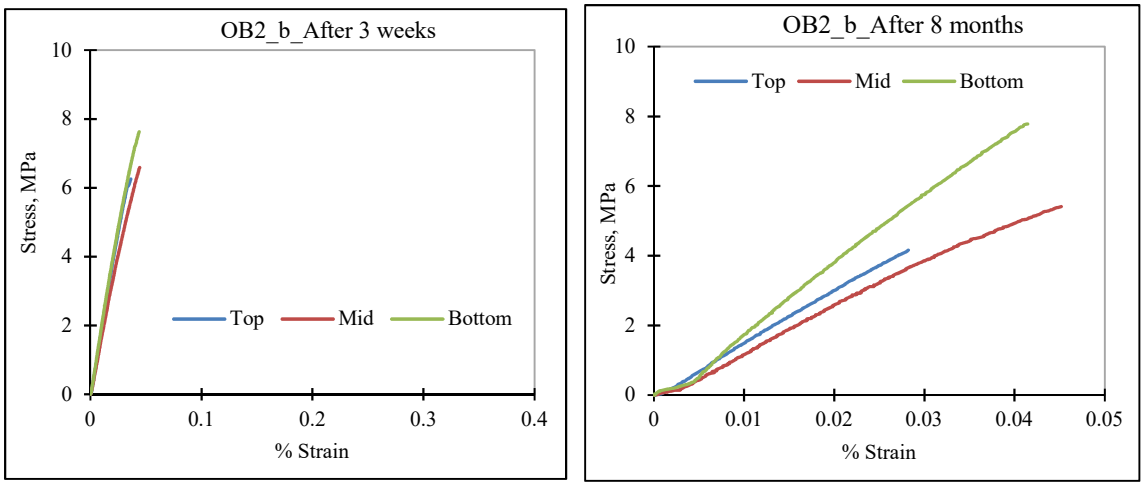

FIGURE 5. 34 Stress-Strain Curve at -24C for OB2_b Treated Section (a) After 3 weeks; (b) After 8 months.

A similar effect of oil-based OB1 sealant was observed in the case of OB2. There is no difference in the creep stiffness among layers after 3 weeks of sealant application, whereas, a reduction in creep stiffness was noted for the top layer after 8 months (Figure 5.33). Creep stiffness after 8 months from all layers were observed to be lower than the stiffness after 3 weeks which explains the potential of OB2 in reversing the oxidation. A significant increase in %Strain at failure was observed after 8 months (Figure 5.34). As expected, bottom layer had the highest strength and %strain at failure, because of being less exposed to air and oxidation.

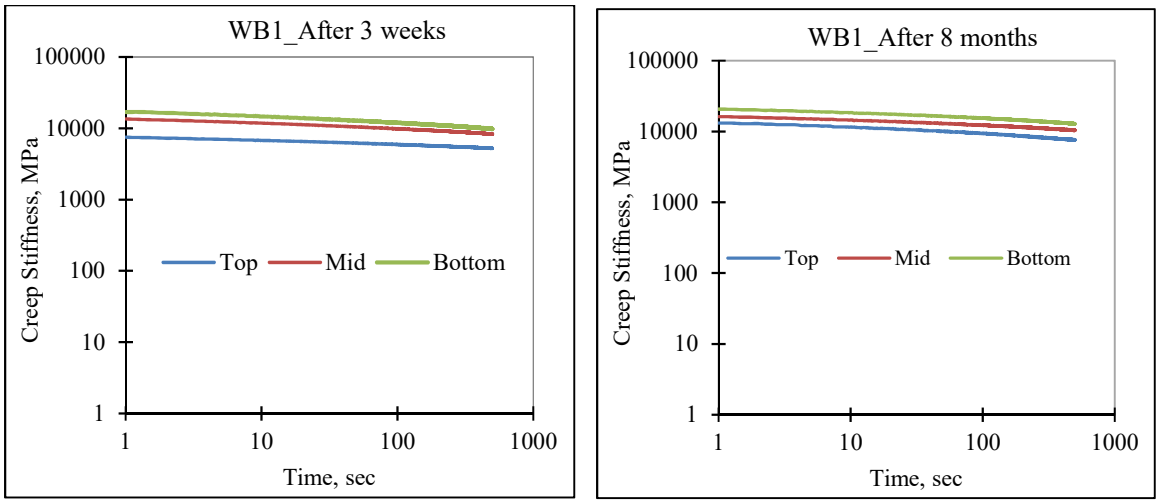

FIGURE 5. 35 Creep Stiffness vs. Time at -24C for WB1 Treated Section (a) After 3 weeks; (b) After 8 months.

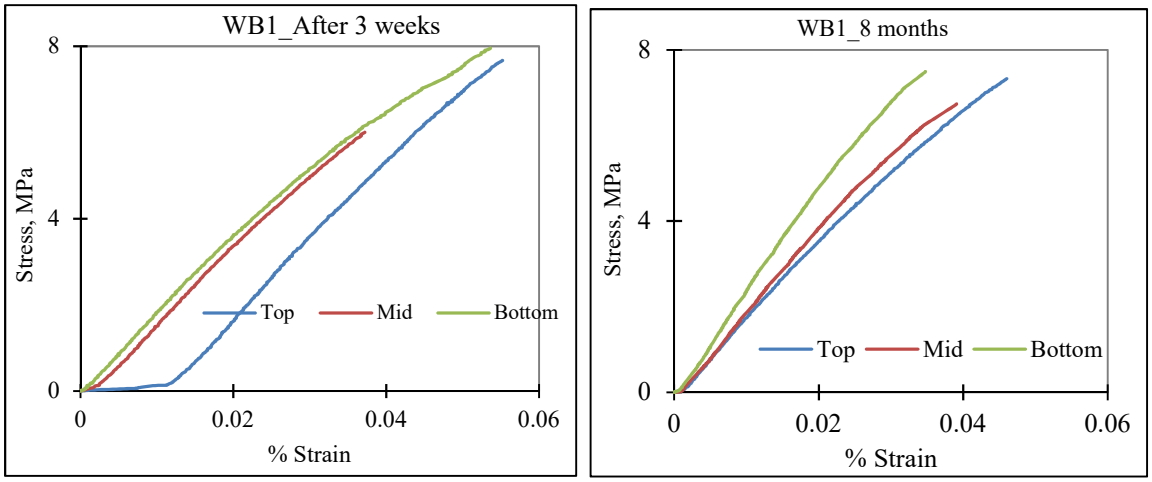

FIGURE 5.36 Stress-Strain Curve at -24C for WB1 Treated Section (a) After 3 weeks; (b) After 8 months.

An increase in creep stiffness and reduction in % strain at failure was observed after 8 months of WB1 application (Figures 5.35 and 5.36).

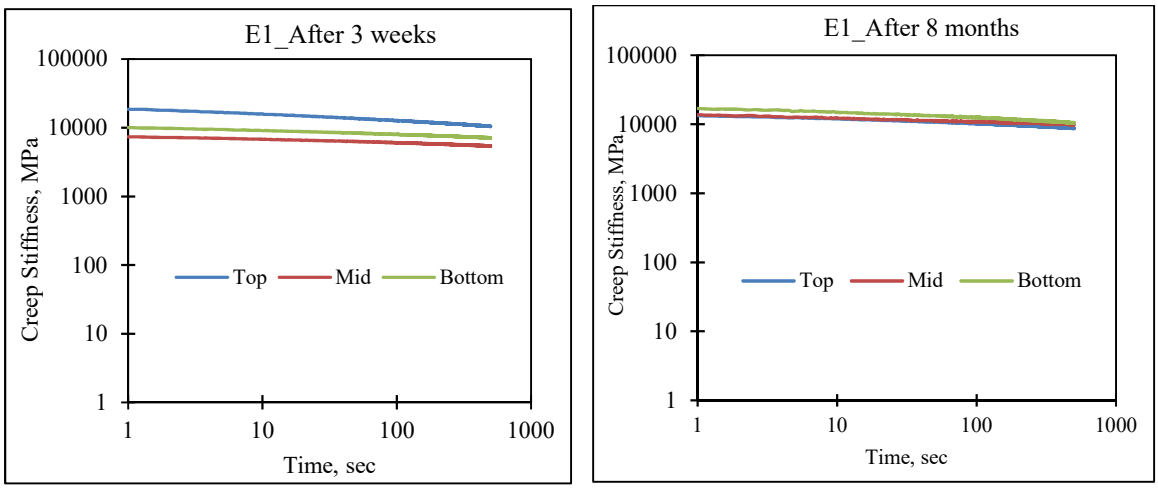

FIGURE 5.37 Creep Stiffness vs. Time at -24C for E1 Treated Section (a) After 3 weeks; (b) After 8 months.

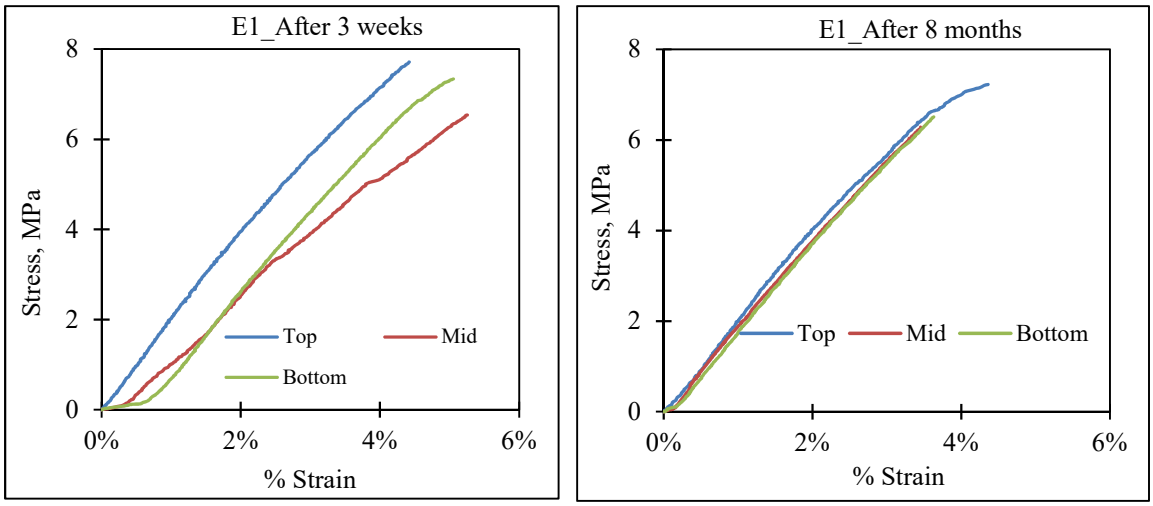

FIGURE 5.38 Stress-Strain Curve at -24C for E1 Treated Section (a) After 3 weeks; (b) After 8 months.

While there is no significant change in strength, an increase in creep stiffness was observed after application of traditional emulsion E1 (Figure 5.37 and 5.38).

5.6.1 Comparison

5.6.1.1 Creep Stiffness and m-value

TABLE 5.3 Creep Stiffness and m-value at -24C of different layers

	Control		**OB1**		**OB2_b**		**WB1**		**E1**	
Layer	Stiffness @ 60sec, MPa	m-value @ 60 sec	Stiffness @ 60sec, MPa	m-value @ 60 sec	Stiffness @ 60sec, MPa	m-value @ 60 sec	Stiffness @ 60sec, MPa	m-value @ 60 sec	Stiffness @ 60sec, MPa	m-value @ 60 sec
After 3 Weeks										
Top	10366	0.094	10542	0.111	14205	0.102	6144	0.060	10645	0.078
Mid	9754	0.080	11538	0.087	11446	0.113	10318	0.087	11013	0.047
Bottom	7567	0.069	11855	0.056	13061	0.089	12608	0.099	12903	0.087
Average	9229	0.081	11312	0.085	12904	0.101	9690	0.082	11520	0.071
% CoV	15%	18%	6%	**33%**	11%	12%	**34%**	**24%**	11%	**30%**
After 8 Months										
Top	11457	0.081	11453	0.107	7811	0.105	9824	0.104	13424	0.102
Mid	10585	0.080	9590	0.083	9722	0.124	12761	0.081	12598	0.056
Bottom	11627	0.078	10007	0.085	8311	0.098	16076	0.088	11244	0.057
Average	11223	0.080	10350	0.092	8615	0.109	12887	0.091	12422	0.072
% CoV	5%	2%	9%	15%	12%	12%	**24%**	13%	9%	**36%**

The coefficient of variation of the average creep stiffness and m-value among layers are within 15%, except for few cases marked in bold (Table5.3). As a result, an average of three layers was considered for a comparative analysis among the treatments to study the ageing effect. Figures 5.39 and 5.40 below presents the comparison.

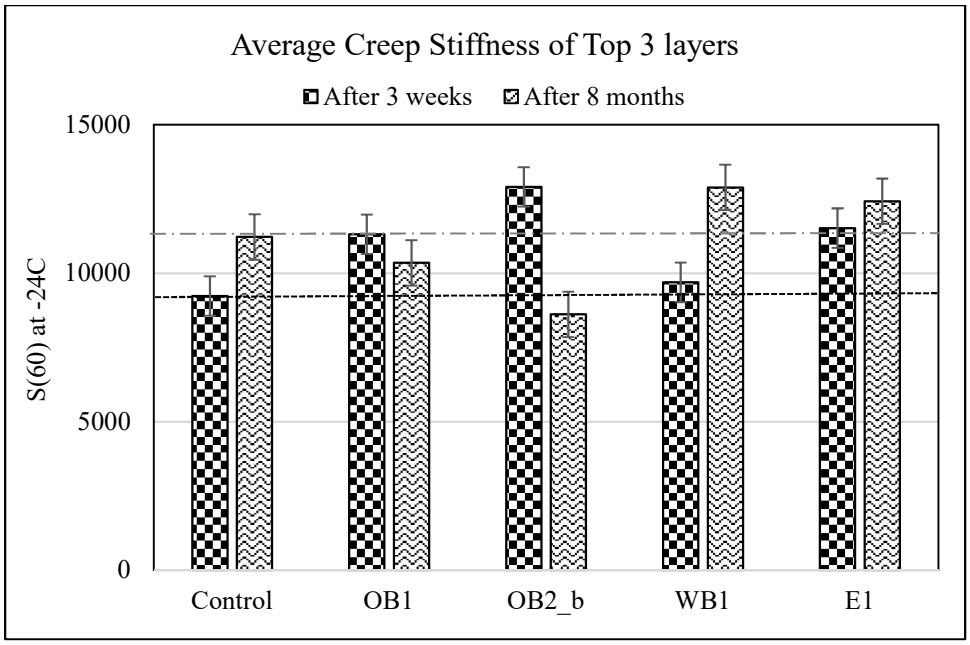

FIGURE 5.39 Average Creep stiffness at -24C for treated and untreated sections.

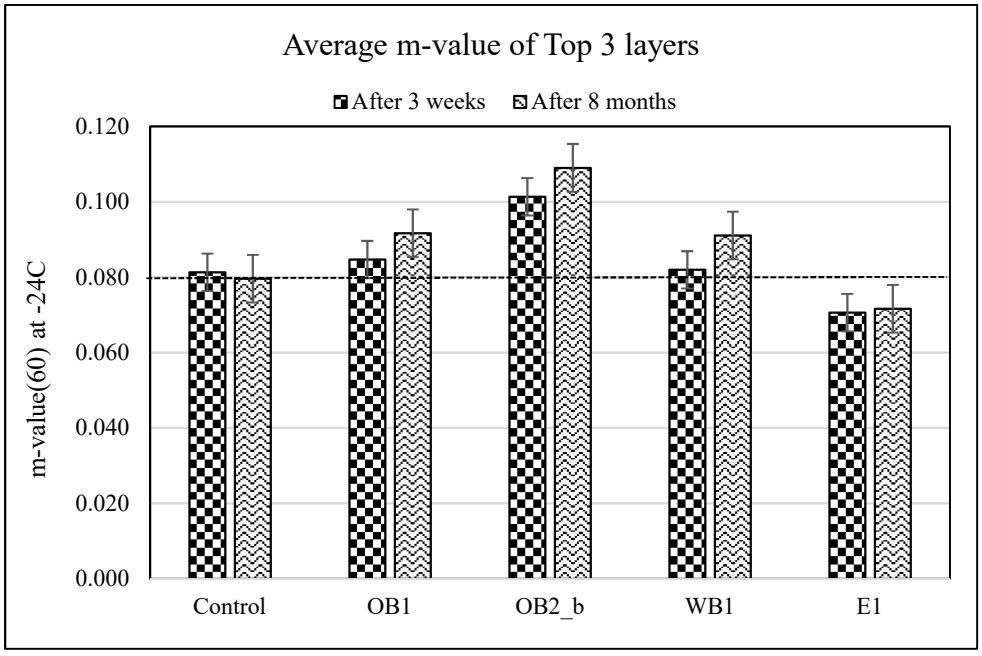

FIGURE 5.40 Average m-value at -24C for treated and untreated sections.

It can be observed that, after 8 months, while the creep stiffness of the control section increased, oil-based OB1 and OB2 treated sections resulted in lower creep stiffness than after 3 weeks (Figure 5.39). The water-based W1 and traditional emulsion, E1 increase the creep stiffness of the section after 8 months. The oil-based sealant treated sections were

also observed to have a higher relaxation modulus in both cases compared to control and other treated sections which are a desirable material property for the low-temperature region (Figure 5.40). Overall, oil-based bio-sealants, OB1 and OB2 have softening effect observed from the reduction in creep stiffness associated with an increase in relaxation modulus. Conversely, water-base bio-sealant, W1, and traditional emulsion E1 have a stiffening effect resulting in higher creep stiffness.

5.6.1.2 Stress and Strain at Failure

TABLE 5.4 Stress and %Strain at Failure of Different Layers at -24C

	Control		**OB1**		**OB2_b**		**WB1**		**E1**	
Layer	Stress @ Failure, MPa	Strain @ Failure, %	Stress @ Failure, MPa	Strain @ Failure, %	Stress @ Failure, MPa	Strain @ Failure, %	Stress @ Failure, MPa	Strain @ Failure, %	Stress @ Failure, MPa	Strain @ Failure, %
Core 1										
Top	8.4	0.063	6.5	0.076	7.0	0.041	7.8	0.069	7.8	0.047
Mid	8.7	0.065	7.9	0.049	8.5	0.076	7.2	0.047	7.9	0.045
Bottom	6.3	0.054	7.4	0.048	9.2	0.086	7.4	0.048	8.7	0.055
Average	7.8	0.061	7.3	0.058	8.2	0.068	7.5	0.055	8.1	0.049
% CoV	17%	9%	10%	**28%**	14%	**35%**	4%	23%	6%	10%
Core 4										
Top	6.9	0.070	5.5	0.074	6.8	0.063	8.6	0.058	8.4	0.050
Mid	7.8	0.049	6.8	0.045	5.4	0.055	6.8	0.039	7.6	0.064
Bottom	9.0	0.053	7.0	0.120	7.8	0.058	8.3	0.044	8.8	0.065
Average	7.9	0.057	6.4	0.080	6.7	0.059	7.9	0.047	8.2	0.059
% CoV	13%	19%	13%	**48%**	18%	7%	13%	20%	7%	14%

The coefficient of variation of fracture properties among the layers was noted to be within 25% except for three cases (marked in bold) (Table 5.4). When compared the average of three layers with each other, oil-based sealants were observed to lower the strength value with an increase in %strain at failure, thus resulting in ductility which is required to resist thermal cracking (Figure 5.41 and 5.42). While no significant change in strength is observed due to the application of WB1 compared to control section, WB1

resulted in a reduction of %Strain at failure. The traditional emulsion E1 resulted in a small increase in strength compared to control section with a reduction in %Strain at failure

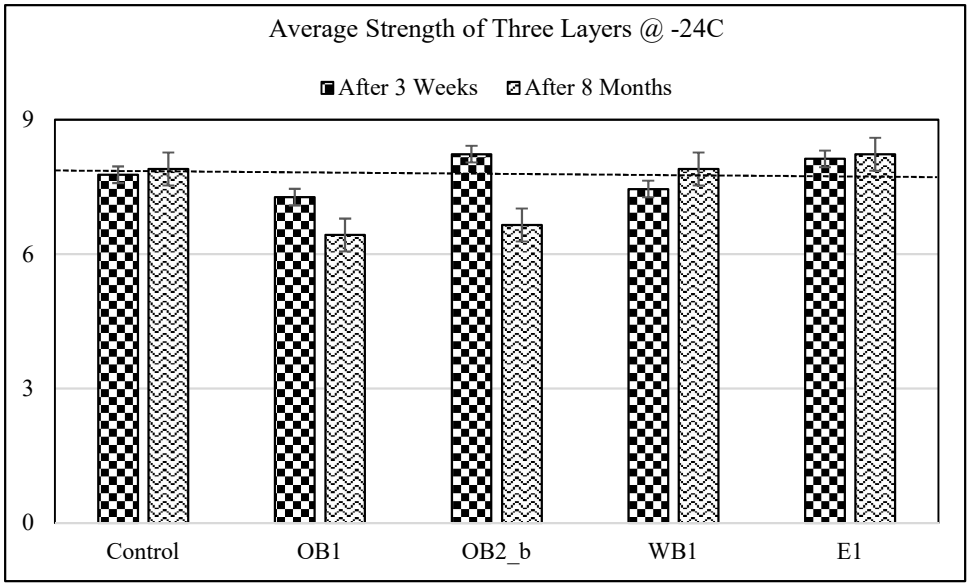

FIGURE 5.41 Average Strength at -24C for treated and untreated sections.

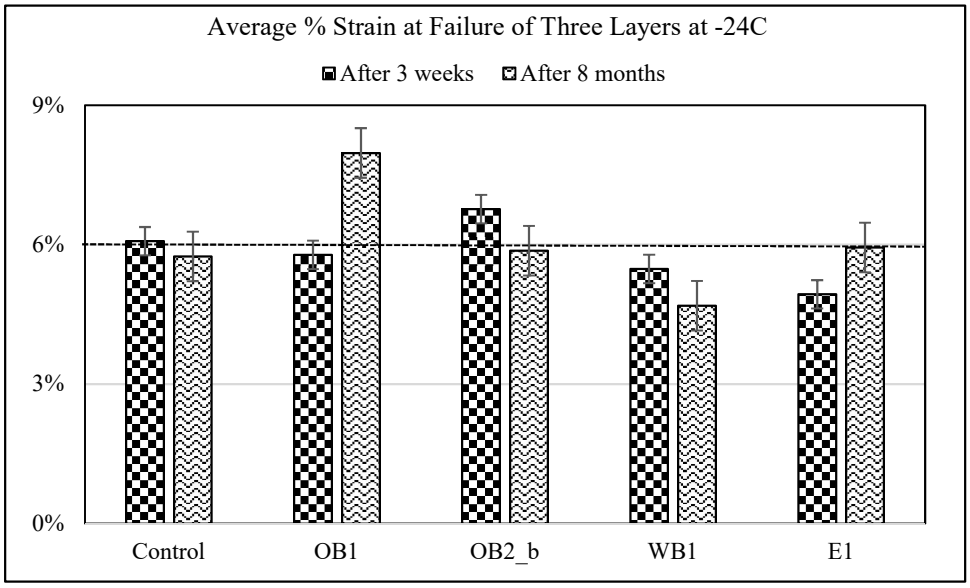

FIGURE 5.42 Average %Strain at Failure at -24C for treated and untreated sections.

5.7 Summary of Asphalt Mixture Testing

Creep and strength tests were performed on mixture beams prepared from field cores. The beams included were both field-treated and laboratory treated. The new pipette method was used to treat the beams in the laboratory, and a comparison was run between the results obtained from field-treated beams and lab-treated beams. Hardly any change in properties was noticed when the beams from the top layer, which was field treated, were compared to the control sections. When the beams from top three layers were analysed together, the changes in rheological and fracture properties of the beams from treated sections were similar to the observations of the laboratory-treated beams. A softening effect was observed in the case of oil-based OB1 and OB2 applications where the beams from field-treated sections or laboratory-treated beams resulted in lower creep stiffness and higher m-value compared to the control section. An increase in %strain at failure was also noticed for the oil-based sealant application. There were no significant changes in fracture properties because of water-based WB1 or traditional emulsion E1 application compared to the control section; however, these treatments did result in higher creep stiffness than the control section. The changes were very significant for the laboratory-treated beams due to a controlled application rate and less exposure to the environment. A more detailed analysis of the mixture results is presented in chapter 6.

Chapter 6: ANALYSIS OF THE EXPERIMENTAL RESULTS

6.1 Introduction

In this chapter, further analysis of the experimental results obtained on the asphalt binder and mixture materials investigated in this study are presented. Statistical analyses were performed to investigate the effect of bio-sealant on binders and mixtures. A semi-empirical model is used to evaluate the feasibility of relating asphalt binder and mixture properties to better understand the effect of sealant application rates to mixture properties.

6.2 Analysis of Asphalt Binder Experimental Results

A one-way ANOVA test for single factor was performed to determine the statistical significance of sealant application on the low-temperature properties of treated binders. For binder testing, only two replicates were used. The results of the ANOVA test are presented in Table 6.1. For a significance level of 5%, the variables with *p*-values smaller than 0.05 are significant and presented in bold. In some cases, the p-value is even less than 0.01 which indicates the probability of 99% that the bio-sealants have the effect on control binder. The positive and negative signs in Table 6.1 represents an increase and respectively, a decrease in properties compared to the control.

The statistical analysis verifies the findings of laboratory experiments. For the binder, the most significant effect is observed for the case when the hot binder and sealants were mixed together, as indicated by the very small p-values. The positive and negative sign in the parenthesis implicates the stiffening and softening effects, respectively (Table 6.1).

TABLE 6.1 One-Way ANOVA Test for Binder at Low-temperature

Creep Stiffness Test of Binder @ -24ºC								
P-value from One-Way ANOVA Test								
	RTFO (8 drops)		RTFO (16 drops)		PAV (8 drops)		PAV(mixing)	
	Stiffness	m-value	Stiffness	m-value	Stiffness	m-value	Stiffness	m-value
OB1	**(-)0**	**0.001**	**(-)0.0003**	0.277	**(-)0.02**	0.059	**(-)0.001**	**0.002**
OB2	**(-)0.003**	0.239	**(-)0.003**	0.487	**(-)0.02**	0.062	**(-)0.003**	**0.002**
WB1	(-)0.899	0.687	(-)0.073	0.727	**(+)0.07**	0.053	(-)0.63	0.139
E1	(+)0.051	0.766	**(+)0.015**	0.572	**(+)0.02**	0.222	(+)0.65	0.176

6.3 Analysis of Asphalt Mixture Experimental Results

A one-way ANOVA test for single factor was performed to determine the statistical significance of sealant application on the low-temperature properties of treated mixtures. Mixture beams from respective layers of all cores were used as replicates in the analysis. For mixture creep-stiffness and m-value, a total of 9 replicates where used, whereas for strength and strain at failure, 12 replicates were used. The results of the ANOVA test are presented in Tables 6.2 and 6.3 for two different temperature, -24ºC and -12ºC, respectively. For a significance level of 5%, the variables with *p*-values smaller than 0.05 are significant and presented in bold. In some cases, the p-value is even less than 0.01 which indicates the probability of 99% that the bio-sealants have the effect on control binder/mixture. The positive and negative signs in Tables 6.2 and 6.3 represent an increase and respectively, a decrease in properties compared to the control.

The statistical analysis verifies the findings of laboratory experiments. For the mixtures, only a few significant effects are observed for the field mixtures, while significant changes in almost all properties investigated are seen for the laboratory treated mixtures.

TABLE 6. 2 p-value from One-Way ANOVA Test for Mixture at -24ºC

Creep Stiffness and Strength Test of Mixture Beams @ -24ºC									
		Stiffness, MPa		**m-value**		**Strength, MPa**		**Strain @ Failure**	
Sealants		Field	Lab	Field	Lab	Field	Lab	Field	Lab
Oil-Based	OB1	**0.040**	**(-)0.000**	0.210	**(+)0.000**	*0.059*	**(-)0.001**	*0.057*	**(+)0.000**
	OB2_a	0.310	**(-)0.001**	**0.011**	**(+)0.000**	0.293	0.803	0.340	**(+)0.000**
	OB2_b	0.740	**(-)0.000**	0.450	**(+)0.000**	**0.041**	**(+)0.016**	*0.060*	**(+)0.000**
Water-Based	Wb1	0.250	0.170	*0.060*	**(+)0.002**	0.357	**(+)0.015**	0.473	*0.070*
	E1	0.230	**(-)0.004**	0.690	**(+)0.005**	0.327	0.432	0.170	0.222

TABLE 6. 3 p-value from One-Way ANOVA Test for Test Results at -12ºC

Creep Stiffness and Strength Test of Mixture Beams @ -12ºC									
		Stiffness, MPa		**m-value**		**Strength, MPa**		**Strain @ Failure**	
Sealants		Field	Lab	Field	Lab	Field	Lab	Field	Lab
Oil-Based	OB1	0.632	**5.02E-07**	0.972	**0.000**	0.534	**2.19E-13**	0.246	**1.06E-11**
	OB2_a	0.474	**9.16E-08**	0.126	**0.000**	0.366	**0.0038**	**0.014**	**1.39E-05**
	OB2_b	0.189	**4.79E-08**	0.064	**0.001**	0.812	**0.0059**	**0.027**	**2.34E-06**
Water-Based	WB1	**0.037**	**0.0126**	0.074	**0.000**	0.274	0.6757	**0.037**	**0.00037**
	E1	0.672	0.335	0.953	**0.007**	0.641	**0.0396**	0.277	**0.032**

6.4 Application of Hirsch Model to Experimental Binder and Mixture Data

In this analysis, Hirsch semi empirical model is used to relate binder and mixture properties and to investigate if it is possible to predict treated mixture properties from treated binder properties. The goal is to determine if changes in mixture behavior are due to the addition of sealant. In the calculations, only the creep stiffness results at -24ºC were used. After a number of iterations, it was decided to only use the experimental binder creep stiffness results obtained on samples treated in the laboratory using the pipette method. Both RTFO-aged and PAV-aged binder beams were treated with sealants to predict the

mixture creep stiffness. The predicted mixture creep stiffness was then compared with the obtained experimental mixture creep stiffness data for Core 3 only, for both field treated (top layer) and lab-treated (bottom layer) samples. Core 3 results were used since it was the only core from which the top was not removed, and therefore was the closest to real field conditions.

6.4.1 Forward Problem

Christensen et al. (2003) proposed a semi-empirical model based on Hirsch model (Hirsch, 1962) which can estimate the extensional and shear dynamic modulus. This model is used to solve the forward problem of predicting mixture stiffness from experimental binder stiffness. The general equation for the semi-empirical model is

$$S_{mix}=P_c[E_{agg}*V_{agg}+S_{binder}*V_{binder}]+(1-Pc)*[(V_{agg}/E_{agg})+(1-V_{agg})^2/(S_{binder}*V_{binder})]^{-1} \quad (1)$$

where:

S_{mix}= effective creep stiffness of the mixture,

E_{agg}, V_{agg}= modulus and volume fraction of the aggregate,

S_{binder}, V_{binder}= creep stiffness and volume fraction of binder and

P_c= contact volume is an empirical factor defined as:

$P_c=0.1*LN(E_{binder}/a)+0.609$; a= 1000 MPa.

Volume fraction of aggregate and binder were calculated from the information provided in the mix design data-sheet. The total binder was 4.8% of which 3.9% was the newly added fresh binder along with the rest of it coming from the RAP. The calculation was performed using both Pb=3.9% and Pb=4.8%, where Pb is the percent binder used.

The observed difference was very negligible. Therefore, the plots obtained using Pb=4.8% are presented.

Since the modulus of aggregate is not known, based on a study by Zofka et al., both E_{agg}=19GPa and E_{agg}=29GPa were used. Zofka et al. (2005) used a value of aggregate modulus different from the original formulation, proposed by Christensen (2003) (19GPa instead of 29GPa) with better fitting results. As a result in this study, both values were used. The results are shown in Figures 6.1-6.10.

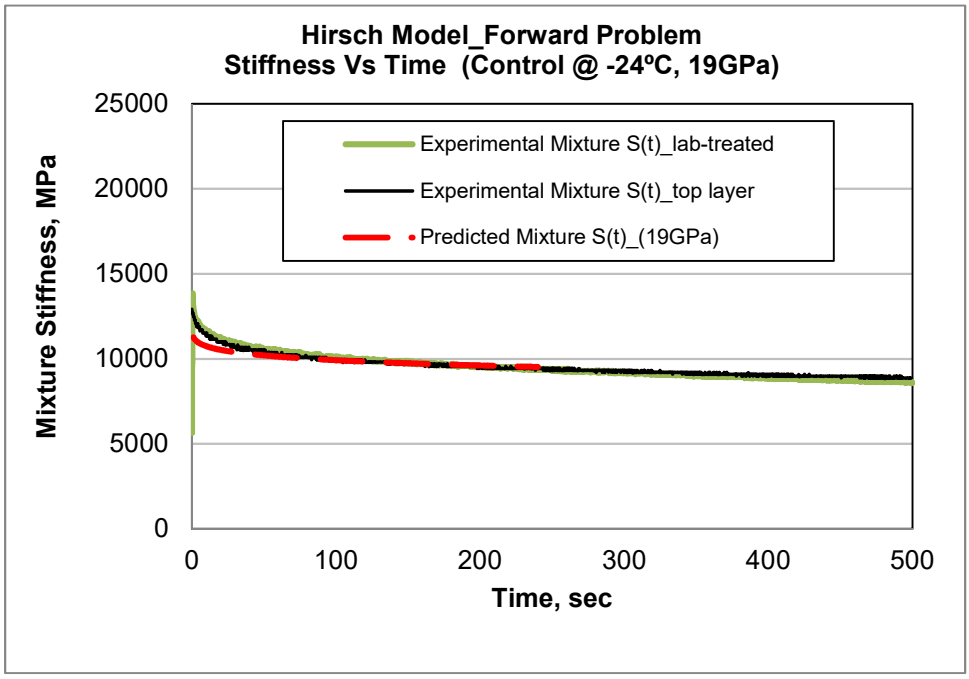

FIGURE 6.1 Hirsch Model using E_{agg}=19 GPa for Control RTFO-aged PG 58-28.

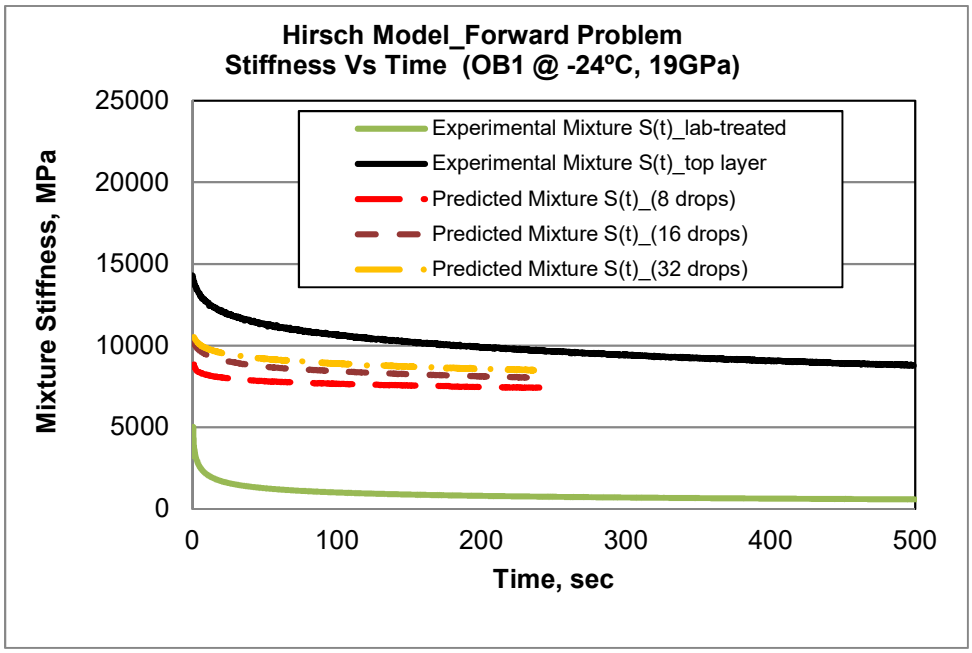

FIGURE 6. 2 Hirsch Model Using Eagg=19 GPA for RTFO-aged PG 58-28 Treated with OB1.

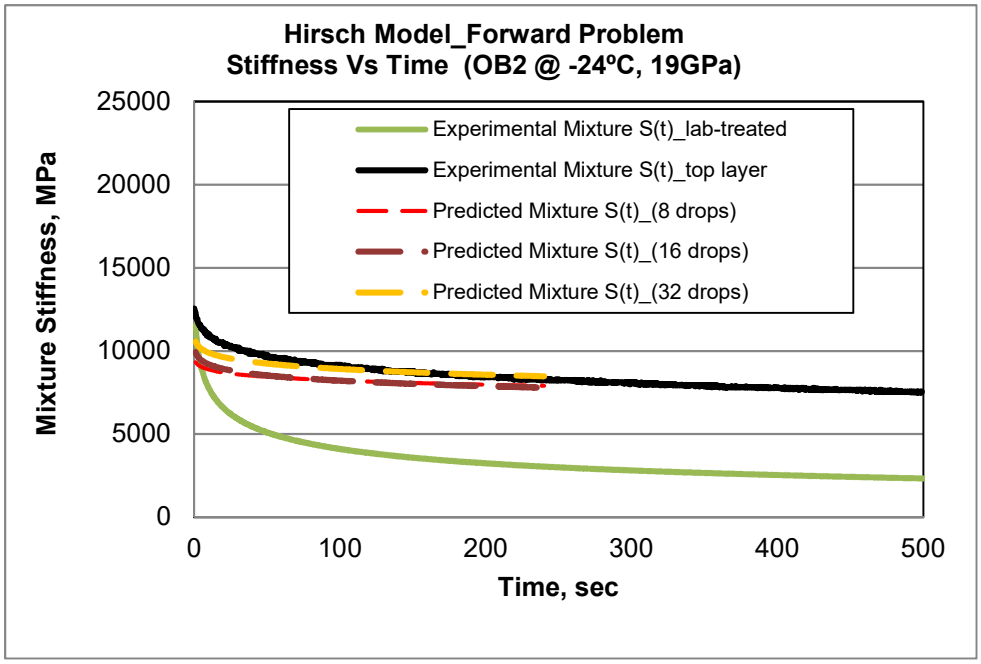

FIGURE 6. 3 Hirsch Model Using Eagg=19 GPA for RTFO-aged PG 58-28 Treated with OB2.

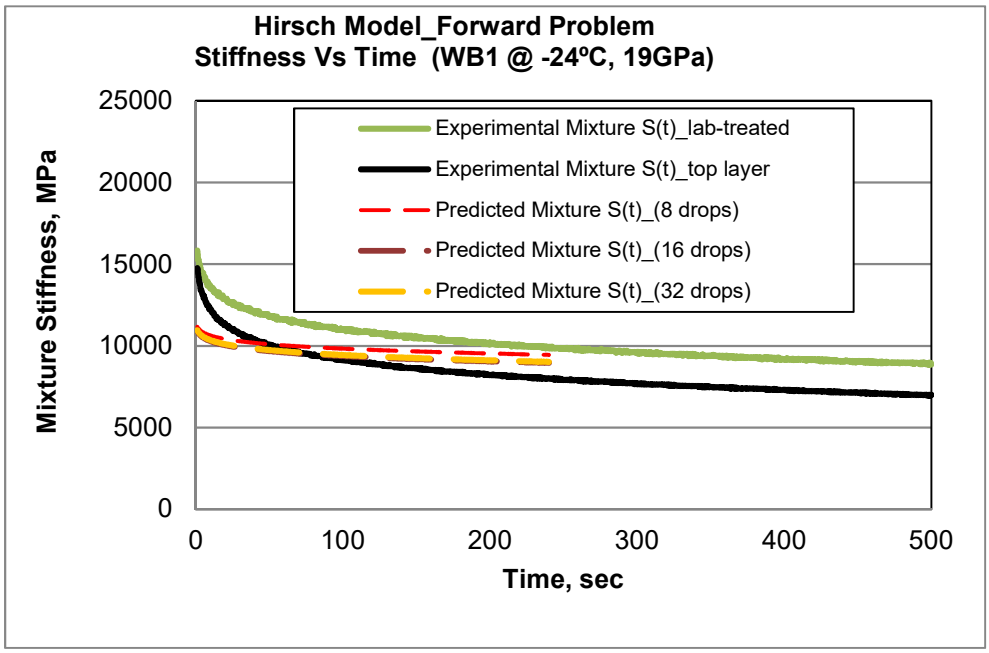

FIGURE 6. 4 Hirsch Model Using Eagg=19 GPA for RTFO-aged PG 58-28 Treated with WB1.

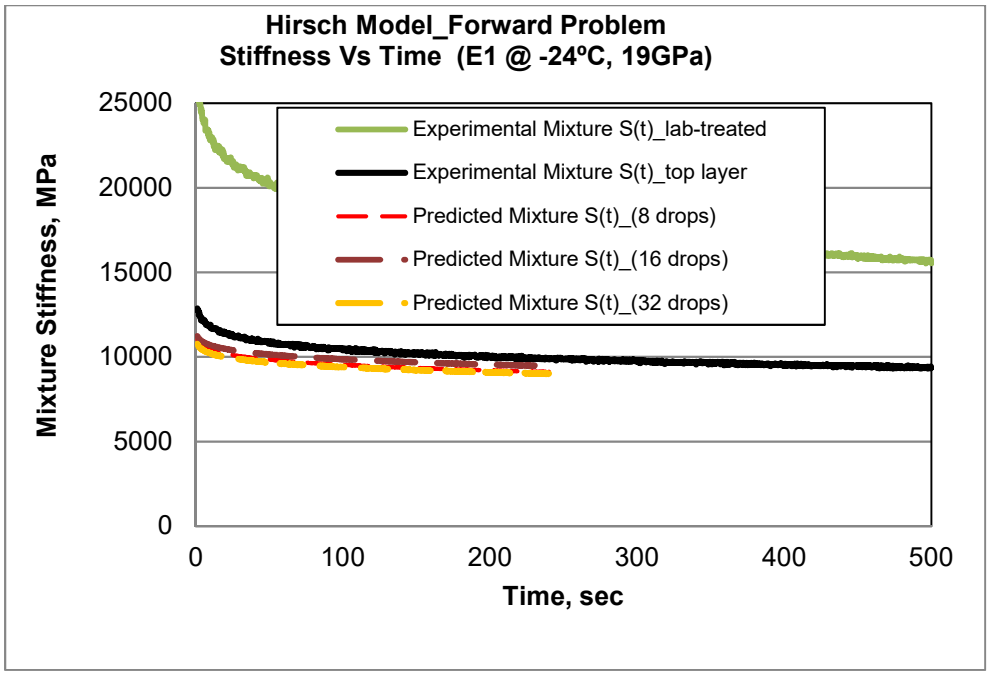

FIGURE 6. 5 Hirsch Model Using E_{agg}=19 GPA for RTFO-aged PG 58-28 Treated with E1.

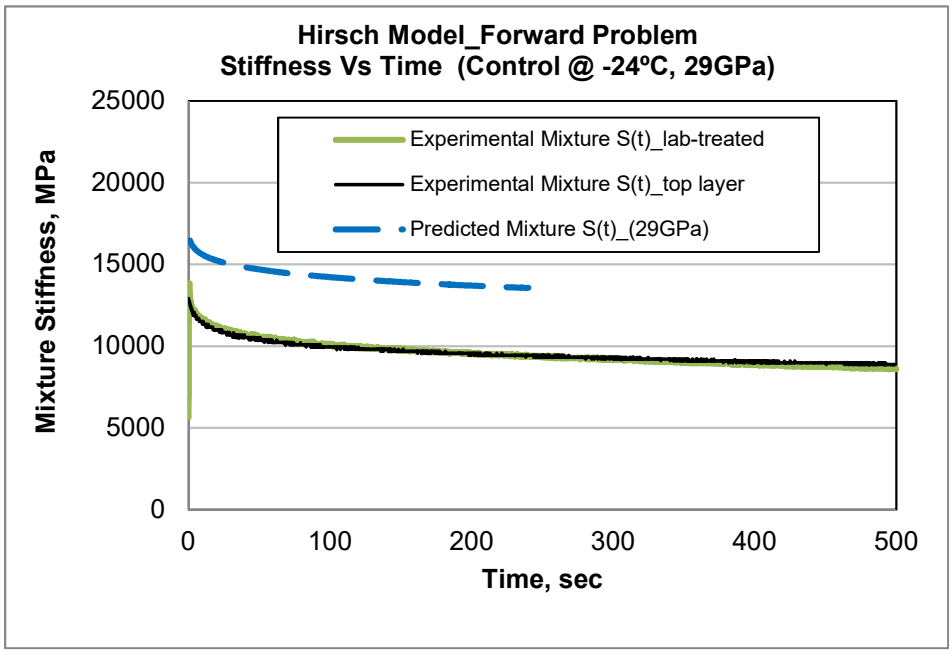

FIGURE 6.6 Hirsch Model using Eagg=29 GPa for control RTFO-aged PG 58-28.

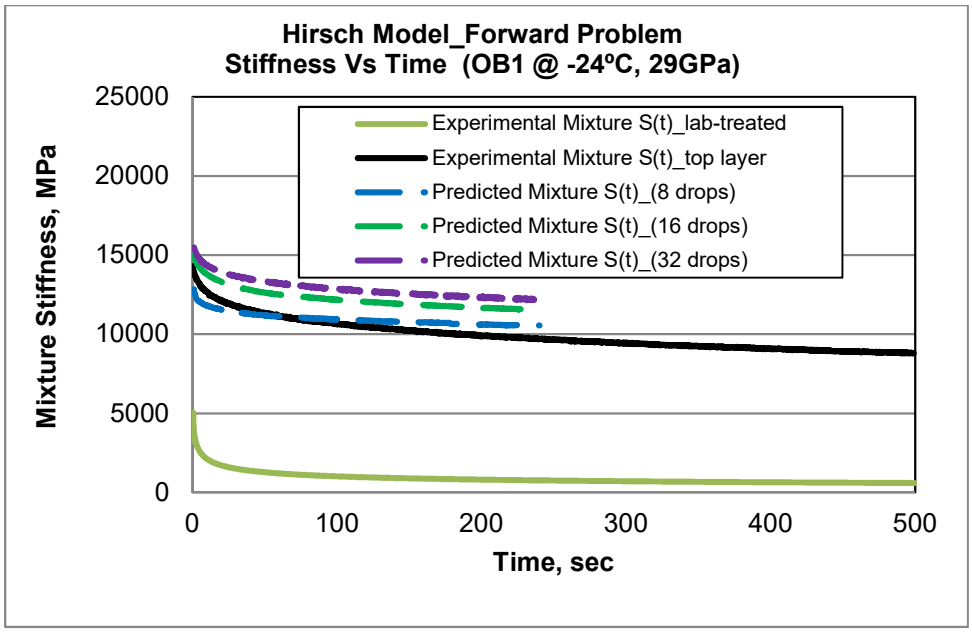

FIGURE 6. 7 Hirsch Model Using Eagg=29 GPA for RTFO-aged PG 58-28 Treated with OB1.

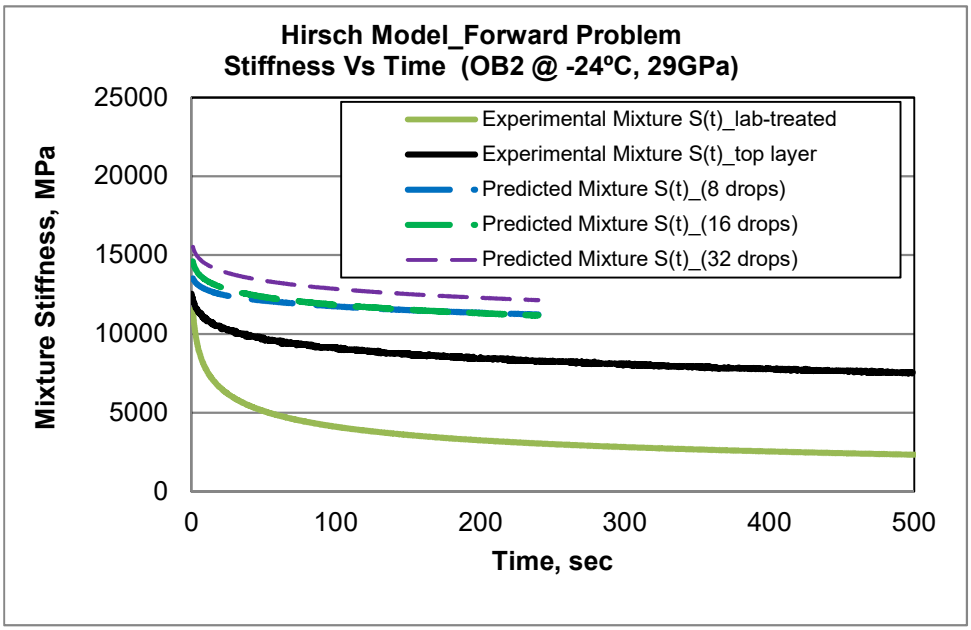

FIGURE 6. 8 Hirsch Model Using Eagg=29 GPA for RTFO-aged PG 58-28 Treated with OB2.

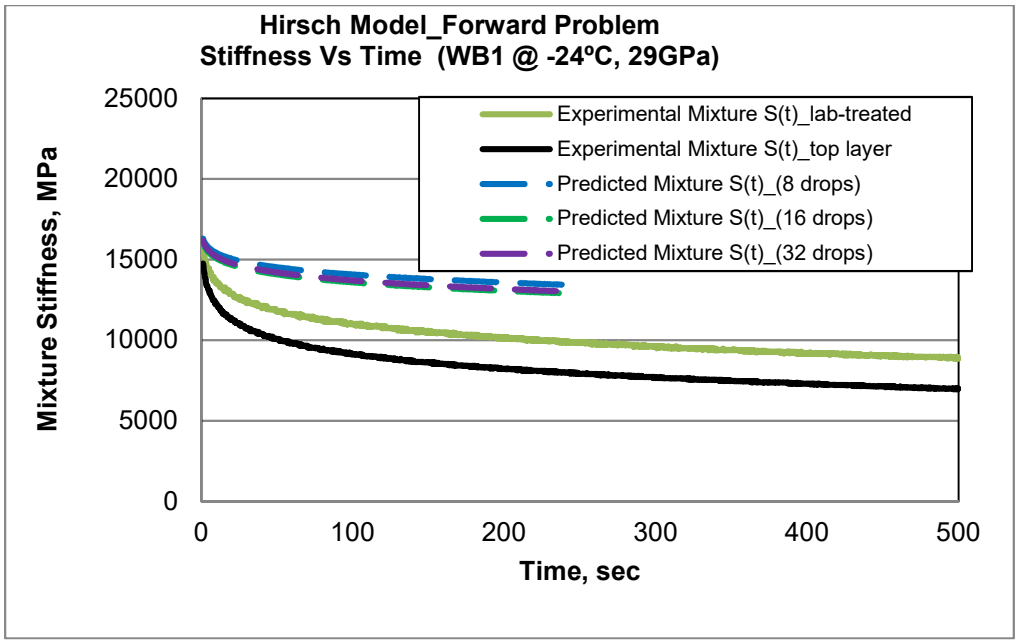

FIGURE 6. 9 Hirsch Model Using Eagg=29 GPa for RTFO-aged PG 58-28 Treated with WB1.

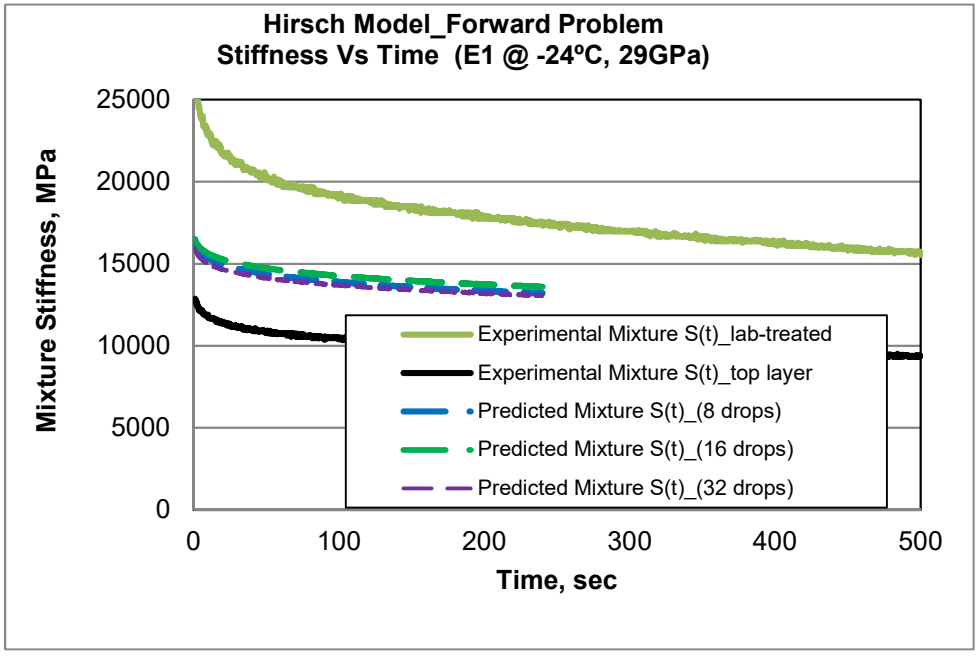

FIGURE 6.10 Hirsch Model Using Eagg=29 GPa for RTFO-aged PG 58-28 Treated with E1.

The Hirsch model using E_{agg} = 19GPa predicts reasonable well the field mixture properties for the control binder and binder treated with WB1 and E1; the model under predicts the mixture stiffness for the oil based sealants (Figure 6.1-6.5). Hirsch model using E_{agg} = 29GPa over predicts the mixture stiffness for all four sealants (Figures 6.7-6.10). The opposite trend is also visible for two different aggregate modulus when increasing the application rate of the sealant. The predicted mixture stiffness using E_{agg} = 19GPa gets closer to the field-treated mixture stiffness with increase in no. of drops or application rate of sealant, while the predicted mixture using E_{agg} = 29GPa moves away from the field-treated mixture stiffness (Figures 6.1-6.10). In addition, it can be observed that the stiffness values for the laboratory treated mixture beams is much lower for the oil-based sealants and it is higher for the water based sealants, compared to the predicted values. These results may indicate some other changes occur in the mixture beams prepared in laboratory conditions.

6.4.2 Inverse Problem

For the inverse problem, in which binder creep stiffness is predicted from experimental mixture creep stiffness, a simplified procedure developed by Zofka et al. (2005) was used. In this procedure, binder stiffness values between 50 to 1000MPa are selected and the corresponding mixture creep stiffness is obtained using Equation 1. Then, a simple function (Equation 2) is fitted to the plot obtained in this manner (Figure 6.11), and the function coefficients are obtained.

$$S_{mix} = a^* \ln (S_{binder}) + b \quad (2)$$

where a and b are regression parameters. The advantage of this simple equation is that S_{binder} can be easily calculated from S_{mix}, which could not be done using equation 1 directly. Examples of the inverse problem results are shown in Figures 6.12 to 6.14. Additional results are presented in appendix A.

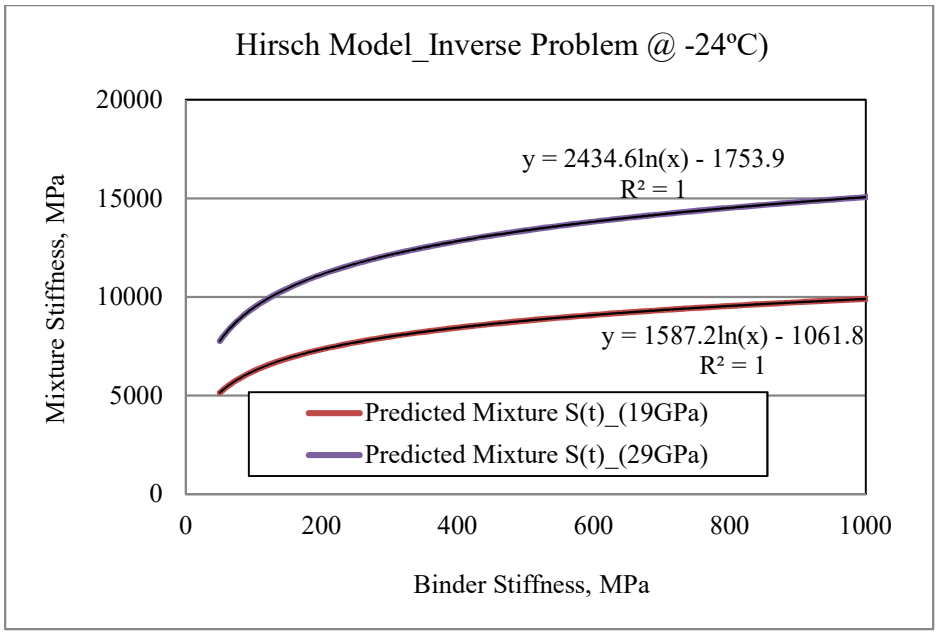

FIGURE 6.11 Simplified Mixture stiffness function.

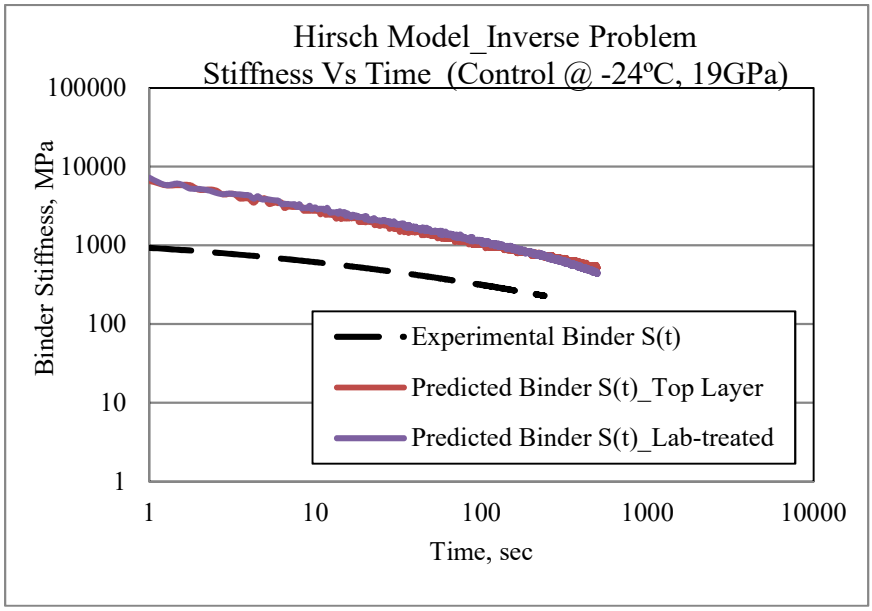

FIGURE 6.12 Hirsch Model Using Eagg=19 GPa for Control Mixture Section.

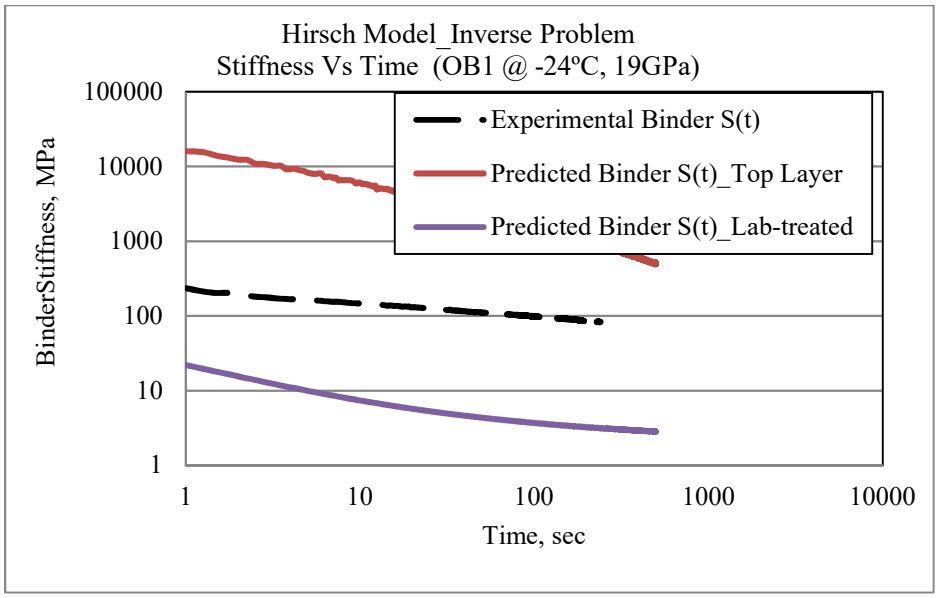

FIGURE 6.13 Hirsch Model Using Eagg=19 GPa for Mixture Treated with OB1.

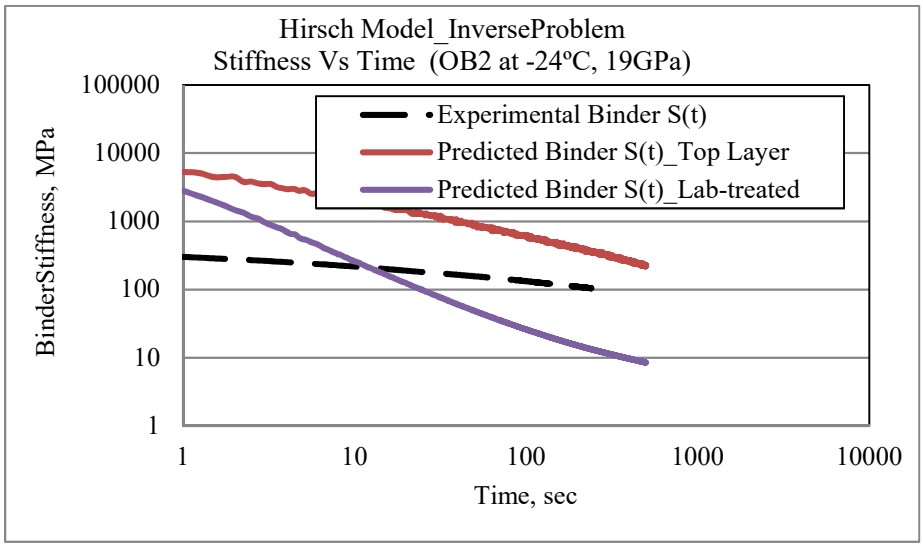

FIGURE 6.14 Hirsch Model using Eagg=19 GPa for Mixture treated with OB2.

In general, the results of the inverse problems were not consistent and were very sensitive to small errors in the experimental data. As a result, the use of this method was not pursued further.

6.5 FTIR Analysis

To better understand the results of the mechanical testing presented in the previous section, Fourier Transform Infrared absorption spectroscopy (FTIR) evaluations were performed on two sealants and on the corresponding extracted binders obtained from the mixture beams used in the experimental laboratory testing. This was done to detect the presence of these sealants on the surface of the field cores and in the laboratory treated asphalt mixture beams. The presence of the other two sealants could not be tested since their corresponding spectrum matched the asphalt binder spectrum. Test specimens were prepared by evaporating residue from liquid samples and then configuring them as Cap Film on NaCl Window specimens.

Stacked absorbance spectra are shown in Figures 6.15 and 6.16 for wavenumbers in the region between 455.13 and 3995.85 cm-1. In both cases, it is noticed that traces of the sealants were detected only in the laboratory treated samples and not in the field treated samples. It is not clear what the mechanism responsible for this difference is.

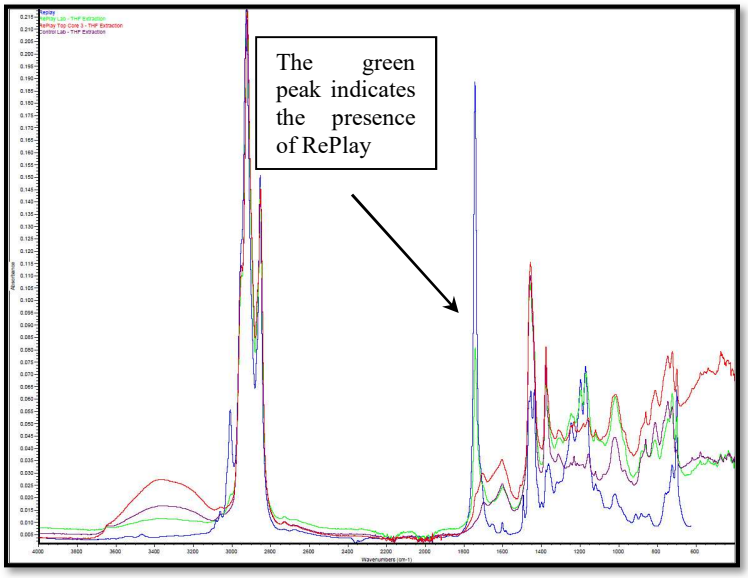

FIGURE 6.15 Stacked absorbance spectra for OB1 and OB1 treated samples.

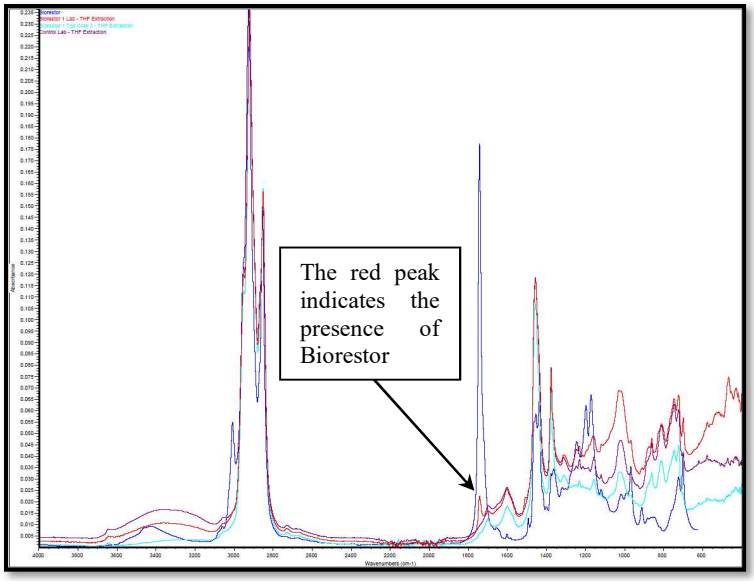

FIGURE 6.16 Stacked absorbance spectra for OB2 and OB2 treated samples.

6.6 Field Investigation

As part of the field performance testing and monitoring, distress surveys of the shoulder test sections were performed after product installations (September 28 and October 29, 2014), the following spring (April 23, 2015) and the year after that (April 14, 2016). The relative performance of cracking values from 2015 and 2016, as compared to baseline values from 2014, is shown in the Figure 6.17 (E. Johnson and A. Joseph, "LRRB 974 Field Investigation of Non-traditional and Bio-Based Asphalt Sealers", working report, Minnesota Local Road Research Board and Minnesota Department of Transportation, Minnesota). The trend of transverse crack of mile depending on the various treated sections shows resemblance and similar pattern with creep stiffness of lab-treated samples at -24C (Figure 6.17). The treated sections with lower stiffness experienced less number of cracks and vice versa.

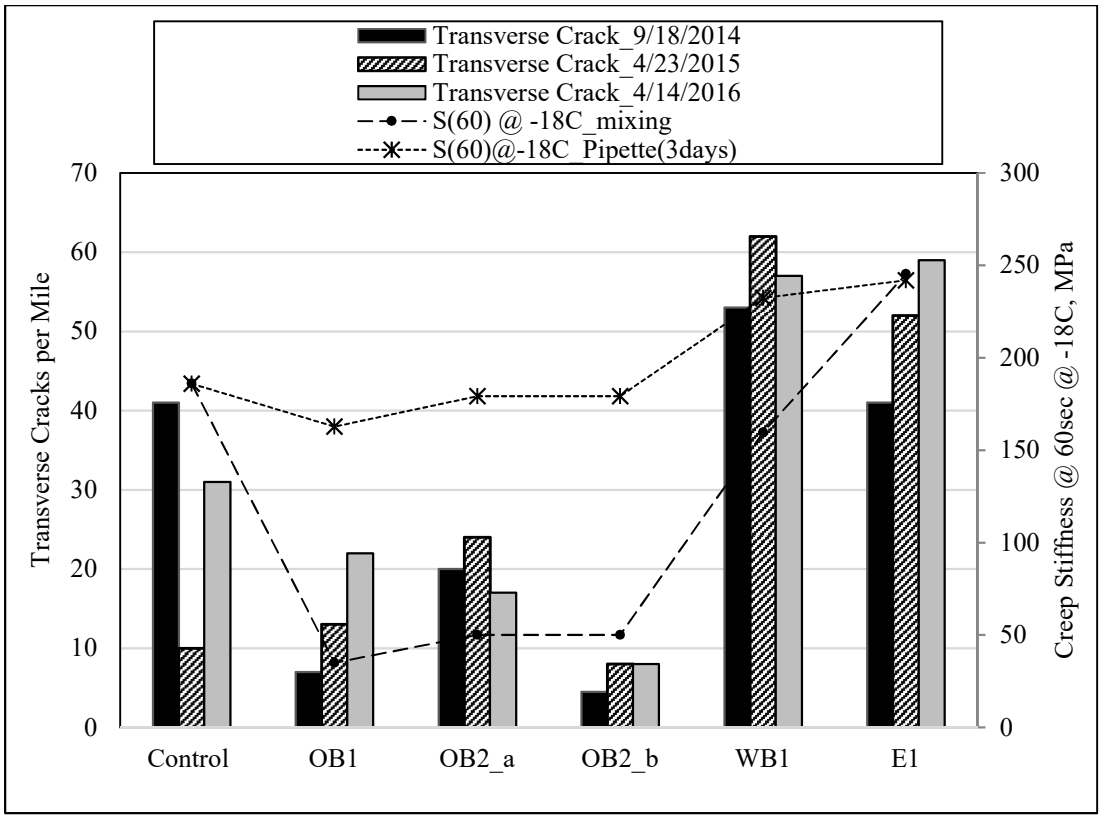

FIGURE 6.17 Transverse Cracking Histories.

However, since the sections already had some pre-existing cracks prior treatment, it is more reasonable and important to compare the crack growth rate after treatment. The cracking rate on each section was compared by fitting linear least squares from the cracking history data to produce slope and intercept values in units of cracks per mile per year. Figure 6.18 is a plot of the difference between those cracking rates when compared to the control section.

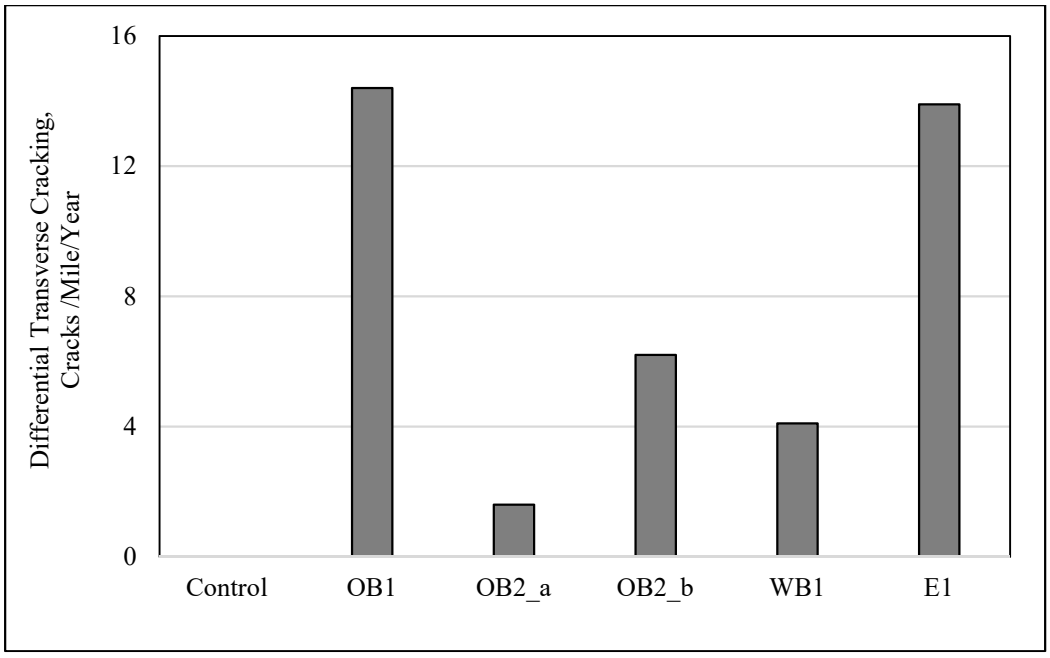

FIGURE 6. 18 Differential Cracking Rates. (E. Johnson and A. Joseph, "LRRB 974 Field Investigation of Nontraditional and Bio-Based Asphalt Sealers", working report, Minnesota Local Road Research Board and Minnesota Department of Transportation, Minnesota).

The greatest rate difference values occurred in the E1 and OB1 treated sections. A similar trend of rate difference was observed in the laboratory testing when plotted the change in creep stiffness of lab-treated samples at -24C with respect to control section. The OB1 and E1-treated sections experienced the most softening and stiffening effect, respectively due to the sealant application (Figure 6.19). Their change in creep stiffness was nearly 100% in laboratory experiment along with resulting in the highest crack-growth rate per year in the field investigation (Figure 6.18 and Figure 6.19). This indicates that both extreme stiffening and softening might be detrimental to the pavement. Therefore, it is important to investigate application rate of sealant to control the stiffness and crack-growth rate.

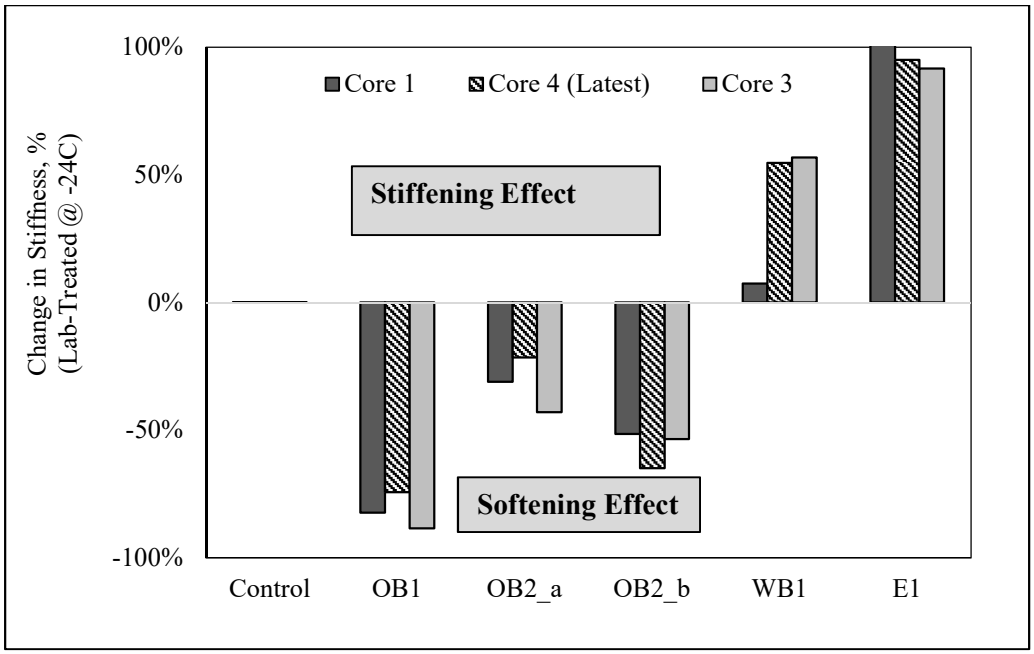

FIGURE 6.19 Change in Creep Stiffness Due to Sealant-Application.

6.7 Summary of Result Analysis

In this chapter, the results obtained through asphalt binder and mixture testing were analysed using one-way ANOVA test, Hirsch Model and FITR evaluation. Finally, distress survey from field performance testing and monitoring was used to establish correlation with the laboratory findings. The p-value from ANOVA test verifies laboratory findings resulting in statistical significance for the laboratory-treated samples. Hirsch model can be used to predict asphalt mixture stiffness using experimental binder stiffness efficiently. The results of the field distress survey of the treated and untreated sections show good correlation with the laboratory findings.

Chapter 7: DEVELOPMENT OF BINDER STRENGTH TEST

7.1 Introduction

The current Superpave specifications address the low-temperature properties of asphalt binders using experimental data from two laboratory instruments developed during the Strategic Highway Research Program (SHRP) research effort: The Bending Beam Rheometer (BBR) (AASHTO T313, 2012) and the Direct Tension Tester (DTT) (AASHTO T314, 2012). The BBR was used to perform low-temperature creep tests on beams of long term aged asphalt binders conditioned at the desired temperature for 1 hour. The DTT was used to perform low-temperature uniaxial tension tests at a constant strain rate. Average stress and strain at failure were obtained.

7.1.1 Background

The development of the Performance Grade (PG) criterion (AASHTO M320, 2010) for low-temperature cracking assumed that the 2-hour mixture stiffness correlated well with the severity of thermal cracking in the field (Anderson & Kennedy, 1993; Readshaw, 1972). This assumption was extended to asphalt binder stiffness obtained in low-temperature creep tests. The time-temperature superposition principle (Ferry, 1980) was used to expedite the testing process and show that, for asphalt binders in general, the stiffness at 60 seconds at T1ºC is approximately equal to the stiffness at 2 hours at T1-10ºC (Anderson & Kennedy, 1993; AASHTO T313, 2012). The effects of physical hardening were not considered to keep the PG binder specification to a reasonable level of simplicity, (Bahia, 1991; Anderson et al., 1994; Anderson & Marasteanu, 1999) although one of the major findings during SHRP was the significant effect of physical hardening on binder physical properties. The validity of these simplifications is discussed in detail elsewhere (Basu, Marasteanu, & Hesp, 2003; Marasteanu, Basu, Hesp, & Voller, 2004).

The slope at 60 seconds of the stiffness vs. time curve on a double logarithmic scale, the m-value (AASHTO T313, 2012), was introduced as an additional parameter to control the rheological type of asphalt binders and to eliminate heavily blown asphalts, which in fact were associated with poor fatigue performance. This additional criterion was based on

the idea that a low m-value corresponded to slower relaxation of the thermal stresses that build up at low temperatures, which was detrimental to performance.

A simple fracture test (AASHTO T314, 2012) was also developed as part of the original SHRP binder research. A dog bone shaped specimen is pulled with a constant strain rate of 3%/minute, and the tensile failure stress and strain are obtained. A second critical temperature was obtained as the temperature at which the failure strain is 1%. The 0ºC shift was also applied to this temperature, using the extensive work performed by Dongré, (1994) in which he showed that TTSP also applied to the failure properties of the SHRP core binders. According to Dongré, the strain rate and the strain limit were chosen based on practical considerations: to shorten the duration of the test to less than one minute and to obtain limiting temperatures similar to the limiting temperatures obtained from BBR creep data. Due to DTT cost and low repeatability of the results, the direct tension test is not always used in the selection process. While rheological experiments are highly repeatable, as seen for DSR and BBR data, fracture experiments are known to be less repeatable. The analysis of the test data for large sets of binders has shown that the repeatability issue is significant only for certain types of binders, which indicates that the reduced repeatability may be a material property or a specimen preparation problem and not a testing problem. The repeatability issue, the complex sample preparation, and the high cost of the instrument made this testing approach less appealing to the industry. Also, current DTT devices are not capable of maintaining a constant strain of 3%/minute at the beginning of the test (Marasteanu and Anderson, 2000), which makes the use of the experimental data less applicable to modeling of binder behavior.

7.1.2 Objective

Many agencies do not perform DTT and entirely depend on the creep properties of the binder at low-temperature. The creep stiffness obtained with the BBR can be related to thermal stress accumulation as temperature moves into negative values; however, without knowledge of failure properties, it is impossible to correctly predict the cracking resistance of these materials, especially for modified binders. Developing an alternative test method,

which can be easily performed and implemented, to determine the failure properties of asphalt binders at low temperature becomes, therefore, an important objective.

7.2 Literature Review of Binder Strength Test

In previous work, the authors have proposed a new strength testing method using a modified BBR device, called BBR-Pro, which is equipped with proportional valve air bearing system (Marasteanu et al., 2012b). This device can apply loads up to 44N with different loading rates for performing strength tests. Figure 7.1 presents the BBR-Pro and the corresponding three-point bending (3PB) testing configuration while Figure 7.2 presents the traditional DTT set up. The test method using BBR and DTT is presented next.

7.2.1 Strength Test Using Bending Beam Rheometer

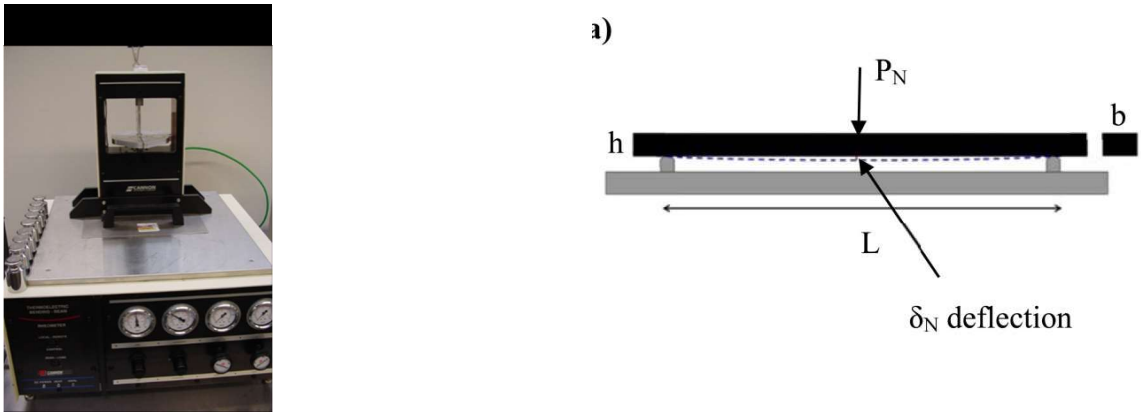

FIGURE 7.1 (a) BBR-Pro and (b) testing configuration.

BBR strength tests were performed with the BBR-Pro device and nominal strength, σ_N_BBR, and nominal strain, δ_N_BBR, were computed according to the following equations:

$$\sigma_{N\_BBR} = \frac{3 \cdot P_{N\_BBR} \cdot l_{BBR}}{2 \cdot b_{BBR} \cdot h_{BBR}^2} \tag{7.1}$$

$$\varepsilon_{N\_BBR} = \frac{6\delta_N h_{BBR}}{l_{BBR}^2} \tag{7.2}$$

where P_N_BBR is the maximum measured load (N), and δ_N_BBR is the deflection (mm) of the beam corresponding to maximum load P_N_BBR.

Tests were conducted on asphalt binder beams identical to the beams used for BBR creep testing: l_{BBR} = 102mm, b_{BBR} = 12.5mm, h_{BBR} = 6.25mm, with a total volume V_{BBR} = 7969mm^3. The duration of specimen conditioning was set to 1h; a different conditioning time was also used. Tests were conducted in ethanol, as prescribed in the current BBR creep standard (AASHTO T313, 2012), in potassium acetate, as prescribed in the current DTT standard (AASHTO T314, 2012), and air.

7.2.2 Strength Test Using Direct Tension Tester

DTT was run according to the current AASHTO standard (AASHTO T314, 2012) with a strain rate of 3% per minute. The total specimens volume is V_{DTT}=1946 mm^3 and consist of small dog-bone shape samples of asphalt binder subjected to long term aging with the Pressure Aging Vessel (PAV) apparatus (AASHTO T314, 2012). Conditioning and testing were performed in potassium acetate (Dongré & D'Angelo, 1998), and nominal stress and nominal strain were recorded until failure. Figure 7.2 provides a picture of the testing device and a schematic of the DTT test.

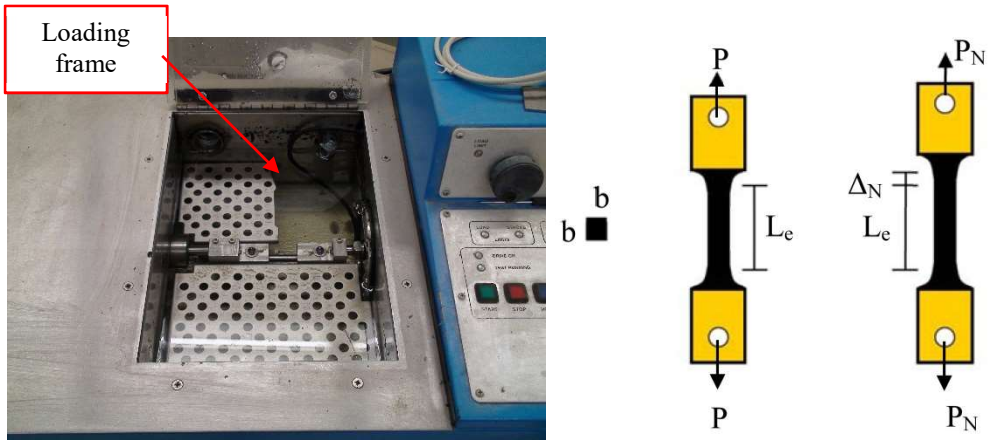

(a) (b)

FIGURE 7.2 (a) DTT device and (b) test schematic.

The nominal strength, σ_{N_DTT} (MPa) and nominal failure strain ε_{N_DTT} are calculated as:

$$\sigma_{N\_DTT} = \frac{P_{N\_DTT}}{A} \quad (7.3)$$

$$\varepsilon_{N\_DTT} = \frac{\Delta_N}{L_e} \quad (7.4)$$

where P_{N_DTT} is the failure load (N), A is the original area of the cross section (mm^2), $A=b_{DTT}\times b_{DTT}$, b_{DTT} is the cross-section side (b=6 mm), ΔN is the elongation at failure (mm), and Le is the effective gage length (33.8mm).

7.2.3 Preliminary Testing

In previous work, the authors have proposed a new strength testing method using a modified BBR device, called BBR-Pro (Marasteanu et al., 2012). In their investigation, the authors demonstrated that, by taking into account the size effect and the cooling medium effect, the two testing method results in strength values that are similar (Marasteanu et al., 2012; Falchetto et al., 2012). However, they did not provide a clear path towards the development of a specification that can replace DTT. Additional testing and viscoelasticity concepts are presented next to overcome this obstacle.

7.2.4 Summary

This preliminary investigation identifies potassium acetate and air as cooling medium for failure tests and provides support to the idea that the DTT and BBR strength methods provide similar information about the failure properties of asphalt binders at low temperature. However, it does not provide a clear path towards the development of a simple failure test that can replace DTT. The main obstacle is selecting the appropriate loading rate to obtain comparable results and to keep the testing time within reasonable limits. Additional testing and viscoelasticity concepts are used next to overcome this obstacle.

7.3 Experimental Analysis

7.3.1 Preliminary Testing of Selecting Initial Loading Rate of BBR Strength Test

Several BBR strength tests were performed on PG 58-28 binder using various loading rates to match the DTT strain rate of PG 58-28 (FIGURE 7.3). However, to match the strain rate of DTT (slope of strain vs. time), the loading rate of BBR was observed to be too fast to obtain a reasonable amount of test duration for the stress-strain curve (FIGURE 7.3 a). Another attempt was made to match the slope of the stress-strain curve of DTT, where the loading rate of BBR strength test was too slow to break the binder beam and obtain stress or strain at failure (FIGURE 7.3 b). Finally, a loading rate of 0.53N/sec for BBR strength test was selected to match the stress rate in the DTT (FIGURE 7.3 c).

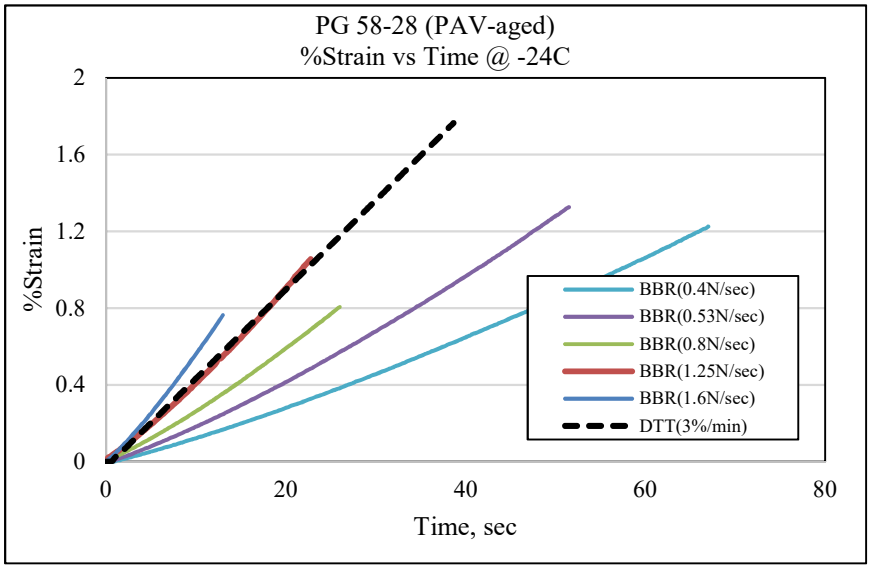

(a)

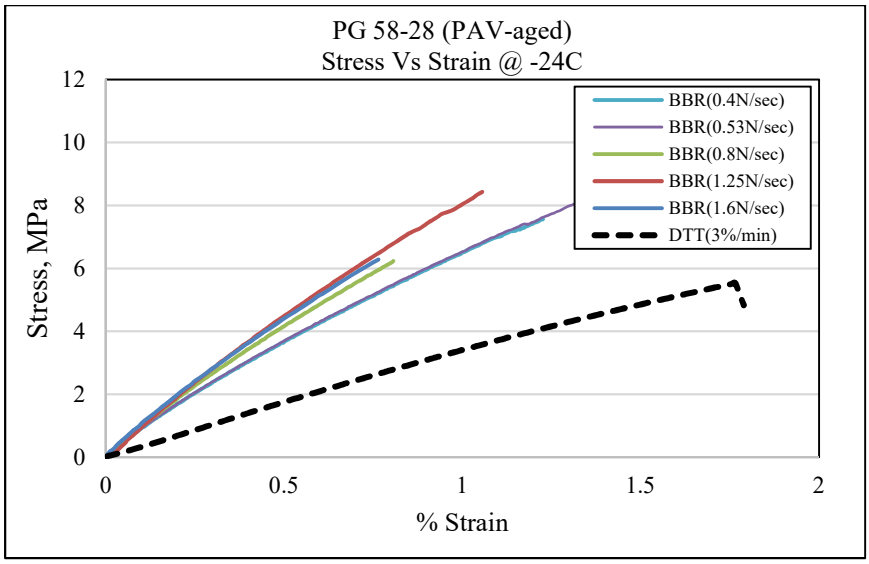

(b)

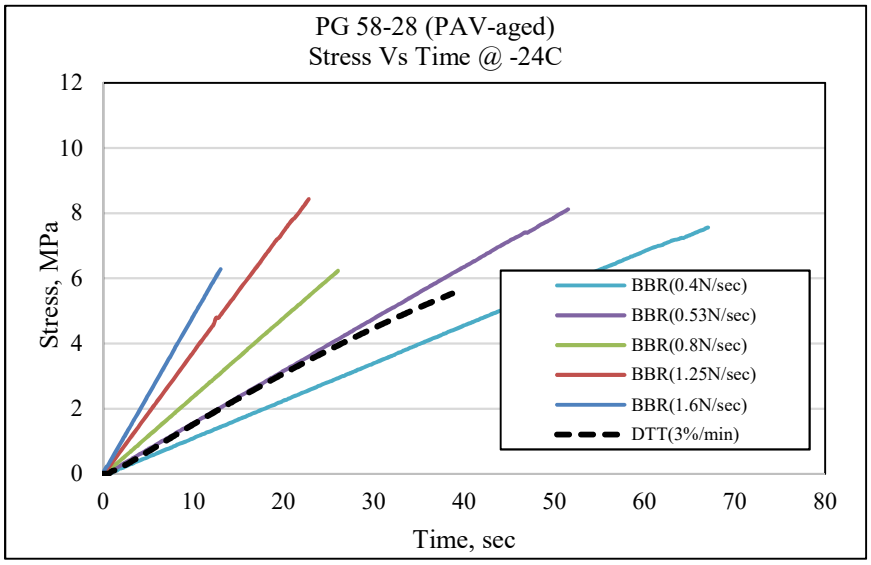

(c)

FIGURE 7.3 Selection of Loading Rate for BBR Strength Test.

7.3.2 Preliminary Testing of a Plain and Modified Asphalt Binder

To better understand the limitations and benefits of the two methods, DTT and BBR, linear viscoelasticity concepts are used to analyze the experimental data obtained on two binders: a plain PG64-28 (U), and an SBS-modified PG64-28 (M). The binders have

similar creep properties, as indicated by the similar performance grade. However, the DTT responses are quite different, as shown in Figures 7.4 and 7.5. The idea was to determine if BBR strength can also differentiate between the two binders.

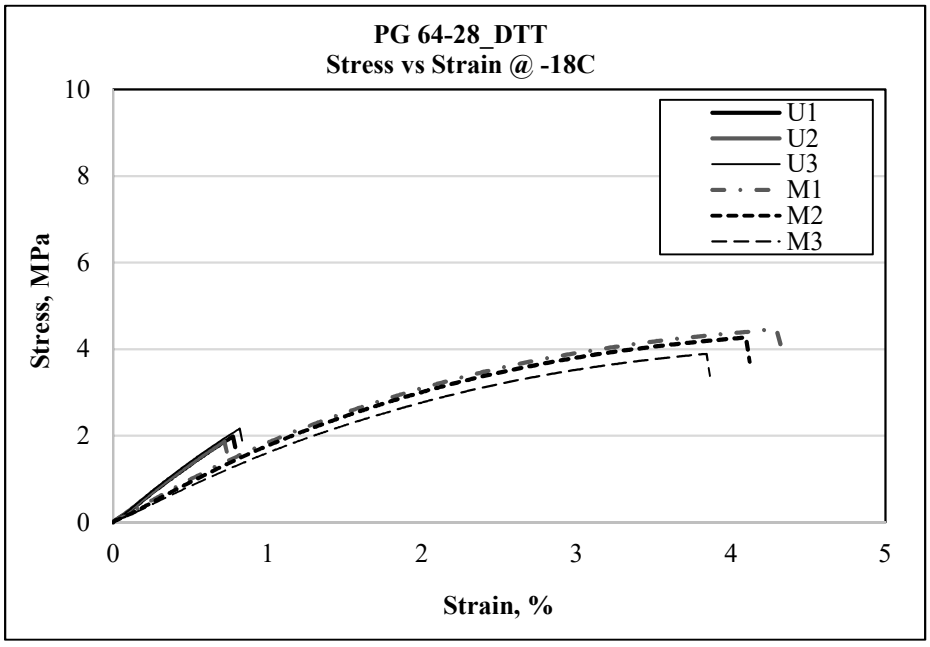

FIGURE 7.4 DTT Stress vs. Strain @ -18C for PG 64-28_U (unmodified) and PG 64-28_M (SBS-modified).

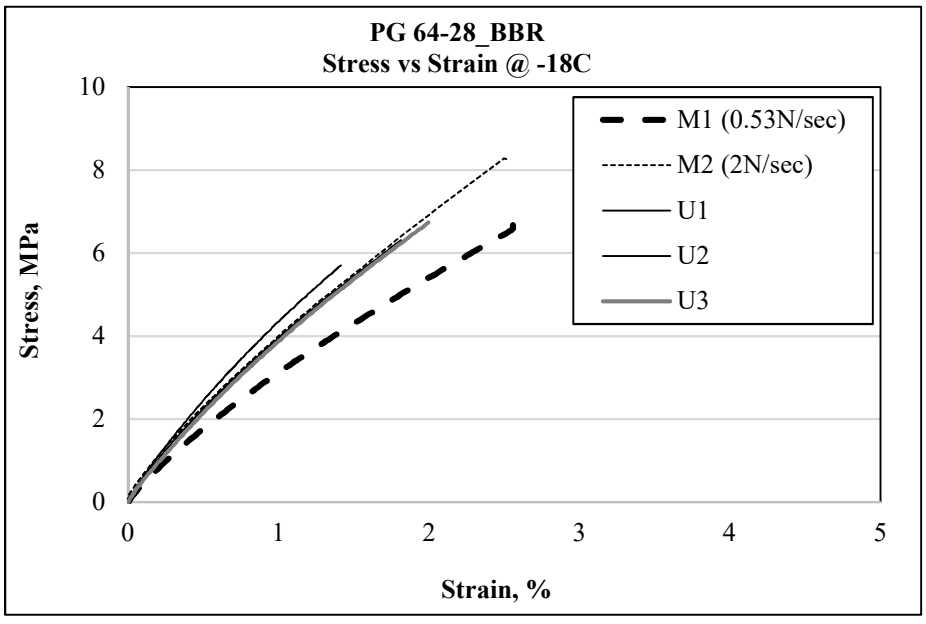

FIGURE 7.5 BBR Stress vs. Strain @ -18C for PG 64-28_U (unmodified) and PG 64-28_M (SBS-modified).

First, the constant strain rate condition was checked, and it was found that the condition is not met, especially in the beginning of the test, where the stiffness of the binder is very high. An example is shown in FIGURE 7.6 for tests performed at -18C.

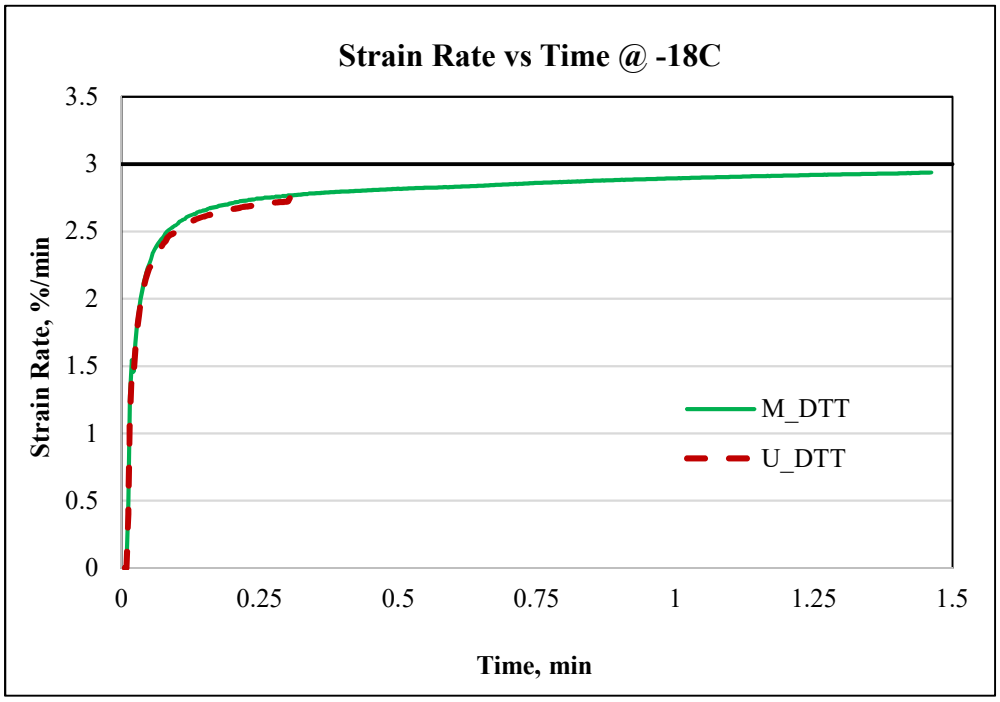

FIGURE 7.6 Strain rate of PG 64-28 asphalt binders at -18C.

This means that linear viscoelasticity interconversions for constant strain rate experiments may not work. The stress-strain data obtained under a constant strain rate can be directly converted to relaxation modulus. When a specimen is subjected to a strain that increases in direct proportion to the time, i.e. $d\varepsilon / dt = \dot{\varepsilon} =$ constant, the following equation is obtained:

$$\sigma(t) = \dot{\varepsilon} \int_{-\infty}^{t} E(t - t')dt' \tag{7.5}$$

where

$\sigma(t)$ = tensile stress,

$\dot{\varepsilon}(t)$ = time dependent tensile strain,

$\dot{\varepsilon}(t)$ = derivative of tensile strain with respect to time, and

$E(t)$ = tensile relaxation modulus.

Replacing $\varepsilon(t) = \dot{\varepsilon}t$ in equation 8.5 results in:

$$F(t) \equiv \frac{\sigma(t)}{\varepsilon(t)} = \frac{1}{t}\int_{-\infty}^{t} E(t-t')dt' \tag{7.6}$$

Where F(t) is a modulus termed the constant-strain-rate modulus which represents the response to a constant strain rate (Smith, 1976). Differentiation of equation 8.6 concerning t yields:

$$E(t) = F(t) + t\frac{dF(t)}{dt} \tag{7.7a}$$

which can be rewritten as:

$$E(t) = F(t)\left[1 + \frac{d\log F(t)}{d\log t}\right] \tag{7.7b}$$

This approach diminishes the noise considerably in the experimental stress-strain data. For this reason, equations 7.7a and 7.7b are the forms preferred for transforming experimental data into E(t). The direct differentiation of the stress-strain curve to obtain the relaxation modulus E(t) inherits all the noise in the experimental data and should be avoided (Smith, 1976).

First, the stress-strain data is converted to secant modulus, which is simply the ratio of stress and strain at a given time. Then the logarithm of the secant modulus with respect to the logarithm of the time is approximated with a fourth order polynomial to obtain the slope at any given time. The approximated values were in all cases within 4% of the initial values. The slope was simply calculated as the first derivative of the fourth order polynomial with respect to time.

The relaxation moduli obtained using equation 7.7b were compared next to the relaxation moduli obtained from BBR creep data using Hopkins and Hamming numerical algorithm. Typical plots of moduli from the BBR creep and DTT stress-strain data are shown in FIGURE 7.7.

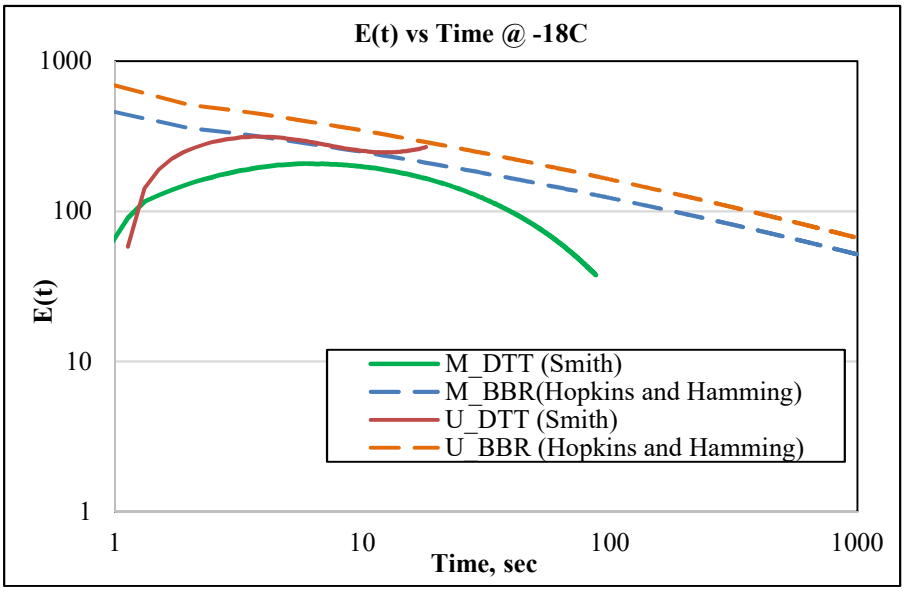

FIGURE 7.7 Relaxation modulus for PG 64-28 asphalt binder at –18°C, converted BBR and converted DT data.

Visual inspection of the plots shows that the BBR and DT moduli are different. The difference at short times can be explained by the difference in strain rate at the beginning of the DT test. The difference beyond 10s can be explained most likely by deviation from the linear behavior of the material in DT testing. This was shown before in previous work by Marasteanu and Anderson (2000). In the same paper, the authors performed DT tests using 2 strain rates. If the data is obtained in the linear viscoelastic region, then the stress-strain curves measured at different strain rates superpose to yield a single composite curve on a plot of stress divided by strain rate versus time. The example shown in FIGURE 7.8 indicated that departures from linearity conditions are most likely present in the DT test.

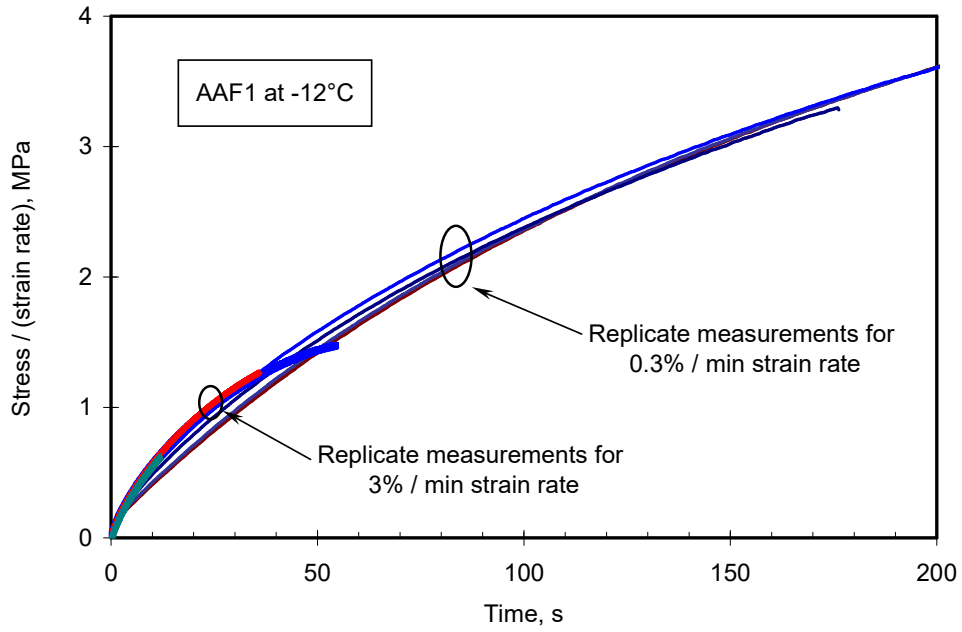

FIGURE 7.8 Stress divided by strain rate composite curve for AAF1 at -12°C (Marasteanu and Anderson, 2000).

Based on preliminary testing performed to match the stress rate in the DTT and BBR-strength test, an initial rate of 0.53N/sec was selected for the BBR strength test for both temperatures studied: -18ºC and -24ºC (Marasteanu et al., 2017). The test summary is presented in Table 7.1, and the stress-strain curves are shown in Figures 7.9 and 7.10. It should be noted that the modified binder beams did not break at -18ºC, even when the rate was increased four times, and the test stopped when the maximum deflection limit of 7mm was reached. Both DTT (Figures 7.7 and 7.8) and BBR (Figures 7.12 and 7.13) tests identify the modified binder as the better performer at both temperatures. The results of ANOVA also confirm these findings with a *p*-value less than 0.05 (Table 7.2). This suggests that BBR strength test has the potential to be used as an index test to determine the more fracture resistant material.

TABLE 7. 1 BBR strength and DTT strength results for binders in PAV condition.

Binder PG	T [°C]	DTT		BBR		DTT		BBR	
		Stress @ Failure [MPa]	Avg Stress, [MPa]	Stress @ Failure [MPa]	Avg Stress, [MPa]	Strain @ Failure [%]	Avg Strain [%]	Strain @ Failure [%]	Avg Strain [%]
64-28 U	-18	2.11	2.13	5.56	6.10	0.80	0.80	1.41	1.74
	-18	2.00		6.16		0.75		1.81	
	-18	2.29		6.58		0.85		2.00	
64-28 U	-24	3.18	2.38	5.01	5.88	0.75	0.55	0.77	0.97
	-24	2.91		4.16		0.68		0.60	
	-24	2.55		8.48		0.58		1.54	
	-24	0.90				0.20			
64-28 M	-18	4.56	4.30	Beams did not break		4.36	4.14	Beams did not break	
	-18	4.36				4.16			
	-18	3.99				3.90			
64-28 M	-24	4.59	5.00	9.12	8.44	1.62	1.84	2.53	2.26
	-24	4.58		8.52		1.57		2.40	
	-24	4.78		7.68		1.65		1.84	
	-24	6.04				2.50			

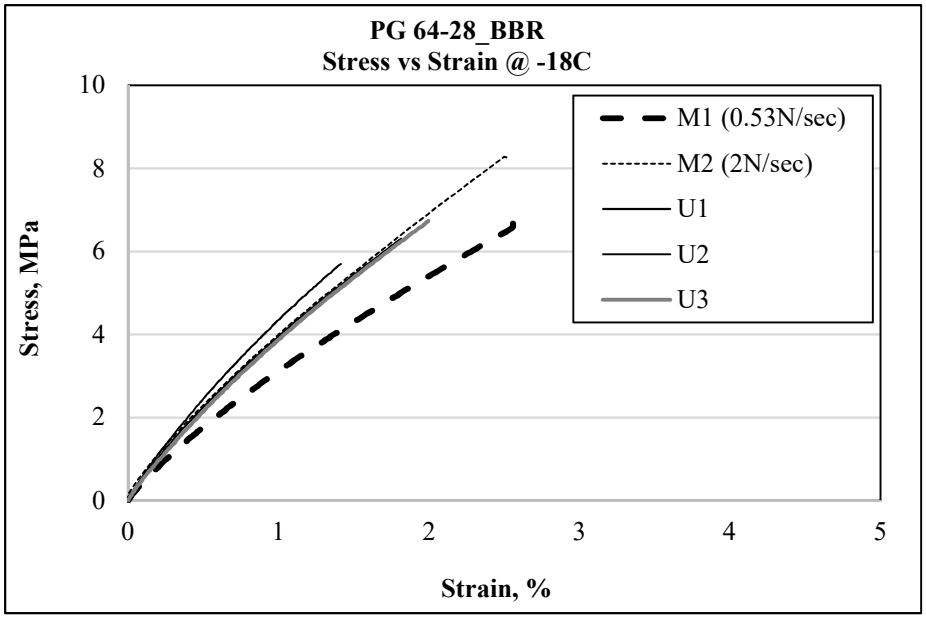

FIGURE 7.9 BBR_ Stress vs. Strain @ -18C for PG 64-28_U (unmodified) and PG 64-28_M (SBS-modified).

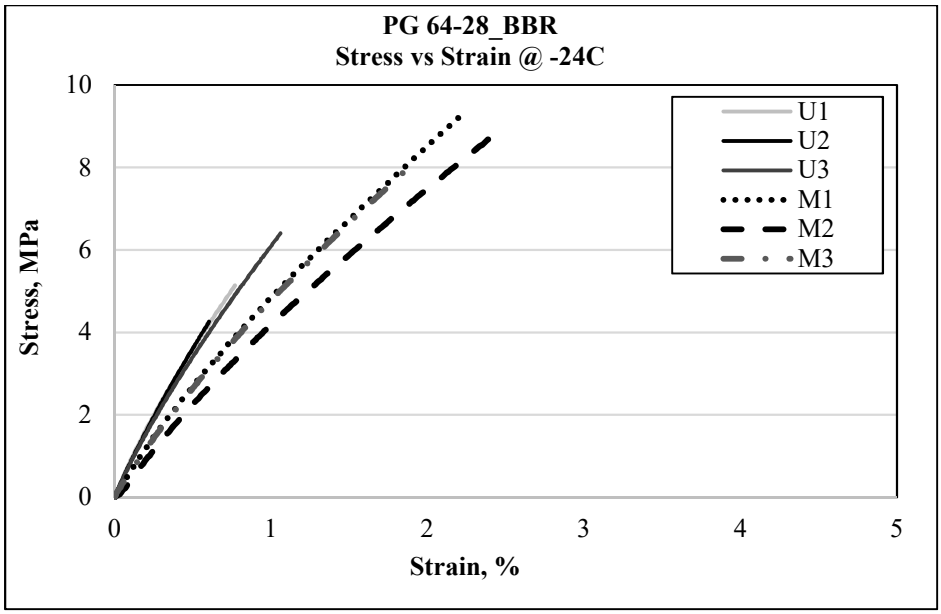

FIGURE 7.3 BBR_ Stress vs. Strain @ -24C for PG 64-28_U (unmodified) and PG 64-28_M (SBS-modified).

TABLE 7.2 One Way ANOVA test Results

One Way ANOVA Test_p-value				
Test Method	Effect of Modifier		Effect of Temperature	
	-18C	-24C	Unmodified (U)	Modified (M)
	Stress @ Failure			
DTT	0.0003	0.0056	0.7000	0.1746
BBR	0.0000	0.0085	0.8806	0.0000
Strain @ Failure				
DTT	0.0000	0.0022	0.0750	0.0000
BBR	0.0000	0.0226	0.0845	0.0004

As seen for the SBS-modified binders, the beams did not break by the time the deflection reached the maximum measurable value and a higher loading rate could be necessary. To be able to calculate a loading rate that would result in a deflection of 7mm (equivalent to a strain of 2.6%) prior information related to the strain evolution with time is needed. Since the test is stress controlled, this could be determined if the stress strain curve is known for a given loading rate. This information can be in fact obtained using linear viscoelasticity concepts.

In a test in which the stress is increased linearly starting from zero, the resulting strain will reflect the superposition of a series of retarded compliances (Ferry, 1980). If $\dot{\sigma} = \mathrm{d}\sigma/\mathrm{d}t$ is the rate of stress increase, then:

$$\gamma = \dot{\sigma} t J_g + \dot{\sigma} \int_0^t \int_{-\infty}^{\infty} L(1 - e^{-u/\tau}) d \ln \tau \, du + \frac{\dot{\sigma} t^2}{2\eta_o} \tag{7.8}$$

$$\gamma = \dot{\sigma} t J_g + \dot{\sigma} \int_{-\infty}^{\infty} L\left[t - \tau\left(1 - e^{-t/\tau}\right)\right] d \ln \tau + \frac{\dot{\sigma} t^2}{2\eta_o} \tag{7.9}$$

When the stress-strain curve under this condition is differentiated, the result is the creep compliance:

$$\frac{d\gamma}{d\sigma} = (1/\dot{\sigma}) \frac{d\gamma}{dt} = J_g + \int_{-\infty}^{\infty} L\left(1 - e^{-t/\tau}\right) d \ln \tau + t/\eta_o = J(t) \tag{7.10}$$

This also means that if creep compliance is known, the variation of strain with stress is known for a constant loading rate test. If the loading rate is known, then the entire stress-strain curve can be determined for a given stress rate. A detailed example is provided below.

First, a BBR creep test is performed, and the creep compliance is calculated as a function of time. We then make the reasonable assumption that the creep compliance D(t) follows a power law.

Next, we consider a hypothetical BBR strength test performed using a constant stress rate $\dot{\sigma}$. The stress at any time can be simply calculated as

$$\sigma(t) = \dot{\sigma} * t \tag{7.11}$$

Therefore, we can relate the creep compliance from the performed BBR creep test to the stress from the hypothetical BBR strength test using a power law:

$$D(t) = a * \{\dot{\sigma} * t\}^b = \; a * \{\sigma(t)\}^b \tag{7.12}$$

Coefficients *a* and *b* can be simply calculated from fitting equation 7.12 to the creep compliance vs. stress plot, for an assumed loading rate. The loading rate is required to match the times for the creep compliance (vertical axis) and the stress data (horizontal axis). An example is presented in Figure 7.11.

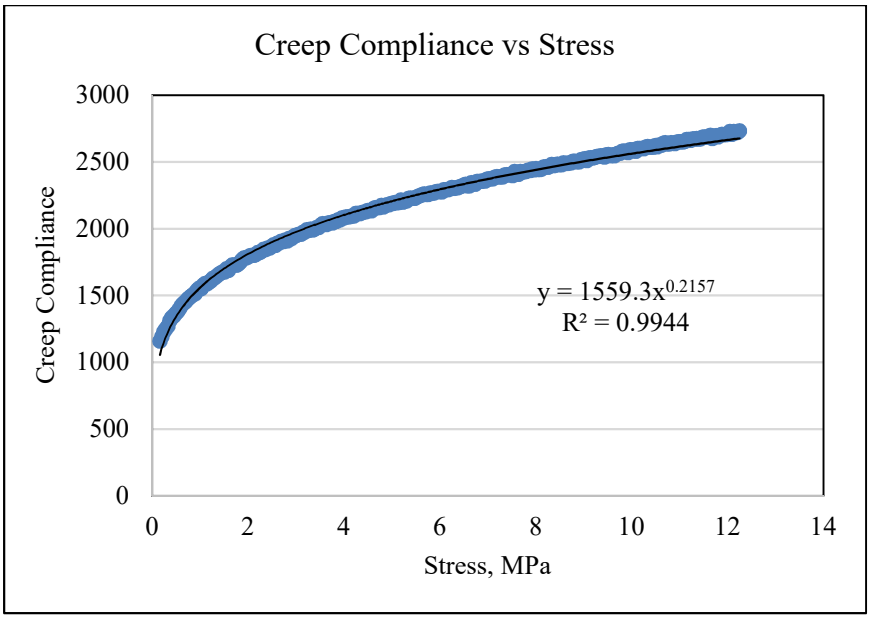

FIGURE 7.11 Creep Compliance (BBR creep test) vs. Stress (hypothetical BBR strength test) for PG 64-28_M @ -24C and a stress rate of 0.53N/s.

From equation 7.10, the first derivative of the strain-stress curve is the creep compliance, $D(t)$, and, therefore, we can rewrite equation (7.12) as:

$$D(t) = \mathrm{d}\varepsilon(t)/\mathrm{d}\sigma(t) = a * \{\sigma(t)\}^b \tag{7.13}$$

The strain can then be obtained as:

$$\varepsilon(t) = \frac{a*\{\sigma(t)\}^{b+1}}{b+1} + c \tag{7.14}$$

Constant c is zero, since the plot starts in the origin.

For the example shown in Figure 8.11, using equation (8.14) and the values of coefficients a and b, the strain is calculated as

$$\varepsilon(t) = \frac{[1559.3*\{\sigma(t)\}^{0.215}\quad]}{0.2157+} \tag{7.15}$$

Examples of predicted stress-strain curves for the two 64-28 binders at -24ºC and a loading rate of 0.53N/s are shown in Figure 7.12. The predicted stress-strain curves match very well the experimentally obtained stress - strain curves from the BBR strength test.

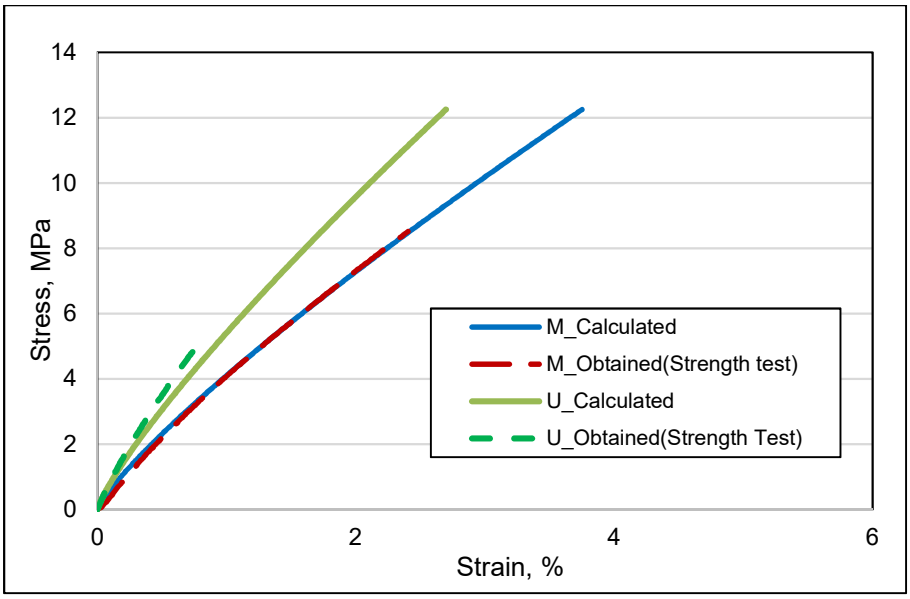

FIGURE 7.12 Predicted and experimentally determined stress-strain curves for PG 64-28 binders at -24ºC and a stress rate of 0.53N/s

The same observation can be made for the comparison performed based on BBR creep and BBR strength results at -18 ºC (Figure 7.13). Therefore, it can be concluded that the BBR creep data can be successfully used to predict the entire stress-strain curve. The prediction helps determine, prior to performinging BBR strength tests, if a deflection of 7mm, equivalent to a strain of 2.6%, is reached during the test, for a stress rate of 0.53N/s (or any other rate).

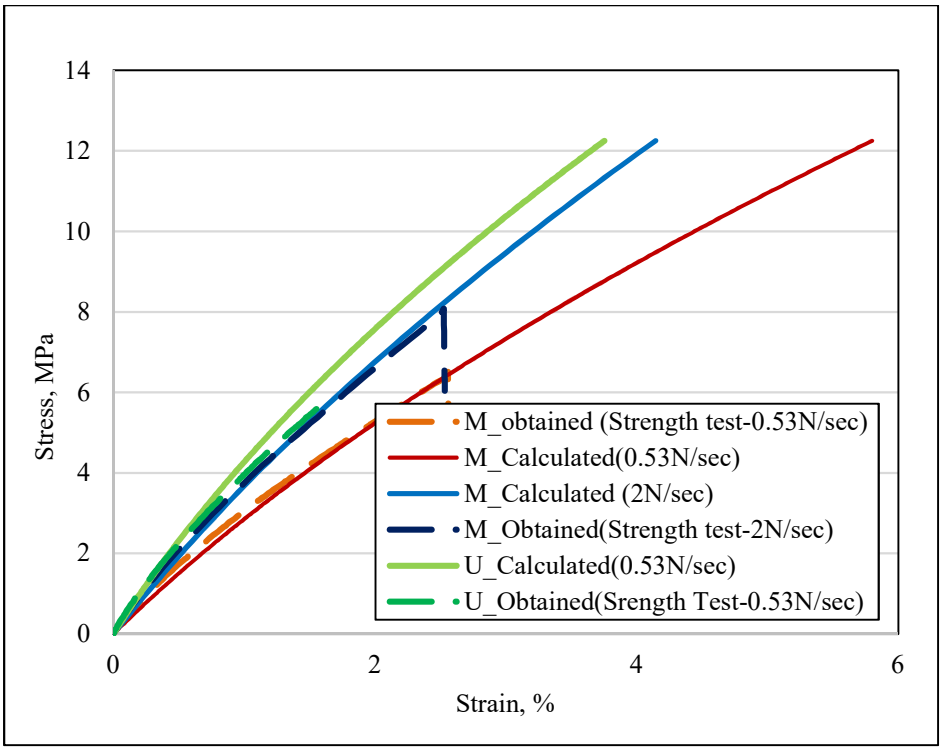

FIGURE 7.13 Predicted and experimentally determined stress-strain curves for PG 64-28 binders at -18ºC and different stress rates.

The BBR strength results from all the binders tested varied between 2 and 10MPa and never went above 12 MPa, which could be set as an upper limit to be reached within a given period of time that will make the duration of the test reasonable. For example, similar to the approach used for DTT, one can set a loading rate such that 12MPa is reached in 60 seconds. Since this is a stress controlled test, this rate can be easily calculated to be 39N in 60 sec or approximately 0.65N/sec, very close to the rate used to test the PG64-28 binders.

Based on these results, an initial procedure was proposed to select the binder with the best failure properties out of a group of binders with similar creep stiffness and m-values (16):

- Perform BBR creep tests at two temperatures, according to the current specifications, to determine the grade of the binder.

- Use the experimental creep compliance data to predict the stress-strain curves for a stress rate of 0.65N/s, which will limit the duration of the test to 1 minute or less.

- Use the stress-strain curves to determine if the 2.6% strain limit is reached within 1 minute. If the limit is reached, increase the stress rate accordingly. If the strain is less than 2.6%, perform strength test using the 0.65N/s rate.

- Perform BBR strength tests and obtain stress-strain curves and the stress and strain at failure.

-Select the binder with the highest failure stress and strain as the most crack resistant.

This approach introduces an additional level of complication that may not be necessary, apart from testing some modified binders, and from theoretically proving that the BBR strength test is performed under linear viscoelastic conditions, which can help develop a failure criterion in the future. Therefore, a simple procedure is proposed in which a constant loading rate of 0.65N/s is used for all testing. A deflection exceeding the 7mm threshold is considered an indication of ductile to brittle behavior that makes the material more crack resistant. Additional testing at a lower temperature can be performed but it is not mandatory.

7.3.2 Final Investigation

The simple procedure described above was used to test five asphalt binders used in MnROAD cells 16, 20, 21, 22, 23. Both creep and fracture properties were obtained using a Bending Beam Rheometer Pro at PGLT+10C and PGLT+4C in the air. Since low-temperature failure is a criterion of aged pavement, to simulate long-term aging condition, all the binders were short and then long-term aged using RTFO and PAV prior to testing. All binders were PAV aged, and all testing was performed in air. Six replicates were tested for each binder at each temperature. After the beams had been conditioned for 1h, a creep test was performed according to AASTHO T313. The beam was allowed to recover for 240 sec followed by a strength test at a constant loading rate of 0.65N/s. Tables 7.3 details the binders used.

TABLE 7.3 Asphalt Binder Tested

Cell No.	Binder Type	Replicates	Temperature	Test Method	Properties Obtained
16	PG 64S-22	6	-12C and -18C	Creep and Strength Test	Creep Stiffness, m-value, Strength, Strain at Failure
20	PG 52S-34	6	-24C and -30C		
21	PG 58H-34	6	-24C and -30C		
22	PG 58H-34	6	-24C and -30C		
23	PG 64E-34 (highly modified)	6	-24C and -30C		

Tables 7.4 and 7.5 below present creep and strength test results for the five binders at two temperatures. The values presented are the average of six replicates.

TABLE 7.4 Creep Stiffness and m-value of Asphalt Binder

Cell No.	**Mix Design**	**Binder**	**Creep Stiffness, S (60), MPa**				**m-value, m(60)**			
			PGLT+10C		**PGLT+4C**		**PGLT+10C**		**PGLT+4C**	
			Avg	**CoV, %**	Avg	**CoV, %**	Avg	**CoV, %**	Avg	**CoV, %**
16	SPWEB540L	PG 64S-22	174	4%	432	10%	0.372	1%	0.298	7%
20	SPWEB540A	PG 52S-34	262	9%	531	14%	0.337	4%	0.266	6%
21	SPWEB540C	PG 58H-34	241	9%	435	7%	0.328	1%	0.266	6%
22	SPWEB540C	PG 58H-34	213	11%	432	5%	0.333	4%	0.271	4%
23	SPWEB540I	PG 64E-34 (highly modified)	190	4%	407	10%	0.344	4%	0.290	6%

TABLE 7.5 Strength and Strain at Failure of Asphalt Binder

Cell No.	Mix Design	Binder	BBR Binder Strength, MPa				% Strain at Failure			
			PGLT+10C		PGLT+4C		PGLT+10C		PGLT+4C	
			Avg	CoV, %	Avg	CoV, %	Avg	CoV, %	Avg	CoV, %
16	SPWEB540L	PG 64S-22	4.1	20%	3.7	17%	1.38	25%	0.54	23%
20	SPWEB540A	PG 52S-34	5.2	12%	5.3	49%	1.2	17%	0.72	52%
21	SPWEB540C	PG 58H-34	5.7	38%	5.0	31%	1.50	51%	0.70	37%
22	SPWEB540C	PG 58H-34	4.9	17%	6.0	23%	1.29	20%	0.92	24%
23	SPWEB540I	PG 64E-34 (highly modified)	7	11%	5.5	10%	2.3	14%	0.85	14%

The coefficient of variation was observed to be between 15% and 10% for creep stiffness and m-value, respectively which indicates reasonable repeatability. The strength properties obtained from strength test has a coefficient of variation below 25% except for the binders from Cell 20 and 21 (Table 7.5). The obtained properties from creep and strength test; creep stiffness at 60 sec, m-value at 60sec, strength, and strain at failure is graphically presented below for better understanding (Figures 7.14-7.17).

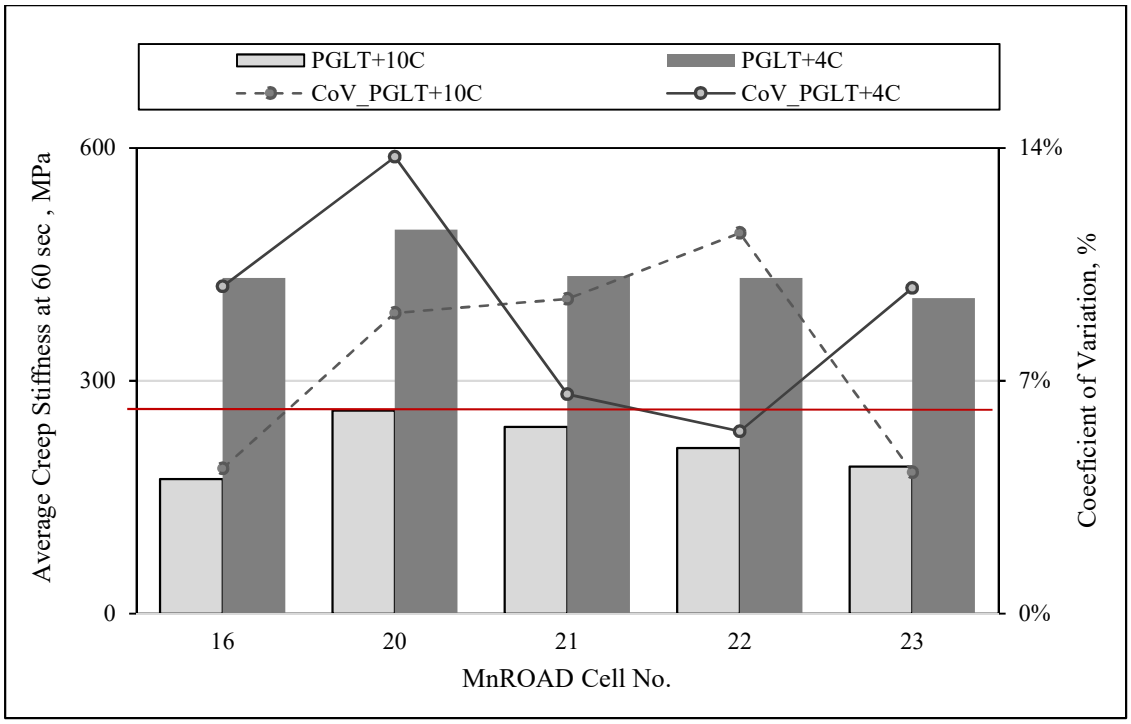

FIGURE 7.14 Creep Stiffness at 60 sec at PGLT+10C and PGLT+4C for binders from Cell 16, 20-23.

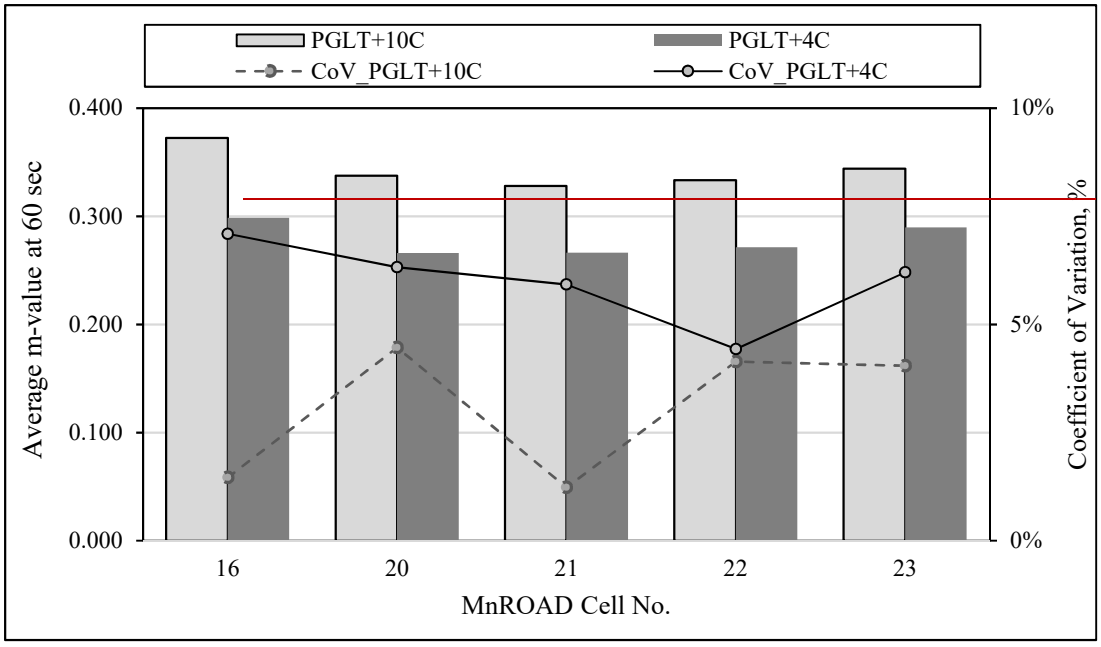

FIGURE 7.15 m-value at 60 sec at PGLT+10C and PGLT+4C for Binders from Cell 16, 20-23.

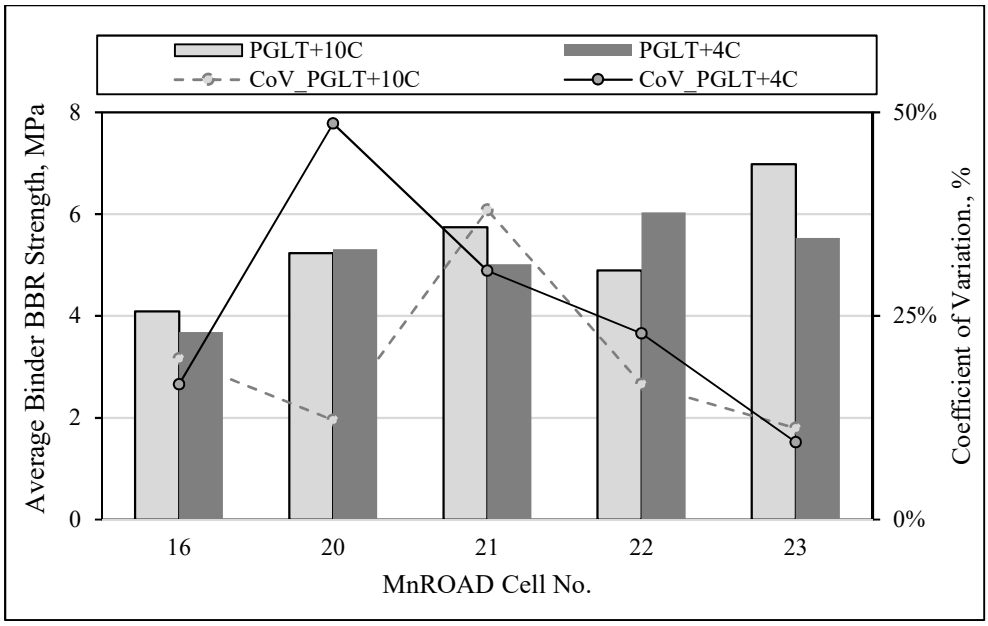

FIGURE 7.16 BBR Strength of Binders from Cell 16, 20-23.

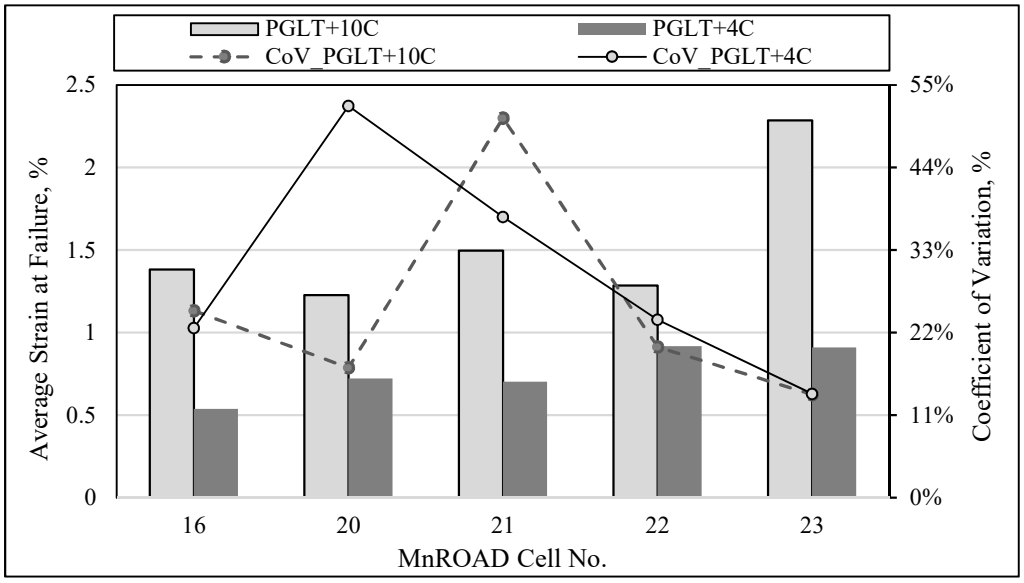

FIGURE 7.17 Strain at Failure of Binders from Cell 16, 20-23.

The results show a clear difference between the different types of asphalt binder. All binders pass the stiffness criterion of being below 300 MPa at PGLT+10C, according to AASHTO T313, as well as having minimum m-value of 0.3 (Figures 7.14 and 7.15). The binder from Cell 16 has similar stiffness value of the binder from Cell 23. However, the binder from Cell 16 has the lowest strength, whereas the binder from Cell 23 has the

highest strength. So, creep stiffness and m value are not sufficient to rank the binder in term of performance. The strength and strain at failure obtained from strength test showed that the test can distinguish among different material which reflects anticipated cracking potential. This is also confirmed by the creep stiffness and stress-strain curves shown in Figures 7.18 and 7.19. A less obvious difference is observed for binders from cell 20 and 21 that have almost the same creep stiffness and m-value, as shown in Figure 7.18. However, stress-strain curves in Figure 7.19 indicate that the binder from cell 21 may perform better than the binder from cell 22.

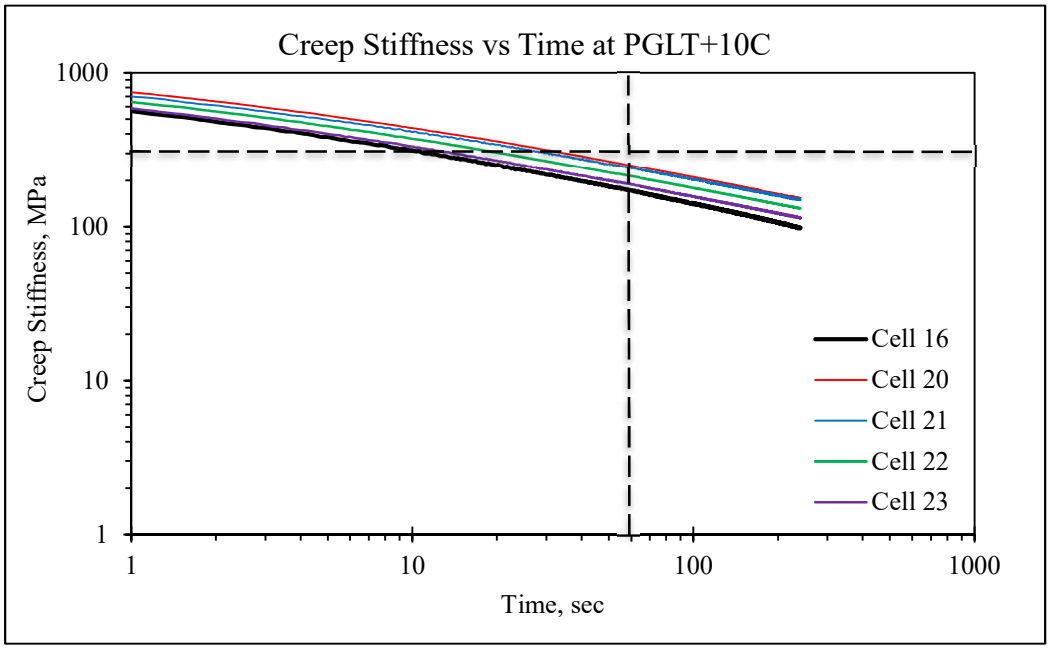

FIGURE 7.18 Creep Stiffness vs. Time at PGLT+10C.

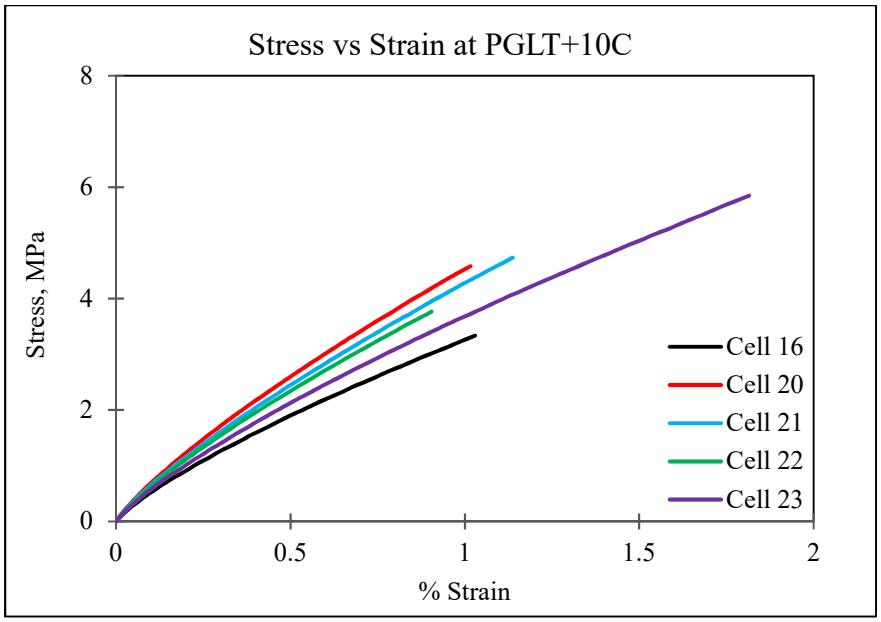

FIGURE 7.19 Stress-Strain Curves at PGLT+10C.

The results from the BBR strength test also reflect the same trend obtained from asphalt mixture fracture testing. DC(T) tests were performed for the mixtures from cells 16-23 to determine low-temperature fracture energy (Figure 7.20). From the results shown in Figure 7.20, it is observed that Cell 23 mixture has the highest fracture resistance, while Cell 22 mixture has the lowest fracture resistance, although they use binders with similar low temperature PG limit.

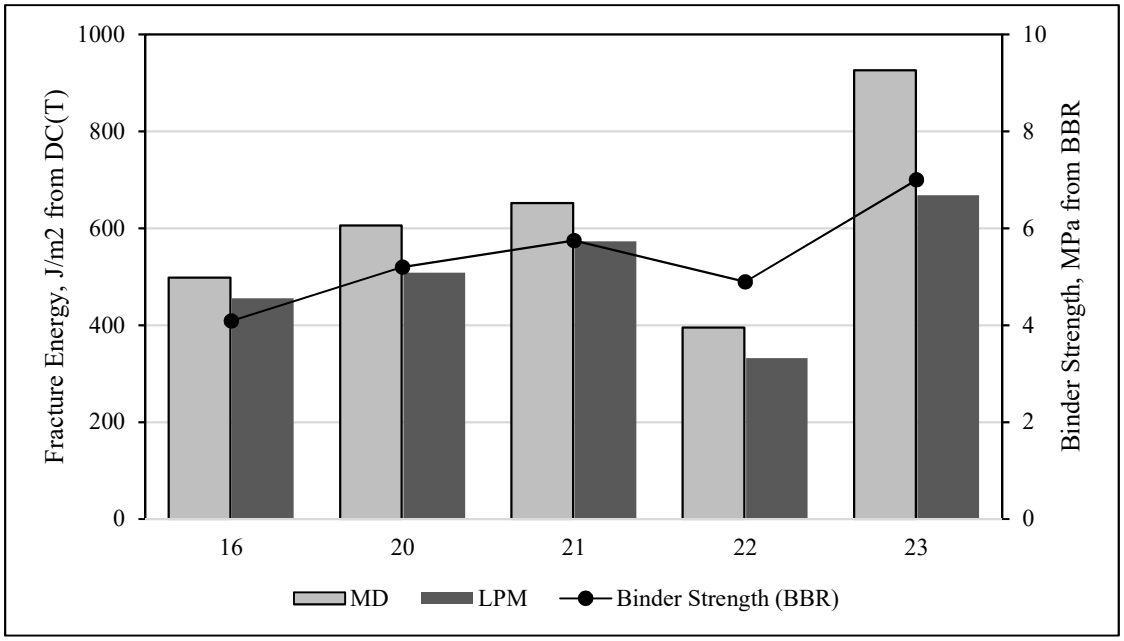

FIGURE 7.20 Fracture Energy from DC(T) test at -21.4C for Mixtures from Cell 16, 20-23.

The procedure previously described to predict stress-strain curves from creep data was applied to the test data for the five binders. It was found that in all cases the predicted stress-strain curve matched the experimental stress-strain curve, which indicates that all strength testing was performed under linear viscoelastic conditions. An example is presented in Figure 7.21.

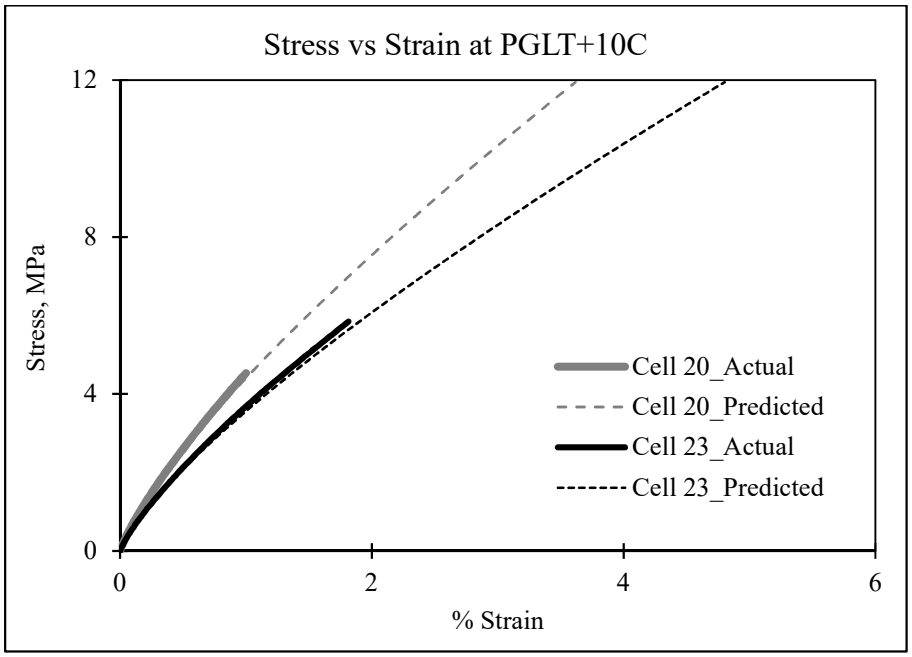

FIGURE 7.21: Predicted and experimentally determined stress-strain curves for binders from MnROAD cells at PGLT+10ºC and 12MPa/sec stress rate.

Chapter 8: CONCLUSIONS AND RECCOMENDATIONS

A number of conclusions can be drawn from the experimental work and statistical analyses performed in this investigation.

8.1 Effect of Bio-Sealant on Asphalt Binder and Mixture

For asphalt binder, the oil-based sealants decreased rutting and fatigue resistance. However, it helped low temperature grading. The water based sealant and the traditional emulsion didn't bring any significant changes to the binder grade except that theemulsion showed a stiffening effect. It was found that the simple mixing procedure produced unrealistic results, with significant softening of the treated aged binders, particularly at the high temperature. The pipette procedure appears to produce more realistic results, more consistent with field observations. The largest softening effect is noticed on the aged binder treated with oil-based OB1 and OB2, whereas stiffening effect was noticed when binder was treated with the water-based WB1 and traditional emulsion E1. It was also observed that storage time may have affected the softening effect at high temperature; it is not clear which mechanism was responsible for this effect, so further investigation is needed.

For asphalt mixtures, the analysis performed on the bending creep and strength results at low temperature showed that the application of sealants in the field resulted in only a few statistically significant changes in the properties of the control section, while for the laboratory-treated samples, significant differences were observed in almost all cases. This is especially true for the oil-based sealants that significantly affected all rheological and fracture properties of the mixtures treated in laboratory conditions. It can be hypothesized that the significant differences observed between the field-treated and the laboratory-treated samples are due to a number of factors:

- Cores were collected 3 weeks after sealant was applied in the field. Samples prepared from these cores were tested approximately 9 months after core collection. It is possible that some of the sealant was absorbed by the aggregates or evaporated. Laboratory samples were tested after only 1 month in very stable environmental conditions.

- The application rate in the laboratory was very well controlled, while less control can be achieved in the field.
- Application of sealant on laboratory samples could have produced localized damage that might have influenced the results significantly, as seen with some of the test specimens treated with the oil-based products.

FTIR analysis detected no trace of sealants in the field-treated mixture beams from the top layer, which supports the above hypothesis. Very few statistically significant changes due to sealant application were observed in the control section when considering beams from the top layer only. A field study by PennDOT on OB1, described in the literature review, also concluded that there was no visible effect of sealant application after 18 months.

However, when considering beams from all three layers of the cores for each treated section, changes were observed similar to those observed for the laboratory-treated beams.

The aging effect was also considered in the analysis. It was observed that, after 8 months, while the creep stiffness of the control section increased, the oil-based OB1 and OB2 treated sections resulted in lower creep stiffness than after 3 weeks and compared to the control section as well. For the water-based W1 and traditional emulsion, E1 sections, the creep stiffness increased after 8 months. The oil-based sealant treated sections also had higher m-value indicating increased ability to relax stresses in both cases compared to the control and the other treated sections, which is a desirable material property for the low-temperature region. Overall, the application of oil-based bio-sealants, OB1 and OB2 had a softening effect observed from the reduction in creep stiffness associated with an increase in m-value.

The Hirsch model analysis appears to indicate that the pipette method can replicate the sealant application procedure used in the field, which means that laboratory experiments could be performed to determine the amount of sealant required to obtain specific changes in mixture properties.

The results of the field distress survey of the treated and untreated sections correlated well with the laboratory findings. From the field investigation, it was observed that OB1 and E1 treated sections resulted in the highest transverse cracking differential. Both laboratory-treated beams and field-treated beams from top three layers of the core resulted in lowest the creep stiffness due to application of oil-based OB1, and highest creep stiffness due to the application of E1. While it is expected for the treated section with high creep stiffness to be more susceptible to cracking due to resulting brittleness, the presence of highest crack per mile for the oil-based OB1-treated section, which had the lowest stiffness is unexpected. During laboratory testing it was observed that OB1-treated beams tended to break at the aggregate-binder interface after sealant application, suggesting a reduction in bonding at the interface.

Based on the results and analyses performed in this study, an optimum application rate can be determined. However, additional materials and application rates should be investigated before a definitive conclusion can be made regarding the benefit of the application of these products in terms of pavement performance improvements.

8.2 Development of Binder Strength Testing Protocol

A simple testing protocol was developed to obtain the failure properties of asphalt binders at low temperatures using a BBR Pro device. By imposing constraints related to the duration of the test (1 minute for practical reasons) and knowing that the maximum stress value is approximately 12MPa, a loading rate of 0.65N/s is proposed for all testing. The tests should be performed at PGLT+10ºC and at PGLT+4ºC, similar to current BBR and DTT specifications. The strength tests can be conducted after a 240s recovery period immediately after BBR creep testing, or can be performed as a separate test on new binder specimens. The first method of conducting strength test right after creep test on the same binder sample is much shorter and requires less asphalt binder.

The proposed testing protocol was applied on a set of asphalt binders from five MnROAD cells constructed in 2016. The results showed that the new protocol can be

used to discriminate between asphalt binders with similar rheological properties but different failure properties. In addition, it was shown that the ranking provided by the BBR binder strength test matched very the ranking of asphalt mixtures resistance to cracking based on DC(T) fracture energy.

REFERENCE

Alvarez, A. E., Martin, A. E., Estakhri, C. K., Button, J. W., Glover, C. J., & Jung, S. H. (2006). *Synthesis of current practice on the design, construction, and maintenance of porous friction courses*(No. FHWA/TX-06/0-5262-1).A. Johnson *Best Practices Handbook on Asphalt Pavement Maintenance*. Minnesota T2/LTAP Program. Center for Transportation Studies, University of Minnesota. Minneapolis, MN. February 2000.

Johnson, A. M. (2000). Asphalt Pavement Maintenance Field Handbook. *Best practices handbook on asphalt pavement maintenance* (No. MN/RC-2000-04). Center for Transportation Studies, University of Minnesota. Minneapolis MN.

AASHTO (American Association of State Highway and Transportation Officials). Standard method of test for determining the flexural creep stiffness of asphalt binder using the bending beam rheometer (BBR). Specification T 313-12. Washington D. C., 2012.

AASHTO (American Association of State Highway and Transportation Officials). Standard method of test for determining the fracture properties of asphalt binder in Direct Tension (DT). Specification T 314-12. Washington D. C., 2012.

AASHTO (American Association of State Highway and Transportation Officials). Standard specification for performance-graded asphalt binder. Specification M320-10, Washington D. C., 2010.

AASHTO, T. (2006). 313-06. "Determining the flexural creep stiffness of asphalt binder using the Bending Beam Rheometer (BBR)", American Association of State Highway and Transportation Officials, Washington, DC.

AASHTO, T. (2009). 315. "Standard method of test for determining the rheological properties of asphalt binder using a dynamic shear rheometer (DSR)". American Association of State Highway and Transportation Officials, Washington, DC.

AI-Qadi, I., Fini, E., Elseifi, M., Masson, J. F., and McGhee, K. (2006). "Viscosity determination of hot-poured bituminous sealants". Transportation Research Record: Journal of the Transportation Research Board, Washington, DC.

Ali, H., and Sobhan, K. (2012). "On the road to sustainability: properties of hot in-place recycled Superpave mix". Transportation Research Record: Journal of the Transportation Research Board, (2292), 88-93.

Anderson, D. A., & Kennedy, T. Development of SHRP binder specification. *Journal of the Association of Asphalt Pavement Technologies, 62*, 1993, pp. 481-507.

Anderson, D. A., & Marasteanu, M. O. Physical hardening of asphalt binders relative to their glass transition temperatures. *Transportation Research Record, 1661*. doi: 10.3141/1661-05, 1999, pp. 24-37.

Anderson, D., Christensen, D., Bahia, H. U., Dongre, R., Sharma, M., Antle, C., & Button J. Binder characterization and evaluation vol. 3: physical characterization (SHRPA-369). Washington, D.C.: Strategic Highway Research Program, National Research Council, 1994.

Asli, H., E. Ahmadinia, M. Zargar, and M. R. Karim. Investigation on Physical Properties of Waste Cooking Oil–Rejuvenated Bitumen Binder. *Construction and Building Materials,* Vol. 37, 2012, pp. 398–405.

ASTM. *Standard Test Method for Standard Practice for Pull-Off Strength of Coatings Using* 18 *Portable Adhesion Tester*. ASTM D: 4541, American Society for Testing and Materials, 19 West Conshohocken, PA, 2009.

ASTM. *Standard Test Method for Standard Practice for Tack of Pressure-Sensitive Adhesives by Rolling Ball*. ASTM D: 3121, American Society for Testing and Materials, West Conshohocken, PA, 2006.

Bahia H. U. *Low-temperature isothermal physical hardening of asphalt cements* (Ph.D. Thesis). Pennsylvania State University, State College, PA, 1991.

Basu, A., Marasteanu, M. O., Hesp, S. Time-temperature superposition and physical hardening effects in low-temperature asphalt binder grading. Transportation Research Record, 1829, doi: 10.3141/1829-01, 2003, pp. 1-8.

Biorestor (http://www.biosealusa.com/how-bioseal-works.php)

BioSpan Technologies, Inc. RePlay. (2010). Retrieved from BioSpan Technologies, Inc.:http://RePlay.biospantech.com/.

Boyer, R. E., and Engineer, P. S. D. (2000). “Asphalt Rejuvenators “Fact, or Fable”. Transportation systems.

Brownridge, J. (2010). “The role of an asphalt rejuvenator in pavement preservation: use and need for asphalt rejuvenation”. 1st International Conference on Pavement Preservation.

C. K. Estakhri and H. Agarwal, “Effectiveness of Fog Seals and Rejuvenators for Bituminous Pavement Surfaces”, Texas Transportation Institute, Texas A&M University, College Station (TX), **1991**, pp.3-4.

California Department of Transportation. Maintenance Technical Advisory Guide (TAG). Caltrans Division of Maintenance, Sacramento, CA, 2003.

Calvert, J., 2009, presentation on Jointbond. TDOT

Chan, S., Lane, B., Kazmierowski, T., and Lee, W. (2011). Pavement preservation: A solution for sustainability. *Transportation Research Record: Journal of the Transportation Research Board*, (2235), 36-42.

Cheng, D., Lane, L., and Vacura, P. (2014). Performance study of fog or rejuvenating seals on gap and open graded surfaces for Caltrans. *Asphalt Pavements*, 91.

Cheng, D., Lane, L., and Vacura, P. (2015). Performance Evaluation of Fog and Rejuvenating Seals on Gap and Open Graded Surfaces by Caltrans. *International Journal of Pavement Research and Technology*, *8*(3), 159-166.

Chiu, C. T., and Lee, M. G. (2006). Effectiveness of seal rejuvenators for bituminous pavement surfaces. *Journal of Testing and Evaluation*, *34*(5), 1-5.

Christensen Jr, D. W., Pellinen, T., and Bonaquist, R. F. (2003). "Hirsch model for estimating the modulus of asphalt concrete". Journal of the Association of Asphalt Paving Technologists, 72.

Christensen, D. W., and Bonaquist, R. F. (2004). "Evaluation of indirect tensile test (IDT) procedures for low-temperature performance of hot mix asphalt (No. 530)". Transportation Research Board. Washington, DC.

Croteau, J. M., Linton, P., Davidson, J. K., and Houston, G. (2005). "Seal Coat Systems in Canada: performances and practice". Annual Conference of the Transportation Association of Canada, Alberta, Canada.

D. F. Rogge, "Development of Maintenance Practices for Oregon F-mix", Oregon Department of Transportation, Washington, D.C., 2002, pp.37-49.

D. Janisch and F. Gaillard. *Minnesota Seal Coat Handbook*. Sponsored by Minnesota Local Road Research Board, Minnesota Department of Transportation. St. Paul, MN. 1998. Revised in 2006 by T. Wood.

Dongré, R. *Development of direct tension test method to characterize failure properties of asphalt cements*. Pennsylvania State University, State College, PA, 1994.

Doré, G. and Zubeck, H. (2009). Cold Regions Pavement Engineering, McGraw-Hill/ASCE Press, Reston, VA.

Douglas, S. 2006. Fog Seals, *Texas Pavement Preservation Center*, Issue 3, pp. 3–4.

Falchetto, A. C., Turos, M. I., & Marasteanu, M. O. Investigation on asphalt binder strength at low temperatures. *Road Materials and Pavement Design*, *13*(4), 2012, pp. 804-816.

Federal Highway Administration (FHWA). Fog Seal Application. Pavement Preservation Checklist Series 4, U.S. Department of Transportation, http://www.fhwa.dot.gov/pavement/preservation/ppcl00.cfm, 2003.

Ferry, J. D. *Viscoelastic properties of polymers*. U.S.: Wiley& Sons, 1980.

G. King and H. King. *Spray Applied Polymer Surface Seals*. Cooperative Agreement No. DTFH61-01-0004 Final Report. Issued by the Federal Highway Administration to the Foundation for Pavement Preservation. Washington D.C. August 2007.

Galehouse, L. (2002). Strategic Planning for Pavement Preventive Maintenance: Michigan Department of Transportation's" Mix of Fixes" Program. *TR NEWS*, 3-8.

Galenhouse, L., & O'Doherty, J. (2005). Anticipation is Sweet: Research Examines Results of Preventive Maintenance on Pavements After 14 Years in Service. *Roads & Bridges*, *43*(6).

Gayne, D. (2013). "Use of JOINT BOND ® as a Center Line Joint Stabilizer Demonstration on I-95 N.B", Technical Report 13-05, Transportation Research Division. Maine Department of Transportation, Augusta, ME.

Geiger, D. R. (2003). Pavement preservation definitions. *FHWA Memorandum*.

Ghosh, D., Turos, M., & Marasteanu, M. (2016). Evaluation of Bio-Fog Sealants for Pavement Preservation. Final Report, Project No. 2015011, Minnesota Department of Transportation and Local Road Research Board, Minnesota.

Gransberg, D. (2005). "Chip seal program excellence in the United States". Transportation Research Record: Journal of the Transportation Research Board: 72-82, Washington, DC.

Gransberg, D. and James, D. (2005) NCHRP Synthesis 342: "Chip Seal Best Practices. A Synthesis of Highway Practice."

Hajj, E. Y., Loria, L. G., Sebaaly, P. E., Cortez, E., and Gibson, S. (2012). Effective Timing for Two Sequential Applications of Slurry Seal on Asphalt Pavement. *Journal of Transportation Engineering*, *139*(5), 476-484.

Hicks, R. G., K. Dunn, and J. S. Moulthrop. Framework for Selecting Effective Preventive Maintenance Treatments for Flexible Pavements. In Transportation Research Record 1597, TRB, National Research Council, Washington, D.C., 1997, pp. 1–10.

Hugener, M., Partl, M. N., and Morant, M. (2014). “Cold asphalt recycling with 100% reclaimed asphalt pavement and vegetable oil-based rejuvenators”. Road Materials and Pavement Design, 15(2), 239-258.

Im, J. H., & Kim, Y. R. (2013). Development of Fog Seal Field Test Methods and Performance Evaluation Using Polymer-Modified Emulsions. *Transportation Research Record: Journal of Transportation Research Board*, (2361), 88-97.

Im, J. H., and Kim, Y. R. (2015). Performance evaluation of fog seals on chip seals and verification of fog seal field tests. *Canadian Journal of Civil Engineering*, *42*(11), 872-880.

James, A. (2006). “Overview of asphalt emulsion”. Transportation Research Circular E-C102, 1-6. Washington, DC.

Keifenheim, C. (2009) “Evaluation of timing for alternating chip sealing and hot mix asphalt overlays,” Research Paper, MSCE Degree, University of Washington, 2009.

Kim, Y.R. and Lee, J. (2007). Performance-based Analysis of Polymer Modified Emulsions in Asphalt Surface Treatments. Final Report. Report No. FHWA/NC/2007-06. North Carolina State University, Raleigh, NC, http://www.ncdot.org/doh/preconstruct/tpb/ research/download/2007-06finalreport.pdf (7/26/2011).

Lee, J. S. *Performance Based Evaluation of Asphalt Surface Treatments Using Third Scale Model Mobile Loading Simulator.* Ph.D. Dissertation, North Carolina State University, 2007.

Lee, J., and Shields, T. (2010). “Treatment guidelines for pavement preservation”. West Lafayette, IN.

Lin, J., Guo, P., Wan, L., and Wu, S. (2012). Laboratory investigation of rejuvenator seal materials on performances of asphalt mixtures. *Construction and Building Materials*, *37*, 41-45.

Lin, J., Guo, P., Xie, J., Wu, S., and Chen, M. (2012). Effect of rejuvenator sealer materials on the properties of aged asphalt binder. *Journal of Materials in Civil Engineering*, *25*(7), 829-835.

Mahoney, J. P., Slater, M., Keifenheim, C., Uhlmeyer, J., Moomaw, T., and Willoughby, K. (2014). *WSDOT Chip Seals—Optimal Timing, Design and Construction Considerations* (No. WA-RD 837.1).

Marasteanu, M. O., & Anderson, D. A. Comparison of moduli for asphalt binders obtained from different test devices. *Journal of the Association of Asphalt Paving Technologists, 69*, 2000, pp. 574-607.

Marasteanu, M. O., Basu, A., Hesp, S. A., & Voller, V. Time–Temperature Superposition and AASHTO MP1a Critical Temperature for Low-temperature Cracking. *International Journal of Pavement Engineering*, *5*(1), 2004, pp. 31-38.

Marasteanu, M. O., Cannone Falchetto, A., Turos, M., & Le, J-L. *Development of a simple test to determine the low temperature strength of asphalt mixtures and binders* (IDEA Program Final Report, NCHRP-151). Washington D. C.: Transportation Research Board of the National Academies, 2012.

Marasteanu, M. Role of bending beam rheometer parameters in thermal stress calculations. *Transportation Research Record: Journal of the Transportation Research Board*, (1875), 2004, pp. 9-13.

Marasteanu, M., Falchetto, A. C., Turos, M., and Le, J. L. (2012). "Development of a simple test to determine the low temperature strength of asphalt mixtures and binders", No. NCHRP IDEA Project 151.

Marasteanu, M., Ghosh, D., Cannone Falchetto, A., & Turos, M. Testing protocol to obtain failure properties of asphalt binders at low temperature using creep compliance and stress-controlled strength test. *Road Materials and Pavement Design*, 2017, pp. 1-16.

Marasteanu, M., Velasquez, R., Cannone Falchetto, A., and Zofka, A. (2009). "Development of a simple test to determine the low temperature creep compliance of asphalt mixtures". IDEA program final report NCHRP, 133, Washington DC.

Masson, J. F., Collins, P., and Légaré, P. P. (1999). "Performance of pavement crack sealants in cold urban conditions". Canadian Journal of Civil Engineering, 26(4), 395-401.

Medina, J. A., and Tyson, R. C. (2009). "Evaluation of RePlay Soy-Based Sealer for Asphalt Pavement", No. FHWA-PA-2009-020-RP 2008-035, Washington DC.

Mogawer, W. S., Booshehrian, A., Vahidi, S., and Austerman, A. J. (2013). "Evaluating the effect of rejuvenators on the degree of blending and performance of high RAP, RAS, and RAP/RAS mixtures". Road Materials and Pavement Design, 14(sup2), 193-213.

Moraes, R., R. Velasquez, and H. U. Bahia. Measuring the Effect of Moisture on Asphalt-21 Aggregate Bond with the Bitumen Bond Strength Test. In *Transportation Research Record:* 22 *Journal of the Transportation Research Board*, No. 2209, Transportation Research Board of 23 the National Academies, Washington, D.C., 2011, pp. 70–81.

Nahar, S. N., Schmets, A. J. M., Schlangen, E., Shirazi, M., van de Ven, M. F. C., Schitter, G., and Scarpas, A. (2014). "Turning back time: rheological and microstructural assessment of rejuvenated bitumen". In 93rd Annual Meeting Transportation Research Board, Washington, USA.

Olson, J. (2011). "Application of RePlay Agricultural Oil Seal and Preservation Agent", Local Operation Research Assistance Program for Local Transportation Groups Field Report. Local Road Research Board, MN.

Peshkin, D., Smith, K., Wolters, A., Krstulovich, J., Moulthrop, J., and Alvarado, C. (2010) "Guidelines for the Preservation of High Traffic Volume Roadways," Final Guidelines, Project R-26, Strategic Highway Research Program 2, February 1, 2010.

Prapaitrakul, N., Freeman, T., & Glover, C. (2010). Fog Seal Treatment Effectiveness Analysis of Pavement Binders Using the t-Test Statistical Approach. *Petroleum Science and Technology*, *28*(18), 1895-1905.

PS129, A. S. T. M. (2001). Standard provisional test method for measurement of permeability of bituminous paving mixtures using a flexible wall permeameter. *ASTM International*.

Qureshi, N. A., Tran, N. H., Watson, D., & Jamil, S. M. (2013). Effects of rejuvenator seal and fog seal on performance of open-graded friction course pavement. *Maejo International Journal of Science and Technology*, *7*(2), 189.

RePlay (https://pavementrestore.wordpress.com/services-2/)

Romero, P., and Anderson, D. (2005). *Life Cycle of Pavement Preservation Seal Coats* , Final Report (No. UT-04.07.

S. Shatnawi, "Maintenance Technical Advisory Guide, Volume 1: Flexible Pavement Preservation", 2nd Edn., California Department of Transportation, Sacramento (CA), **2008**, p.1.

Shen, J., Amirkhanian, S., and Tang, B. (2007). Effects of rejuvenator on performance-based properties of rejuvenated asphalt binder and mixtures. *Construction and Building Materials*, *21*(5), 958-964.

Simpson, P. L. (2006). "Overview of Asphalt Emulsion Applications in North America". Asphalt Emulsion Technology, Transportation Research Board, Washington, DC.

Stroup-Gardiner, M., Cheng, D., and Hicks, R. G. (2009). Fog and Rejuvenator Seal Test Sections on State Highway 58, Kern County. *Report Number: CP2C-2008-102, California Pavement Preservation Center*.

The Asphalt Institute. *A Basic Asphalt Emulsion Manual*. Manual Series No. 19. Lexington, KY. 1999.

Tran, N. H., Taylor, A., and Willis, R. (2012). "Effect of rejuvenator on performance properties of HMA mixtures with high RAP and RAS contents". National Center for Asphalt Technology. Auburn, AL.

Urbanek, B., Cheng, D., Fraser, B., and Lane, L. (2013). 2013 Caltrans Fog Rejuvenating Seal Pilot Projects in Northern California.

Velasquez, R. A., Marasteanu, M., Labuz, J. F., and Turos, M. (2010). "Evaluation of Bending Beam Rheometer for Characterization of Asphalt Mixtures". Journal of the Association of Asphalt Paving Technologists: 79.

Vitillo, N., Pavement Management Systems Overview, http://www.state.nj.us/transportation/eng/pavement/pdf/PMSOverviews0709.pdf, accessed June 2017.

Wang, F., Wang, Z., Li, C., Xiao, Y., Wu, S., & Pan, P. (2017). The Rejuvenating Effect in Hot Asphalt Recycling by Mortar Transfer Ratio and Image Analysis. *Materials*, *10*(6), 574.

Watson, M. 2009. Memo for Jointbond. Research on Longitudinal Joint Deterioration. Minnesota Department of Transportation, Maplewood, Minnesota. (http://www.dot.state.mn.us/materials/bituminousdocs/Special_Provisions/2009/LJD/JB_Long_Jt_Memo.pdf)

Webb, Z. (2010) "Seal Coat and Surface Treatment Manual." Texas Department of Transportation. Version May 1, 2010.

Wilde, W. J., Thompson, L., and Wood, T. J. (2014). *Cost-Effective Pavement Preservation Solutions for the Real World* (No. MN/RC 2014-33). Department of Transportation, Research Services and Library.

Williams, S. G. (2011). "HMA Longitudinal Joint Evaluation and Construction", TRC-0801 Final Report, AR.

Wood, T. J., D. W. Janisch, and F. S. Gaillard. Minnesota Seal Coat Handbook 2006. Final Report, Minnesota Department of Transportation Research Services Section, St. Paul, MN, 2006.

Wood, T., and Olson, R. (2007). "Rebirth of chip sealing in Minnesota". Transportation Research Record: Journal of the Transportation Research Board: 260-264, Washington, DC.

Yang, X., You, Z., Dai, Q., and Mills-Beale, J. (2014). Mechanical performance of asphalt mixtures modified by bio-oils derived from waste wood resources. *Construction and Building Materials*, *51*, 424-431

Zaniewski, J. P., and Mamlouk, M. S. (1996). *PAVEMENT MAINTENANCE EFFECTIVENESS-PREVENTIVE MAINTENANCE TREATMENTS. PARTICIPANT'S HANDBOOK* (No. FHWA-SA-96-027).

Zaumanis, M., Mallick, R., and Frank, R. (2013). "Evaluation of Rejuvenator's Effectiveness with Conventional Mix Testing for 100% Reclaimed Asphalt Pavement Mixtures". Transportation Research Record: Journal of the Transportation Research Board: 17-25, Washington, DC.

Zimmerman, K. A., & Peshkin, D. G. (2003, August). Integrating preventive maintenance and pavement management practices. In *Proceedings of the 2003 Mid-Continent Transportation Research Symposium, Center for Transportation Research and Education, Iowa State University, Ames, IA*.

Zimmerman, K., and Peshkin, D. (2004). Issues in integrating pavement management and preventive maintenance. *Transportation Research Record: Journal of the Transportation Research Board*, (1889), 13-20

Zofka, A., Marasteanu, M., Li, X., Clyne, T., and McGraw, J. (2005). "Simple Method to Obtain Asphalt Binders Low Temperature Properties from Asphalt Mixtures Properties". Journal of the Association of Asphalt Paving Technologists: 74.

Zubeck, H. K., and Doré, G. (2009). Introduction to cold regions pavement engineering. In *Cold Regions Engineering 2009: Cold Regions Impacts on Research, Design, and Construction* (pp. 337-345).

Zubeck, H., Mullin, A., and Liu, J. (2012). "Pavement Preservation Practices in Cold Regions." Cold Regions Engineering, pp 134-143, Quebec City, Canada.